2014

Modeling of sickle cell anemia utilizing disease-specific induced pluripotent stem cells

BOSTON UNIVERSITY

SCHOOL OF MEDICINE

Dissertation

MODELING OF SICKLE CELL ANEMIA UTILIZING DISEASE-SPECIFIC INDUCED PLURIPOTENT STEM CELLS

by

SARAH SUNDSTROM ROZELLE

B.S., University of California at Davis, 2006

Submitted in partial fulfillment of the

requirements for the degree of

Doctor of Philosophy

2014

Approved by

First Reader

George J. Murphy, Ph.D.
Assistant Professor of Medicine

Second Reader

Martin Steinberg, M.D.
Professor of Medicine

"Promise me you'll always remember: You're braver than you believe, and stronger than you seem, and smarter than you think."

~Christopher Robin

DEDICATION

To D.K.R. and Pumpkin. May we always possess the willingness to embark on new and marvelous adventures together.

ACKNOWLEDGMENTS

First and foremost I must acknowledge and thank the Murphy lab. To G, you have driven me to new heights both intellectually and personally. I am a stronger person than when I entered your lab, and I'm certain it was all due to the fact that you made me work for everything. From my entry into the lab to my exit you have raised the bar of "normal" and truly made me exceed expectations. Hopefully one day I'll be able to follow in your footsteps and be capable of "stealing home."

To Brenden, Amy, Shirley, Whitney, and James, my comrades in arms. Thank you for not killing me in my most psychotic moments and for bringing me back to earth when I needed it. You are all the brightest people I know, and I have been so lucky to have you for colleagues and friends. I have enjoyed your company on the rare early mornings and our late night hours. Thank you for making me laugh, sing, and remember to have fun. I will miss our song and dance parties in the original Murphy TC room and our endless you tube watching.

My Boston friends have been an essential part of getting me out of lab. Whether it is for a bike ride, small group, a run, skiing, shoveling, yard work, and pizza nights, you have made Boston home for me. To Chapter AE, you are a marvelous group of women, so strong, and so fabulous. Thank you all for adopting this CA transplant and making her a Bostonian.

My family. As you once told me "friends come and go, but family is forever." That has never been so true then when you are so far apart. Kevin, you are always so creative and marching to your own drum, literally and figuratively. Thank you for showing me that it's okay to be unique and love who you are. Molly all those years of "practicing" our arguments have made you into the fantastic lawyer you are and myself the very argumentative scientist. As sisters, we share a special bond that has only been strengthened during my time in Boston, mostly due to your desire to call me when stuck in traffic. I love how close we've become and treasure our Sister-Weekends.

Mom and Dad- as a young girl you made all of this possible. You let me be curious, inquisitive to the point of annoyance, and gave me room to follow my dreams. I have always wanted to have a Ph.D. after my name, just like my daddy, the best example of a scientist I have ever met. From celery and colored water, to UCD, and now BU you have supported my dream of being a scientist in more ways then I could ever list.

Dan- you are the only one whom can say they deserve two Ph.Ds. for what we have accomplished in the past 10 years. Thank you for all the love, support, and guidance as you made this dream possible.

MODELING OF SICKLE CELL ANEMIA UTILIZING DISEASE-SPECIFIC INDUCED PLURIPOTENT STEM CELLS

SARAH SUNDSTROM ROZELLE

Boston University School of Medicine, 2014

Major Professor: George J. Murphy, Ph.D., Assistant Professor of Medicine

ABSTRACT

Sickle cell anemia, caused by a point mutation that affects the *HBB* gene, is one of the most common human genetic disorders world-wide and has a high morbidity and mortality. A single FDA approved drug, hydroxyurea, is available for its ability to induce fetal hemoglobin expression, a major modulator of disease severity. Not every patient responds to treatment and additional HbF-inducing drugs are needed. In this thesis, I outline an induced pluripotent stem cell-based approach to the study of sickle cell disease (SCD). In the lab, we are currently building a library of SCD-induced pluripotent stem cell (iPSC) lines from a cohort of SCD patients with different genetic backgrounds and fetal hemoglobin levels. Utilizing a directed-differentiation approach, iPSC can give rise to hematopoietic progenitors that are similar to megakaryocyte-erythroid progenitors and can be further specified to become cells of either lineage. I examined the hypothesis that an iPSC-based system would be capable of producing fully functional erythroid cells and also recapitulate the variation in fetal hemoglobin levels seen in SCD patients. Directed-differentiation of iPSCs produced erythroid-lineage cells that were responsive to oxygen levels and erythropoietin, and were capable of further maturation and increased hemoglobin production. A humanized mouse model demonstrated the ability of these cells to localize to the bone marrow, contribute to the peripheral blood, and survive *in vivo* for over two weeks. The maturation capability of SCD-specific iPSC-derived erythroid lineage cells was correlated with

hemoglobin expression and compared to control cells. Characterization of *in vitro* and *in vivo* differences between control and SCD-specific iPSC-derived erythroid-lineage cells demonstrated variation amongst individuals, similar to the variation seen in patients. Both of these patient-specific iPSC-based *in vitro* and *in vivo* models allow for the examination of the effect of genetic variability on fetal hemoglobin expression and also for the modeling of patient-specific responses to drug treatment. This information will facilitate better clinical treatment of the disease.

TABLE OF CONTENTS

LIST OF TABLES

LIST OF FIGURES

LIST OF ABBREVIATIONS

AGM: aorta-gonad-mesonephros

AhR: aryl hydrocarbon receptor

AhRE: aryl hydrocarbon response element, also known as DRE

AhRR: aryl hydrocarbon receptor repressor

APC: Allophycocyanin

ARNT: aryl hydrocarbon nuclear translocator

CD235: human erythroid marker glycophorin A, GlyA

CD41a: human megakaryocyte marker integrin α_{IIb} also known as platelet GPIIb

CD42b: human megakaryocyte marker Glycoprotein Ib

CD71: human erythroid transferrin receptor, TfR

CLP: common lymphoid progenitor

CMP: common myeloid progenitor

CYP1A1 or CYP1A1: cytochrome P450 1A1 or 1B1

DNA: deoxyribonucleic acid

DRE: dioxin response element, also known as AhRE

Ef1α: constitutively active promoter for human transcription elongation factor alpha

EMM: erythroid maturation media

EPO: erythropoietin

FICZ: 6-fomylindolo[3,2-b] carbazole

FITC: Fluorescein isothiocyanate

FOG1: friend of GATA1

FSC: forward scatter

GAPDH: Glyceraldehyde 3-phosphate dehydrogenase

GMP: granulocyte macrophage progenitor

HbA: adult globin, $\alpha_2\beta_2$

HBA: alpha globin, α

HBB: beta globin, β

HBD: delta globin, δ

HBE: epsilon globin, ε

HbF: fetal globin, $\alpha_2\gamma_2$

HBG: gamma globin, γ

HbS: sickle globin, $\alpha_2\beta^s$

HBZ: zeta globin, ζ

hES: human embryonic stem cells

HP: hematopoietic progenitor

HSC: hematopoietic stem cell

HU: hydroxyurea

IL-3: interleukin-3

iPSC: induced pluripotent stem cells

IRES: internal ribosome entry site

KLF1: kruppel-like factor 1

MEP: megakaryocyte erythroid progenitor

Mk: megakaryocyte

MMTV: mouse mammary tumor virus

NLS: nuclear localization sequence

PAS: Per/ARNT/SIM family of transcription factors

PE: phycoerythrin

PI: propidium iodide

qPCR/RT-PCR: reverse transcriptase polymerase chain reaction

QTL: quantitative trait loci

RBC: red blood cell

SCF: stem cell factor

SD: standard deviation

SNP: single nucleotide polymorphism

SSC: side scatter

TCDD: 2,3,7,8-tetrechlorodibenxopdioxin

TPO: thrombopoietin

β-NF: β-naphthoflavone

CHAPTER 1:

GENERAL INTRODUCTION

The study of hematopoiesis

Hematopoiesis: a brief description of the blood system.

A hierarchal process, hematopoiesis involves a series of cell fate decisions that lead to the production of eight distinct blood cell types, all with unique roles **(Figure 1.1)**. In the adult, the hematopoietic stem cell (HSC) remains quiescent in the bone marrow until signaled to divide, allowing it to produce all blood cell types through a series of differentiation steps and progenitors without stem cell exhaustion[1]. Two major hematopoietic progenitors derived from the HSC, the common myeloid progenitor (CMP) and the common lymphoid progenitor (CLP), will undergo both propagation and differentiation to produce myeloid[2] and lymphoid[3] blood cells.

Both the CMP and the CLP are the source of immune cells. The CLP gives rise to the lymphoid compartment consisting of B and T lymphocytes[3]. B cell lymphocytes are important for adaptive immunity by recognizing foreign antigens and stimulating antibody production for recognition and destruction of foreign objects[4]. T cell lymphocytes direct the immune system's defense in two manners: through the regulation of the immune response and the actual attack of infected cells[4]. The CMP is responsible for the production of granulocytes and monocytes (the most mature form known as macrophages) through the derivation of the granulocyte macrophage progenitor (GMP)[2]. Granulocytes, also known as white blood cells, are identified by the staining properties of their cytoplasm and their unique role in identification of microorganisms in the body. Neutrophils recognize bacteria; eosinophils specialize in parasitic recognition; and basophils release histamine to stimulate inflammatory responses[5]. Imperative to both adaptive and innate immunity, macrophages are accountable for the engulfment and digestion of cellular debris

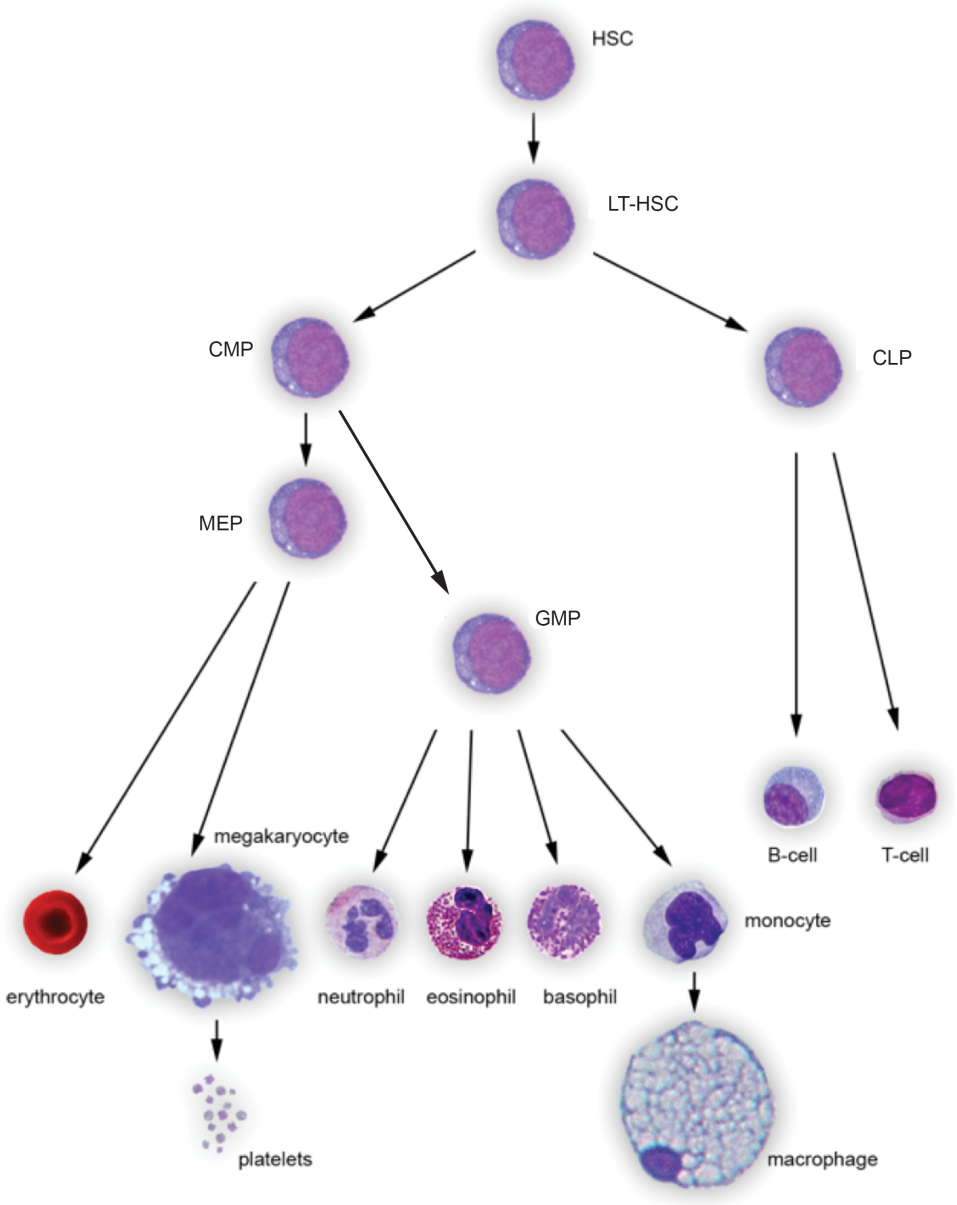

Figure 1.1. Schematic of hematopoiesis. Hematopoiesis is responsible for the derivation of 8 distinct cell types that make up the blood system through the hematopoietic stem cell (HSC) and progenitors such as the common lymphoid progenitor (CLP), the common myeloid progenitor (CMP), the granulocyte macrophage progenitor (GMP) and the megakaryocyte erythroid progenitor (MEP). *Adapted from http://students.uccaribe.net/forums/topic/hematopoiesis-histology-image*

and pathogens[5]. While cells produced by the CLP and CMP are responsible for the immune system, the CMP is also a progenitor for other essential blood cells.

Thrombocytes and erythrocytes are created from the megakaryocyte erythroid progenitor (MEP), another progenitor derived from the CMP[2]. These cells transport oxygen and create clots at the site of injury. Erythrocytes, commonly called red blood cells (RBC), utilize hemoglobin to uptake oxygen in the lungs and exchange it for carbon dioxide in the peripheral tissues[5]. Thrombocytes, also known as platelets, are cell fragments that have been derived from and detached from megakaryocytes. They adhere to endothelial cells in blood vessels at the site of injury to form clots[5].

In *Homo sapiens*, two separate waves of hematopoiesis occur to produce all the cells in the blood system, primitive and definitive. While both arise during embryogenesis, only definitive persists into adulthood. Primitive hematopoiesis is responsible for the production of cells to carry oxygen to the developing embryo. Definitive hematopoiesis is required for the more complex hematopoietic system developed in the embryo and continued throughout adult life.

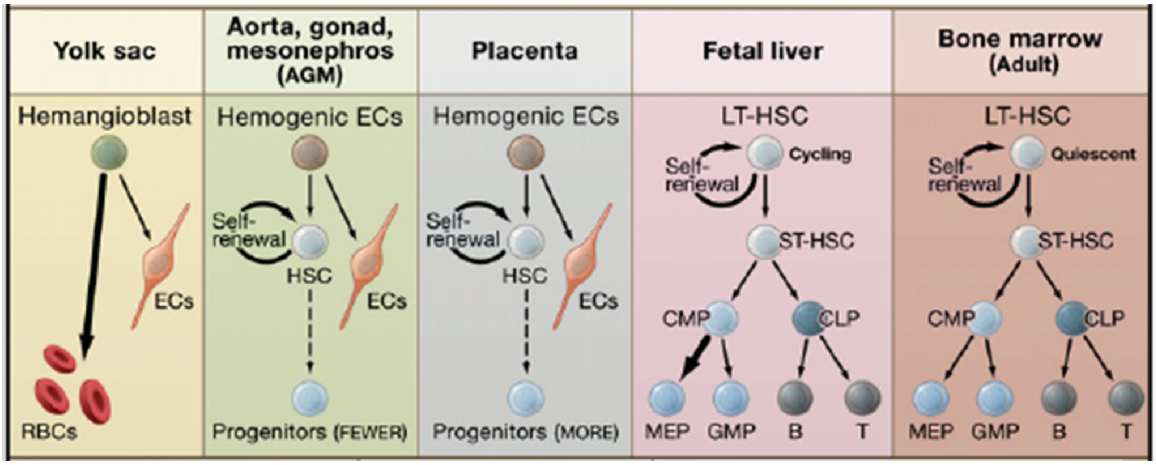

Figure 1.2. The cell source for hematopoiesis changes concurrently with the site of hematopoiesis. As illustrated in mice, as the site of hematopoiesis changes so does the source from which all blood cells are derived. *From Orkin and Zon*[6].

Primitive Hematopoiesis: the earliest phase of hematopoiesis

Hematopoiesis can be classified by the location in which it is occurring, and the source of the hematopoietic lineages. In mammals, the location of hematopoiesis transitions multiple times during development. Initiated in the yolk sac, it is transiently found in the aorta-gonad mesonephros (AGM) region, before residing in the fetal liver and ultimately the bone marrow[6]. Along with the transition in locations, is the transition in the source of hematopoietic lineage cells. Primitive hematopoiesis, the initial wave of hematopoiesis in the yolk sac is essential for the early production of RBCs[7]. This wave of hematopoiesis is termed primitive due to the hallmark expression of embryonic hemoglobin and the belief that the resulting RBCs are not produced from a hematopoietic stem cell, but the hemangioblast **(Figure 1.2)**. The hemangioblast, while short lived, is a multipotent progenitor responsible for the production of hematopoietic and endothelial cells during early development[8–10]. Not long after production in the yolk sac, the site of hematopoiesis transitions to the AGM and fetal liver in which the first few HSCs are found and definitive hematopoiesis can begin[11].

Definitive Hematopoiesis: a HSC mediated production of blood cells

The period when cells in the blood system are produced from the HSC is classified as definitive hematopoiesis. Unlike primitive hematopoiesis, definitive will persist throughout adulthood, despite changes in location. It is unclear whether the HSCs found in the AGM and fetal liver are responsible for colonizing the bone marrow or if a separate wave of HSCs is responsible[6,12] (**Figure 1.2 & 1.3)**. Definitive hematopoiesis can be found in four main locations during embryonic development: AGM, placenta, fetal liver, and the bone marrow[13]. Hemoglobin expression changes during embryonic development with fetal hemoglobin expressed early and transitioning to adult globin at the end of gestation.

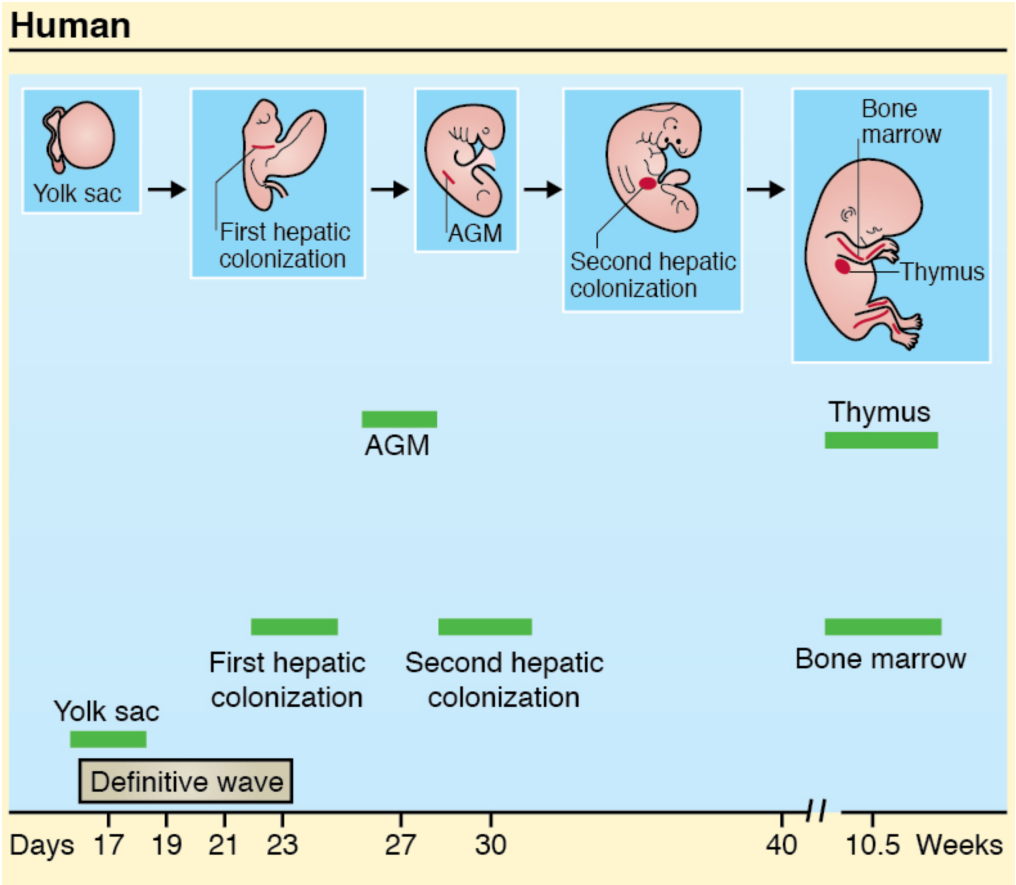

Figure 1.3. Schematic of the development of the human hematopoietic system. The yolk sac is the site of embryonic hematopoiesis, which then proceeds to the fetal liver after the onset of circulation. A second colonization occurs leading to the site of hematopoiesis arriving in the bone marrow at ~10.5 weeks and the thymus at 9-10.5 weeks. *From Jagannathan-Bogdan and Zon*[14].

The study of erythropoiesis

Erythropoiesis: A brief overview of the process of erythropoiesis

Erythropoiesis refers to the process of production of RBCs, which in humans, occurs in red bone marrow. Erythropoiesis is primarily stimulated by erythropoietin (EPO), which is a glycoprotein hormone produced by the kidneys in response to low levels of oxygen. RBC development from the HSC is a multistep process in which many cell fate decisions must be made to specify not only to the myeloid lineage, but also to the erythroid lineage.

The first erythroid lineage precursor, the proerythroblast, will receive multiple signals that cause morphological maturation, hemoglobin switching, hemoglobin accumulation, and ultimately enucleation. This multi-step process will produce biconcave discs, which have a large surface area-to-volume ratio that efficiently allows the diffusion of oxygen and carbon dioxide in and out of the cell. The flexible plasma membrane allows erythrocytes to maneuver through small capillaries, delivering oxygen to all parts of the body **(Figure 1.4)**.

Without a nucleus, RBCs are incapable of repairing themselves after injury. Injured or old RBCs are cleared in the liver and spleen by phagocytosis. Macrophages are the primary recycler of RBC components after phagocytosis, such as the large amounts of iron that accumulated in hemoglobin. A typical RBC lifespan is 120 days, though injury or hemoglobin disorders can cause premature hemolysis. Loss of RBCs, or anemia, results in lower levels of oxygen (hypoxia). While hypoxia can occur naturally, when caused by loss of RBCS, it is extremely important to upregulate erythropoiesis to produce RBCs at a rapid rate.

Erythropoiesis: important cytokine and transcriptional regulation for the production of red blood cells

Specification to the erythroid lineage relies on both concurrent and sequential expression of many transcription factors as well as cytokine signaling. Both external and internal signaling results in morphological changes of the proerythroblast to the erythrocyte, and hemoglobin production. Three important cytokines for erythropoiesis are SCF[15], IL-3[16–18]

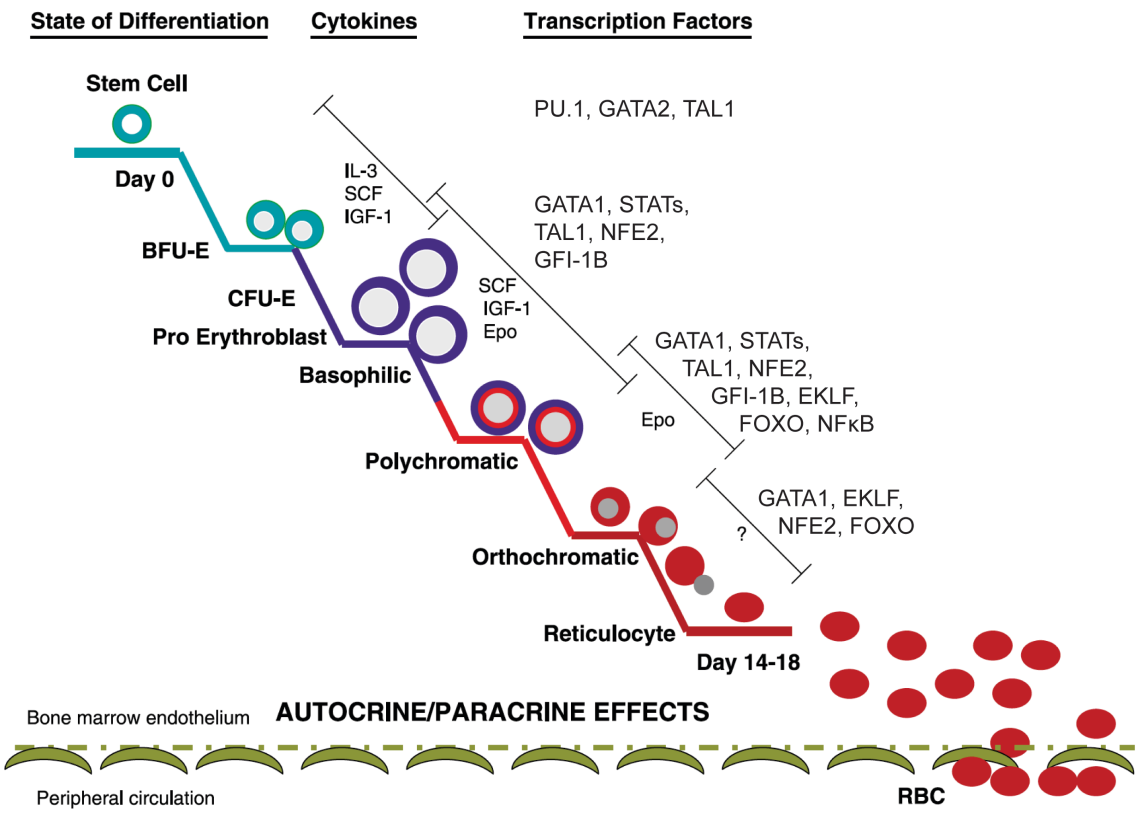

Figure 1.4. Signaling involved in erythroid maturation. Outline of cytokines and transcription factors involved in signaling for erythroid cell maturation. *Image adapted from Wickrema & Crispino, Oncogene (2007), 26:6803-15.*

and EPO[19,20]. While there are many important transcription factors involved in erythropoiesis, GATA1, FOG1[21] and KLF1[22,23] play a crucial role not only in maturation, but hemoglobin expression as well **(Figure 1.5)**.

Erythropoiesis: SCF, a hematopoietic cytokine

Stem cell factor (SCF, also known as Kit ligand) exists both in a soluble and membrane-bound form and binds to the c-kit receptor. C-Kit signaling is important not only for erythroid progenitor proliferation, but also for HSC proliferation, mast cell function, melanogenesis, and spermatogenesis. C-kit is expressed on CD34+ hematopoietic progenitor cells and early erythroid progenitors, however it's expression declines and ultimately disappears in late stage erythroblasts[24]. C-kit transcription is negatively regulated by direct binding of GATA-1 to the c-kit promoter[25]. When SCF binds to the c-kit protein, it induces activation of PI3K resulting in increased proliferation of early and late erythroid progenitors, blast forming units, erythroid and colony forming units-erythroid, as well as terminally differentiated erythroid cells[26,27]. SCF signaling can inhibit cell cycle progression by inducing expression of Myc, which is involved in the final stages of erythroid maturation[25,28]. SCF also plays a role in promoting stress-induced erythropoiesis[29].

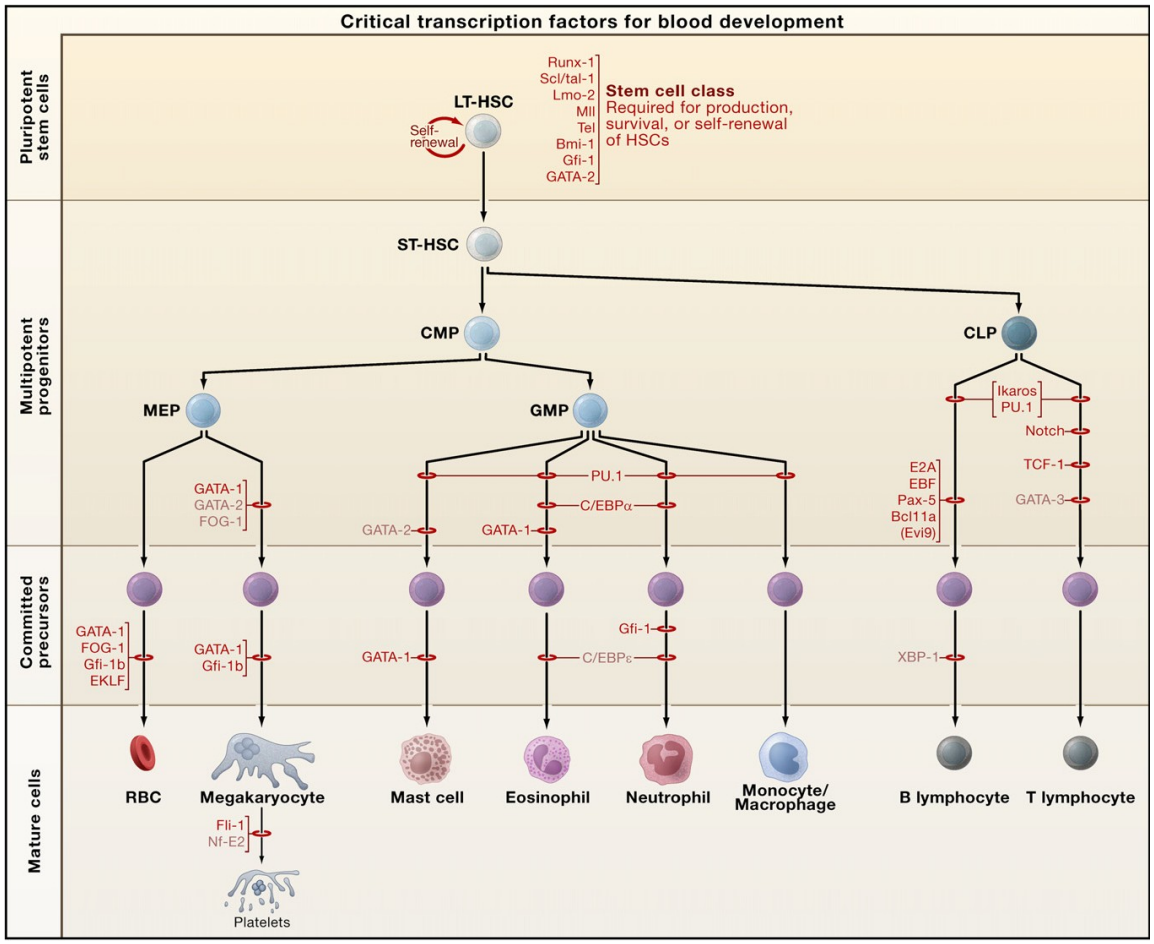

Figure 1.5. Multiple transcription factors are involved in the production of eight types of blood cells. Transcription factors listed at the site of hematopoiesis in which their absence blocks the production of the resultant cells, as noted through conventional gene knockout studies. LT and ST-HSC, long-term and short-term hematopoietic stem cells; CMP, common myeloid progenitor; CLP, common lymphoid progenitor; MEP, megakaryocyte erythroid progenitor; GMP, granulocyte macrophage progenitor. *From Orkin and Zon* [6].

Erythropoiesis: EPO is a stimulant of erythroid progenitor differentiation

Erythroid cell production occurs as a result of EPO signaling in the bone marrow. EPO, produced by the kidney, varies in concentration based on sensing oxygen intake and consumption in the organism. Levels are most commonly elevated in response to anemia and hypoxia[30,31]. Binding of EPO to EPO-receptors on the surface of erythroid progenitors triggers activation of multiple intracellular signal transduction pathways including STAT5 and PI3K whose signaling is essential for renewal divisions and differentiation of erythroid progenitors[32–34]. EPO and SCF activate common signaling pathways such as protein kinase B and the subsequent phosphorylation and inactivation of Foxo3a, while only EPO activates Stat5. Both Foxo3a and Stat5 independently promote erythroid differentiation. In bone marrow, EPO stimulates RBC production through two distinct mechanisms; increasing cell division of erythroblasts and accelerating the maturation of RBCs by accelerating hemoglobin synthesis[35,36]. This quickly results in an increase in the number of RBCs in the blood stream in a very short time span.

Erythropoiesis: IL-3 is a myeloid specific differentiation factor

Interleukin 3 (IL-3) plays an important role in the differentiation of myeloid cells in addition to its better-known role in immunity. IL-3 works in concert with other cytokines such as EPO, to aid in the growth and differentiation of myeloid progenitors. Studies in non-human primates have shown that IL-3 treatment results in an increase both early and late erythroid progenitors. Additionally, combination therapy of NHPs with IL-3 and EPO has shown a synergistic effect on erythropoiesis[18]. Experiments into culture conditions of erythroid lineage cells have found that IL-3 with SCF and EPO enabled not only the purification but the i*n vitro* expansion of large numbers of erythroid progenitors from $CD34^+$ peripheral blood cells[37].

Erythropoiesis: GATA1, a master regulator of differentiation

The transcription factor GATA-1 is required for terminal erythroid maturation and functions as an activator or repressor depending on gene context[38]. GATA-1 is also required in other hematopoietic lineages. Much work has gone into understanding how a "master regulator" transcription factor coordinates tissue differentiation through a variety of DNA and protein interactions. Analysis of the promoter sequences of activated erythroid lineage genes revealed consensus sequences for SCL/Tal1 at GATA1-bound sites, revealing that GATA1 activation of these genes occurs in concert with the SCL/Tal1 co-regulator[39–42]. In erythroid cells, SCL/Tal1 forms a complex with E2A, LMO2 and Ldb1 to form an activating complex with GATA1[43–45]. The components of the GATA1 repressor complexes are much less clear and probably include FOG1, and the repressor Gfi-1b.

Erythropoiesis: KLF1 is an essential erythroid transcription factor

Kruppel like factor 1 (KLF1 or EKLF), is an essential zinc finger transcription factor that recognizes a subset of extended CACC box motifs whose locations are erythroid-restricted[43,46]. When binding sites were compared to GATA1 sites, almost half (48%) of the KLF1 sites were within 1 kb of GATA1 sites and few contained the SCL/Tal1 consensus sequence or overlapped with SCL/Tal1-GATA1 co-occupied sites suggesting that GATA1 and KLF1 may activate genes independently of SCL/Tal1 [47,48]. It is now believed that KLF1 is responsible for bringing transcriptionally active portions of the chromatin to transcription factories, rather than recruiting transcription machinery for the expression of erythroid specific genes[49].

In addition to maturation of erythroid cells, KLF1 is also responsible for regulating hemoglobin expression. This is accomplished by directly binding to the *HBB* promoter and

indirectly through upregulation of *BCLl11A*[50,51]. BCl11A forms a complex with GATA1, FOG1 and the NuRD complex to upregulated β-globin expression.

Erythropoiesis: FOG1, a teammate of GATA1

FOG1 was identified as friend of GATA1, due to its action as a co-factor in GATA1 transcription[21]. A zinc finger protein, FOG1, physically associates with the N finger of GATA-1 via at least one of its fingers. In the absence of FOG1, there is a complete loss of progenitors committed to both the megakaryocyte and erythroid lineages, whereas myeloid-committed GMP progenitors were increased demonstrating the multiple roles FOG1 plays in hematopoiesis[52]. Point mutations that disrupt FOG1 binding affect normal erythroid and MK development in cellular assays, human patients, and engineered mutant mice[53,54]. FOG1 is required for the activation and repression of most GATA1-dependent genes[54–56]. Another partner of FOG1 the nucleosome remodeling and histone deacetylase complex NuRD, which binds to a small conserved motif at the extreme N-terminus of FOG1 [57] has been shown to be involved in differential hemoglobin expression[58].

Erythropoiesis: the role of hemoglobin

In 1840, hemoglobin was discovered by F. L. Hünefeld as the protein responsible for carrying oxygen in the blood[59]. It was Fleix Hopp-Seyler who described hemoglobin's reversible oxygenation and that iron in the globular protein allowed for hemoglobin's oxygen carrying capacity[60]. Each heme group contains one iron atom and can bind one oxygen molecule through dipole forces allowing for the binding in high oxygen environments and release in low oxygen

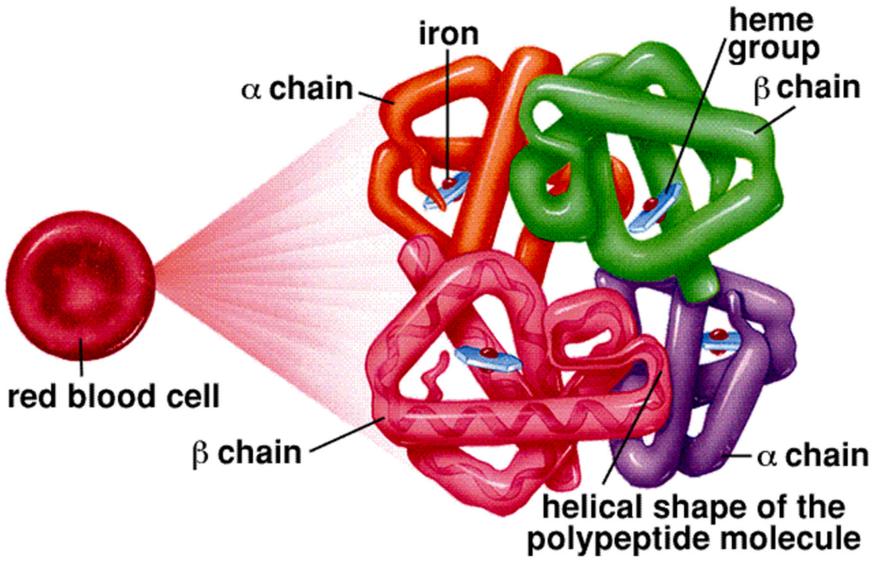

Figure 1.6. Hemoglobin structure showing four heme molecules with attached iron. *Sylvia S. Mader, Inquiry into Life, 8th edition, 1997.*

location. Hemoglobin will bind carbon dioxide in the periphery for transport and release from the lungs. Mammalian hemoglobin, as a tetramer of hemoglobin molecules can bind and carry up to four oxygen molecules **(Figure 1.6)**. While also found outside of RBCs, hemoglobin functions as an antioxidant and a regulator of iron metabolism.

Human hemoglobin has 6 distinct normal variants, each based on a phase of hematopoiesis. Each heterodimer contains one alpha-type globin and one beta-type globin, which change during fetal development. During early human embryonic development first primitive RBCs are derived from yolk sac blood islands [7,61]. As the site of hematopoiesis moves throughout fetal development the type of hemoglobin expressed changes to meet the needs of the fetus. Early RBCs express embryonic globins alpha-type zeta (*HBZ*) and beta-type epsilon (*HBE*) globins, while fetal liver RBCs express alpha (*HBA2* and *HBA1*) and beta-type gamma (*HBG2* and *HBG1*) globins. During this stage of development the fetus is acquiring its oxygen from the maternal peripheral blood system, and therefore fetal hemoglobin, $\alpha_2\gamma_2$ (HbF), which has a higher oxygen

affinity than adult hemoglobin, $\alpha_2\beta_2$ (HbA), is required[62]. The final location of hematopoiesis, the bone marrow is colonized by HSCs around the mid stages of gestation, and it will reside there for the adult life of the individual. Bone marrow HSCs are the source of all definitive hematopoiesis, which results in 97% of RBCs expressing HbA and <1% containing HbF.

Hemoglobin expression, while dependent on erythropoiesis, is not regulated by erythroid maturation. The site of hematopoiesis plays a larger role in the regulation in which hemoglobin molecules are expressed, rather than the maturation state of the cells. This is due to the variety of transcription factors involved in hemoglobin expression and their time/site specific expression. Hemoglobin switching, the process of changing from primarily γ-globin to β-globin expression within the chromosome 11 β-globin locus is an intricate process that begins in mid-gestation and it complete by about 6 months of age. Expression of both genes is under the control of the β-globin locus control region and its dynamic interaction with associated transcription factor complexes allowing for specific globin expression. Hemoglobin switching is further addressed in Chapter 3.

Erythropoiesis: morphology and surface markers of maturation

Under normal conditions RBCs progress through multiple steps of maturation to go from an erythroblast to an erythrocyte. These steps will be explored in chapter 3. Briefly, cells are characterized morphologically based on size, hemoglobin content, and the size and appearance of the nucleus. As maturation continues the hemoglobin content in the cell increases while cell size decreases. All erythroid progenitors are capable of cell division until the stage of the normoblast, the smallest and last nucleate cell in the erythroid lineage. After the nucleus is extruded, the cell is known as a reticulocyte. Macrophages play a crucial role in nuclear extrusion, or the process of expelling the nucleus from the cell, by creating erythroblastic islands in the bone marrow[63–65].

The resultant biconcave shape of the RBC increases the surface area of the cell for optimal oxygen exchange and allows for the deformability necessary to migrate through the microvasculature[66].

Two surface markers are commonly used to assess maturation state of erythroid lineage cells in conjunction with morphology; they are Glycophorin A (CD235) and the transferrin receptor (CD71). CD235 is constitutively expressed on all erythroid cells while CD71 expression is limited to earlier progenitors. These markers will be discussed in further detail in chapter 3.

The history and study of sickle cell disease

Sickle cell disease: a brief history

The first report of sickled cells in the United States was in 1910 from James Herrick who noticed these cells in blood specimens from Walter Clement Noel, a 20-year-old dental student from Grenada[67]. It took 12 years and four more reported cases for the disease, which commonly presents with anemia, to be named sickle cell anemia. Mechanistic studies revealed that deoxygenation of hemoglobin results in the sickling shape of affected individuals[68]. It was Linus Pauling who hypothesized that sickle cell anemia might be caused by abnormal hemoglobin in 1945[69]. Pauling was able to confirm this hypothesis by the differential migration of normal and sickle cell hemoglobin by non-denaturing gel electrophoresis[70]. Around this time, sickle cell anemia was revealed to be inherited in an autosomal recessive manner[71].

It was not long before researchers began noticing differences in clinical manifestations of the disease. Studies of sickle cell disease patient relatives whom showed no symptoms of disease, determined that their RBCs also developed a sickling morphology when deprived of oxygen. This condition became known as “sickle trait”. It was confirmed in 1949 that those whom were

heterozygous for the mutation had the trait, while homozygous individuals had the more severe disease[71]. Sickle cell disease (SCD) is now used to refer to all individuals whom possess the sickle inducing mutation. It was also noted that infants, whom had high levels of HbF at birth, did not have symptoms of the disease until they were older[72].

The mutation causing the abnormal hemoglobin was identified in 1959 as a glutamine-to-valine substitution at the sixth residue of the HBB polypeptide[73]. This amino acid change reveals a hydrophobic region when sickled hemoglobin is deoxygenated, allowing it to bind to a complementary hydrophobic site and polymerize **(Figure 1.7)**. Small amounts of HbF can reduce polymerization of mutant HBB, reducing disease severity and improving the patient's quality of life[74]. Hydroxyurea was first used for its HbF inducing properties in baboons in 1984[75] and humans in 1990[76]. Multi-center studies proved its effectiveness and as the only FDA approved HbF inducing drug, hydroxyurea has been used ever since for treatment of sickle cell anemia[77,78].

Sickle cell disease: disease pathophysiology

While most individuals express normal HbA, nearly 100,000 sickle cell disease patients reside in the United States (~0.03%) and eight percent of African Americans are carriers of the sickle hemoglobin (HbS, $\alpha_2\beta^S{}_2$) mutation. The clinical course of this disease is highly variable and affects many organs[79]. Upon deoxygenation, mutant HBB polymerizes and forms a rigid polymer due to the exposure of hydrophobic regions

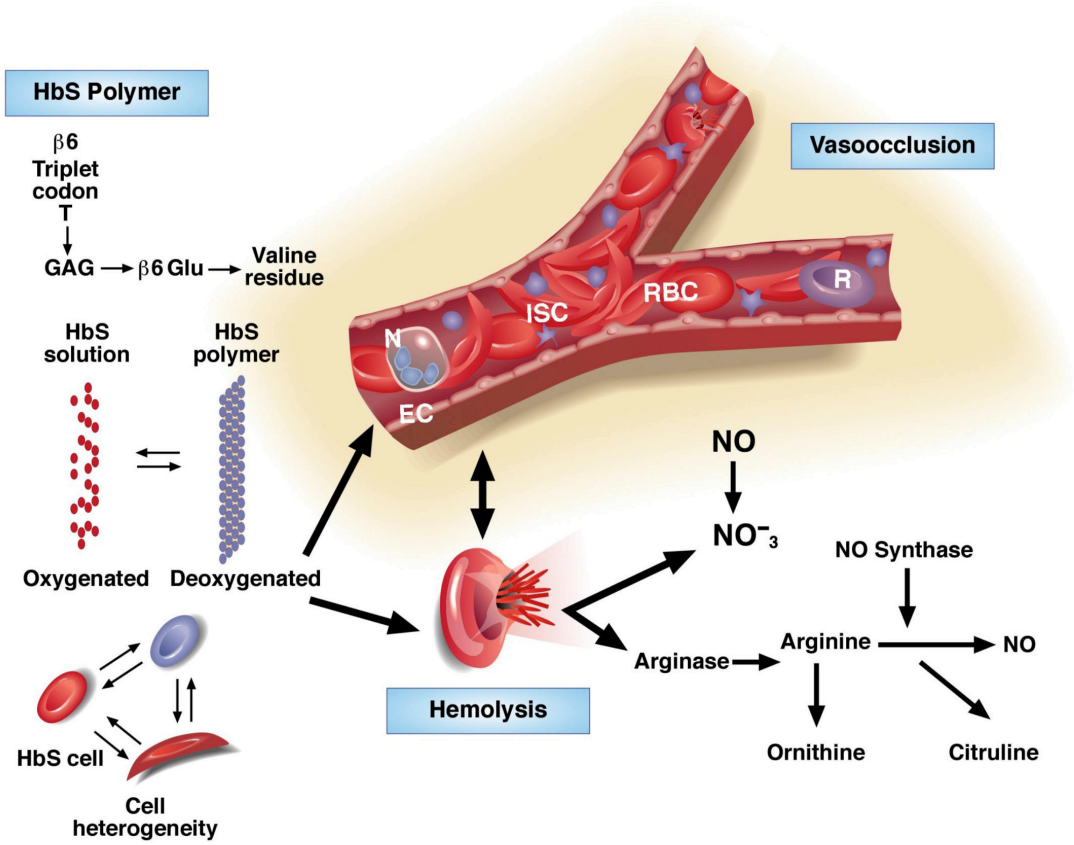

Figure 1.7. Schematic of sickle cell disease demonstrating the cause and resulting complications due to the presence of sickled cells. *From Steinberg, Forget, Higgs, and Weatherall, Disorders of Hemoglobin, 2nd edition, 2009*[79]**.**

created by the mutation. Polymer formation disrupts the cell membrane and cytoskeleton resulting in the characteristic change in erythroid cell shape, from a normal biconcave disc to a diseased sickle cell. This rigid HBB polymer reduces cell flexibility, often resulting in vaso-occulusion and hemolysis **(Figure 1.7)**.

Vaso-occlusion, or the process of blocking blood vessels with sickled cells, is a predominant clinical manifestation of the SCD. In addition to the physical nature of rigid RBCs blocking the vasculature, sickle RBCs are more apt than normal RBC to adhere to endothelial cells in vitro[80,81]. Occlusive episodes result in pain that can be treated with hydration, analgesics, and blood transfusions to decrease the proportion of sickled RBCs. Numerous episodes can result in ischemic injury and permanent organ damage.

Chronic hemolysis, or the rupture of a RBC, leads to the release of hemoglobin. Free hemoglobin has been shown to play a role in endothelial dysfunction through its ability to scavenge the second messenger signaling molecule, nitric oxide[82]. Oxidative stress is another result of hemolysis as is the release of iron from the cell. Other complications of the disease include but are not limited to priapism, autosplenectomy, stroke, chronic pain management and pulmonary hypertension.

Despite the presence of HbS, individuals can present with a range in the severity of the disease phenotype. This indicates that deoxyHbS polymerization is necessary, but not sufficient to account for the heterogeneity of disease manifestations, which are genetically modulated and environmentally effected. Originally noted in infants, researchers have observed that individuals with less severe pathologies persist in making the fetal form of hemoglobin (HbF $\alpha_2\gamma_2$), as adults. They also noted that the levels of HbF present may affect the amount of sickling and side-effects of the disease[72,74,83]. It is now understood that high amounts of HbF lower the concentration of sickle hemoglobin within a cell and neither HbF nor its mixed hybrid tetramer is incorporated

into the HbS polymer, resulting in less polymerization of the abnormal hemoglobin, which can lead to less severe disease phenotypes[74].

Sickle cell disease: haplotypes of SCD

The persistence of HbF into adulthood has allowed for classification of patients based on the genetic markers linked with HbF expression. Using restriction site analysis, five distinct haplotypes of SCD have been identified linked: Senegal, Cameroon, Benin, Bantu (Central African Republic), and Arab-Indian[84,85]. Disease severity and patient outcome have been linked to particular haplotypes[86]. Severe disease outcome is seen most in individuals with the Bantu haplotype while intermediate disease severity is typical with Benin haplotypes. The Senegal and Arab-Indian haplotypes have milder disease symptoms[86,87]. As HbF levels within each haplotype varies, it implies that other factors than elements linked to the *HBB* gene cluster affect HbF concentration.

Sickle cell disease: high levels of HbF, the case of HPFH and QTLs

For reasons that are still being elucidated, there is a large amount of variance in HbF expression during adulthood due to both genetic[88,89] and epigenetic factors[90,91], with some individuals retaining high levels of HbF throughout their adult life. Quantitative trait loci (QTL) play a large role in the modulation of HbF expression. QTLs are genes or stretches of DNA, typically acting in trans, which are responsible for a quantifiable trait, such as hemoglobin expression. There are single nucleotide polymorphisms (SNPs) that have been identified by their ability to affect HbF expression in a patient specific manner. Four QTLs have been identified for their ability to increase HbF expression in adults; they are the Xmn1 restriction site 5' to *HBG2* on chromosome

11p[92], a locus on chromosome 6q (HMIP)[93], *KLF1*[51] and BCL11A on chromosome 2p[94]. These single nucleotide polymorphisms, while occurring on other chromosomes, can modulate gene expression or alter protein interactions to increase HbF expression. While there are multiple QTLs that have been described, their effects on HbF levels are small compared to the variation seen in patients, suggesting that others are still to be found[95].

Sickle cell disease: methods to study SCD and screen for novel therapeutics

As noted previously, HU has been demonstrated to increase expression of HbF in some patients, and while the exact mechanism is unknown, there is evidence to suggest that it may act through the induction of stress erythropoiesis[96,97]. Even modest levels of HbF have a profound effect in preventing polymerization of hemoglobin[97]. Since HU has variable effects, and can induce *de novo* copy number variants even at low doses, constant monitoring is required in every patient[98,99]. Hence, the search for HbF inducing drugs is on-going. Traditionally, prior to testing in *in vivo* models, researchers test HbF inducing drugs in two different cell types: K562, an erythroleukemia cell line or primary CD34+ cells from mobilized peripheral blood. Unfortunately both *in vitro* models have limitations.

K562 cells are an erythroleukemic immortalized cell line with both the potential to differentiate into erythroid- and megakaryocyte-lineage cells[100]. Treatment of K562 cells with sodium butyrate[101] or hemin[102] leads to increased expression of embryonic and fetal hemoglobin, with little expression of adult hemoglobin. Although predominantly expressing fetal globin[103], this cell line has been widely used to study the therapeutic potential of HbF-inducing compounds[104–107]. Other commonly used human cells lines, such as KU812 and HEL cells, behave similarly to K562 cells, and also express primarily fetal and embryonic hemoglobin[108]. Collectively, these immortalized cell lines carry many chromosomal abnormalities, and in the

context of the large, diverse SCD population, represent the genetic background of single individuals, thus limiting the validity of findings.

To circumvent the issue of working with immortalized cell lines researchers also use primary $CD34^+$ cells, which are most commonly isolated from the peripheral blood of patients whom have received granulocyte-colony stimulating factor cytokine treatment and CXCR4 antagonist AMD3100[109,110] in order to mobilize their HSC population. This process yields variable degrees of HSC mobilization even within the same individual[111,112], is time consuming, expensive, invasive and reliant on having medical personnel available for the duration of the collection. While currently there is no evidence that mobilization can have long-term effects on the donor, further long-term studies are needed prior to researchers depending on these cells as a source for high-throughput drug discovery[112]. The main advantage of working with HSCs, defined as cells positive for the hematopoietic progenitor cell-surface marker CD34, is their ability to be differentiated into true adult erythroid cells with accompanying HbA expression. However, they have neither the capacity for extensive proliferation, nor uniform maturation with current culture methods. While one can look at a variety of individual responses using $CD34^+$ cells from peripheral blood they have a limited lifespan and require patients to undergo HSC mobilization treatment every time new cells are required for study. The standard differentiation process involves multiple phases, yielding limited cell numbers and restricting the ability to run high-throughput screens.

Despite the difficulties of working with these two cell populations, they are still being used to identify and validate many new drugs. Some of these drugs include HDAC inhibitors[113–116], DNA-binding drugs which modify the formation of DNA/nuclear protein complexes to control gene expression[117,118], and Cucurbitacin D (CuD)[119] a ROS/p38 MAPK pathway modulator. While these molecules have shown promising results in changing the chromatin status

of the β-globin locus to allow for HbF expression, or generating cells with HbF expression via stress erythropoiesis, very few of these drugs have progressed beyond the pre-clinical stages of drug development, perhaps due to the context in which they are tested for efficacy.

Mouse models of sickle cell disease

For many years transgenic mice have been used to study human hemoglobin switching and erythroid maturation. As murine hemoglobin expression is different from humans, replacement of murine globins with human isoforms is imperative for the *in vivo* understanding of human hemoglobin switching. Studies of the pathophysiology of SCD has been facilitated by the development of a number of mouse models that express either a mixture of mouse globins with HbS, a super-sickling hemoglobin (e.g., SAD, NY1, S-Antilles mice), or human globin chains exclusively (e.g., Berkeley, NY1KO mice). Currently the mouse for studying human fetal-to-adult globin switching is the Berkley-Townes mouse. This animal has all murine hemoglobins knocked out and replaced with overexpressed human versions resulting in murine globin promoters driving the expression of human *HBA* and HBB^{S}[120,121]. While these mice are incredibly useful for studying development, their inbred background prevents full recapitulation of expressed hemoglobin diversity seen in human populations. Therefore it is necessary to study multiple people's hemoglobin expression, not the single example given with the transgenic mouse models. Variability in hemoglobin expression can be observed in cells expressing HbA, which is incredibly difficult to achieve *in vitro*. To observe adult hemoglobin expression in cells produced *in vitro* in an *in vivo* model must be generated resulting in humanized mice *(addressed in further detail in chapter 3)*.

Induced Pluripotent Stems Cells (iPSCs)

Pluripotency and its capabilities

Reprogramming of somatic cells to a pluripotent state was originally achieved by the introduction of four transcription factors, Oct4, Klf4, Sox2 and c-Myc using a series of independent retroviral vectors[122] to produce cells called induced pluripotent stem cells (iPSC). Following the reproduction and extension of these studies in both murine and human cells[123,124], it is widely accepted that iPSC share many of the characteristics of embryonic stem cells (ESC), including gene expression profiles, epigenetic signatures and pluripotency[125–128]. iPSC and ESC are both examples of pluripotent stem cells, or cells that can give rise to all three germ layers. These cells have given scientists the ability to study disease progression outside of the patient, for these cells have the capacity to differentiate into any cell in the body. The directed differentiation of iPSC can reproduce the earliest stages of disease onset, a facet of disease progression not seen with conventional, transformed cell lines. With the ability to produce unlimited amounts of target cells and to differentiate into any cell type, iPSC have the potential to become a valuable tool for examining disease in the exact genetic context of the patient.

Derivation of pluripotent cells from patient samples

There have been many improvements to the methodology of iPSC generation, from individual to polycistronic viral vectors[129–131], to non-integrating viruses and DNA-free techniques[103,132–139]. iPSC can be generated from mature somatic cells such as skin, hair cells[140], and most recently, peripheral blood. The use of peripheral blood mononuclear cells in particular is favorable, as it only requires 4 mL to harvest sufficient numbers of mononuclear cells for the reprogramming process[137,140–143] **(Figure 1.8)**. Mononuclear cells can be expanded, frozen, shipped, and

reprogrammed to produce iPSC from patients worldwide. The practice of iPSC generation from peripheral blood mononuclear cells has the potential to facilitate the creation of large libraries of iPSC, from which researchers can model a plethora of diseases.

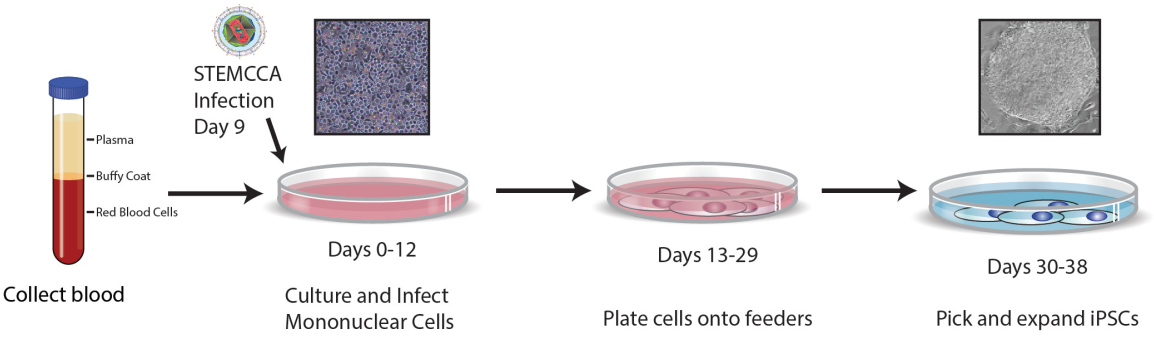

Figure 1.8. Schematic of the production of induced pluripotent stem cells (iPSC) from a peripheral blood sample using the STEMCCA reprograming cassette.

Disease modeling utilizing iPSCs

Disease modeling with iPSC: an overview

iPSC technology offers the prospect of an unlimited supply of material and is ideal for screening drugs against the genetic variations found in a patient population. It is also possible to obtain toxicity and efficacy data in multiple cell types from the same individual, all before human clinical trials[144–146]. Many steps must be taken before iPSC can become the dominant drug screening tool, including optimization of target cell differentiation, competent recapitulation of the disease *in vitro*, and creation of a scalable and automated assay for screening based on the disease phenotype[147]. These steps also depend on the ability to robustly and reproducibly generate high-quality cells, in both undifferentiated (iPSC) and differentiated (target cells) stages. Recently, iPSC have been used to model diseases as well as screen drugs for the treatment of

amyotrophic lateral sclerosis[148], spinal muscular atrophy[149], long QT syndrome[150], familial dysautonomia[151], familial TTR-amyloidosis[152]. Many researchers have already taken steps to demonstrate the efficacy of stem cell-generated cells in both modeling diseases and screening for novel therapeutics[153], thus initiating iPSC into the drug discovery phase of therapeutic development.

Drug screening with iPSC-derived cells

The utilization of iPSC for drug screening presents researchers with the opportunity to explore the effects of a drug on multiple cell types from the same individual, thus examining toxicity well before the initial phases of clinical trial. Common side effects seen during drug testing are due to toxicity damage of tissues of the peripheral nervous system, the liver, and the heart, making examination of these systems crucial for drug screening *in vitro*. Given the pluripotent nature and flexibility of iPSC, it is possible to create a complete "*in vitro* clinical trial" which would allow for both the testing of novel therapeutics in target cells as well as toxicity testing in peripherally affected tissues **(Figure 1.9)**. There are many researchers working on the optimal differentiation conditions to generate these cells and many have screened for toxicity in neurons[154], hepatocytes[155], and cardiomyocytes[150,156,157]. The ability to use iPSC for *in vitro* disease modeling, high-throughput drug screening, as well as drug toxicity screening, may ultimately help to reduce the timeline from the identification of novel therapeutics to FDA approval for treatment in patients.

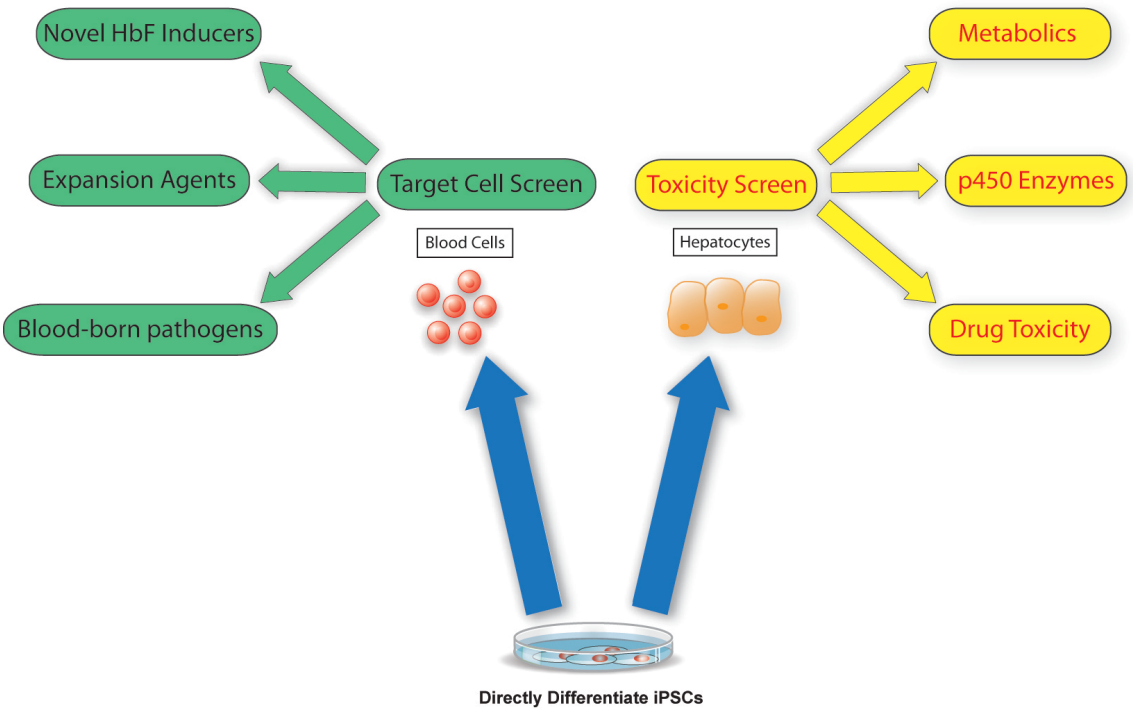

Figure 1.9. Drug screen with cells derived from iPSC allows for *in vitro* screening for both efficacy and toxicity.

In vitro disease modeling of SCD with iPSC

As the mutation for SCD is located on the β-globin gene, expression of HbA is required to view the disease phenotype *in vitro*. Most laboratory models for SCD express HbF, forcing researchers to induce a switch from HbF to HbA expression, a process that has proven elusive. Therefore, for many years, sickle cell researchers have primarily focused on two objectives; firstly, the creation of an *in vitro* model of sickle cell disease whereby HbS expressing cells can be produced and characterized, and secondly, the identification of novel pharmacological agents that are capable of HbF induction in HbS expressing cells. Both goals have been met with limited success. To date, the field is still lacking an *in vitro* model system that can produce sufficiently large numbers of adult red blood cells, and while potential novel therapeutics for SCD have been identified, HU is

still the only drug used in the clinic. The advent of iPSC has renewed vigor in pursuing these goals as the use of iPSC will permit researchers to examine multiple cell lines representing patients world-wide and strengthen our knowledge of how genetic variations result in variance in SCD pathophysiology and drug responsiveness **(Figure 1.10)**.

SCD is an ideal disease to model with iPSC because although all patients suffering with SCD share the same mutation, variability in the severity of the disease is common, illustrating the importance of visualizing SCD through a variety of genetic backgrounds. Traditionally the genetic complexity of SCD is explored by collection of PB-CD34+ cells from multiple individuals. These cells undergo multiple differentiation phases to produce enucleated RBC for analysis[119,158,159]. The difficult culture conditions for progenitor cell expansion and then subsequent specification and maturation[160–162], as well as the lack of markers for HSCs during this process impedes their use in large scale[119,163,164]. This is especially problematic when trying to model SCD pathophysiology within families, let alone worldwide.

Since the advent of ESC and iPSC technology, there has been interest in achieving efficient differentiation of pluripotent cells to RBC, particularly cells that express HbA. To achieve this researchers have employed numerous methods including, but not limited to, embryoid bodies[165–168], co-culture with stromal layers[169–171], and 2D feeder/serum free conditions[172–175]. Some of the most critical limitations of these methods are irreproducibility, the possibility of cross-species contamination, low cell numbers, and a lack of cells expressing HbA. 2D feeder/serum-free differentiation methodologies remove concerns regarding cross-species contamination seen with co-culture methods and the lack of reproducibility with embryoid body differentiation, but the production of cells in sufficient numbers still remains an issue. The use of an aryl hydrocarbon agonist for the efficient production of hematopoietic progenitors will be illustrated in Chapter 2. The ability to achieve large-scale expansion of a progenitor population in

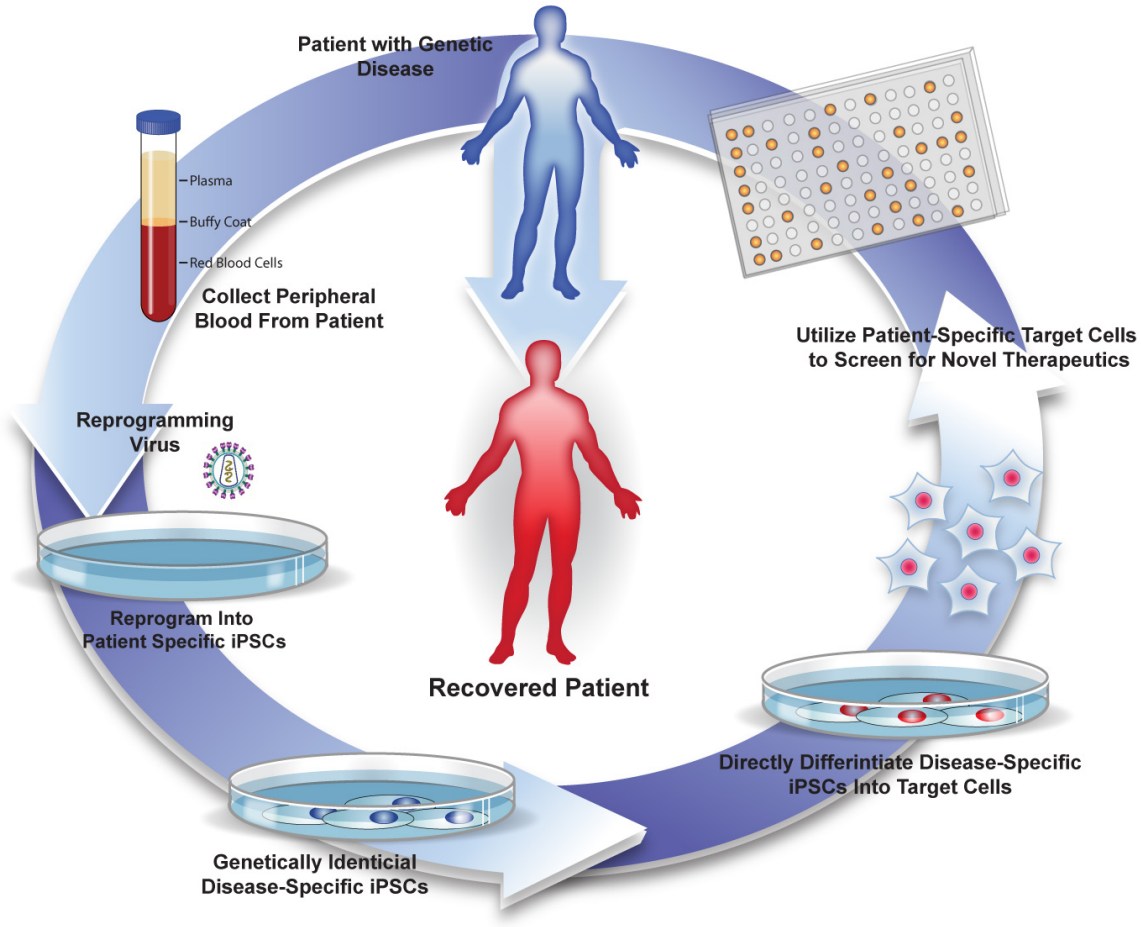

Figure 1.10. The potential of disease modeling with iPSC includes derivation and study of the affected cells as well as high throughput screening of potential therapeutics.

relatively short time frame suggests that progenitors generated in this way may be used as a staging-point for large-scale differentiation of iPSC-derivatives into the erythroid lineage. Even with the efficient derivation of large numbers of iPSC derived erythroid cells, these cells produce HbF and not HbA, suggesting they are a product of primitive hematopoiesis.

As seen with a variety of cell types, end-stage, *in vitro* differentiated cells produced from an embryonic source, such as ESC and iPSC, tend to predominantly express fetal proteins rather than adult proteins[176]. This has been observed in the erythroid lineage, where enucleated red blood cells primarily express HbF, rather than HbA[166,168,171,175,177–181]. It has been reported, however, that stem cell-generated red cell progenitors will enucleate and mature to express HbA when transplanted into recipient mice[182], suggesting that there are unknown factors, such as the proper niche or transcription factors that are required in order for hemoglobin switching to occur, and that a better understanding of final steps of *in vivo* hemoglobin switching may allow researchers to generate this switch *in vitro*.

Specific Aims

The goal of this project is to harness the directed differentiation of iPSCs to produce an unlimited supply of sickle cell disease-specific erythroid-lineage cells that can be utilized to study the expression of HbF. For this proposal, I will use a novel, excisable reprogramming vector able to generate clinical grade iPSCs free of any residual reprogramming transgenes. I propose to characterize erythroid lineage cells derived from multiple SCD-specific iPSC lines for hemoglobin expression, response to HU treatment, and their maturation capabilities. This system allows for the examination of differences in a variety of individuals with varying *in vivo* HbF levels, as well as the *in vitro* HbF response potential therapeutics.

CHAPTER 2:

MODULATION OF THE ARYL HYDROCARBON RECEPTOR DIRECTS HEMATOPOIETIC PROGENITOR CELL EXPANSION AND DIFFERENTIATION

Note: The majority of this chapter has been published in the journal Blood, April 2013. PMID 23723449

Brenden W. Smith,[1,2 *] Sarah S. Rozelle,[1,2 *] Amy Leung,[1,2] Jessalyn Ubellacker,[3] Ashley Parks,[3] Shirley K. Nah,[1,2] Deborah French,[4] Paul Gadue,[4] Stefano Monti,[5] David H. K. Chui,[1] Martin H. Steinberg,[1] Andrew L. Frelinger,[6] Alan D. Michelson,[6] Roger Théberge,[7] Mark E. McComb,[7] Catherine E. Costello,[7] Darrell N. Kotton,[2] Gustavo Mostoslavsky,[2] David H. Sherr,[3] and George J. Murphy[1,2]

*These authors contributed equally and should be viewed as co-first authors

1 Section of Hematology and Oncology, Department of Medicine, Boston University School of Medicine, Boston, MA;

2 Center for Regenerative Medicine, Boston University and Boston Medical Center, Boston, MA;

3 Department of Environmental Health, Boston University School of Public Health, Boston, MA;

4 Center for Cellular and Molecular Therapeutics, Children's Hospital of Philadelphia, Philadelphia, PA;

5 Section of Computational Biomedicine, Department of Medicine, Boston University School of Medicine, Boston, MA;

6 Center for Platelet Research Studies, Division of Hematology/Oncology, Boston Children's Hospital, Dana-Farber Cancer Institute, Harvard Medical School, Boston, MA;

7 Center for Biomedical Mass Spectrometry, Boston University School of Medicine, Boston, MA

Abstract

The evolutionarily conserved aryl hydrocarbon receptor (AhR), a member of the basic helix-loop-helix Per-ARNT-Sim family, has been studied for its role in environmental chemical-induced toxicity. However, recent studies now demonstrate that the AhR may regulate the hematopoietic and immune systems during development in a cell-specific manner. As a roadmap for assessing the possible role of the AhR receptor in hematopoietic cells, we performed an *in silico* analysis of transcriptional profiles of 71 primary human hematopoietic cell isolates which indicated AhR-upregulation at both the hematopoietic stem cell and bipotential hematopoietic progenitor (HP) stages. This result, together with the absence of an *in vitro* model system enabling production of large numbers of primary human HPs capable of differentiating into megakaryocyte- and erythroid-lineage cells, motivated us to determine if AhR modulation could facilitate both HP expansion and megakaryocyte and erythroid cell differentiation. Here we show that a functional AhR is expressed in hematopoietic cells at the HP stage of development. Our chemically defined, serum and feeder-free directed differentiation strategy employs a potent AhR ligand, which allows for the capture in culture and expansion of populations of HPs, megakaryocyte- and erythroid-lineage cells. Further modulation of the AhR in these cells directs cell fate, with AhR agonism permissive to erythroid differentiation and antagonism favoring megakaryocyte specification. These results highlight the development of a new platform for studying human red blood cell and platelet development, and demonstrate that the AhR plays a critical physiological and functional role in hematopoiesis.

Introduction

The aryl hydrocarbon receptor: environmental roles

The AhR is a member of the evolutionarily conserved Per/ARNT/SIM (PAS) family of transcription factors[183]. It is the only PAS family member activated by either endogenous or exogenous ligands. PAS proteins contribute to several important physiological processes[184–187]. When bound by a ligand, cytosolic inactive AhR is released from its chaperone complex and binds to the AhR nuclear translocator (ARNT) and translocates to the nucleus. The AhR/ARNT complex binds to a specific DNA sequence, TnGCGTG, known as both the dioxin or AhR response element (DRE or AhRE). Binding increases transcription of cytochrome P450 genes, CYP1A1 and CYP1B1, which are crucial for the metabolism of xenobiotic toxins for removal. AhR/ARNT signaling is repressed by also upregulating expression of the aryl hydrocarbon receptor repressor, which will compete for binding of ARNT, as part of a negative feedback loop **(Figure 2.1)**. Historically, the evolutionarily conserved AhR was studied in the context of its activation by a variety of ubiquitous environmental pollutants including dioxins, polychlorinated biphenyls, and polycyclic aromatic hydrocarbons, and subsequent transactivation of cytochrome P450-encoding genes[188–198] **(Figure 2.2)**. Recently, the AhR field has undergone a major paradigm shift following the demonstration that the AhR plays important physiological roles in the absence of environmental ligands[197–204].

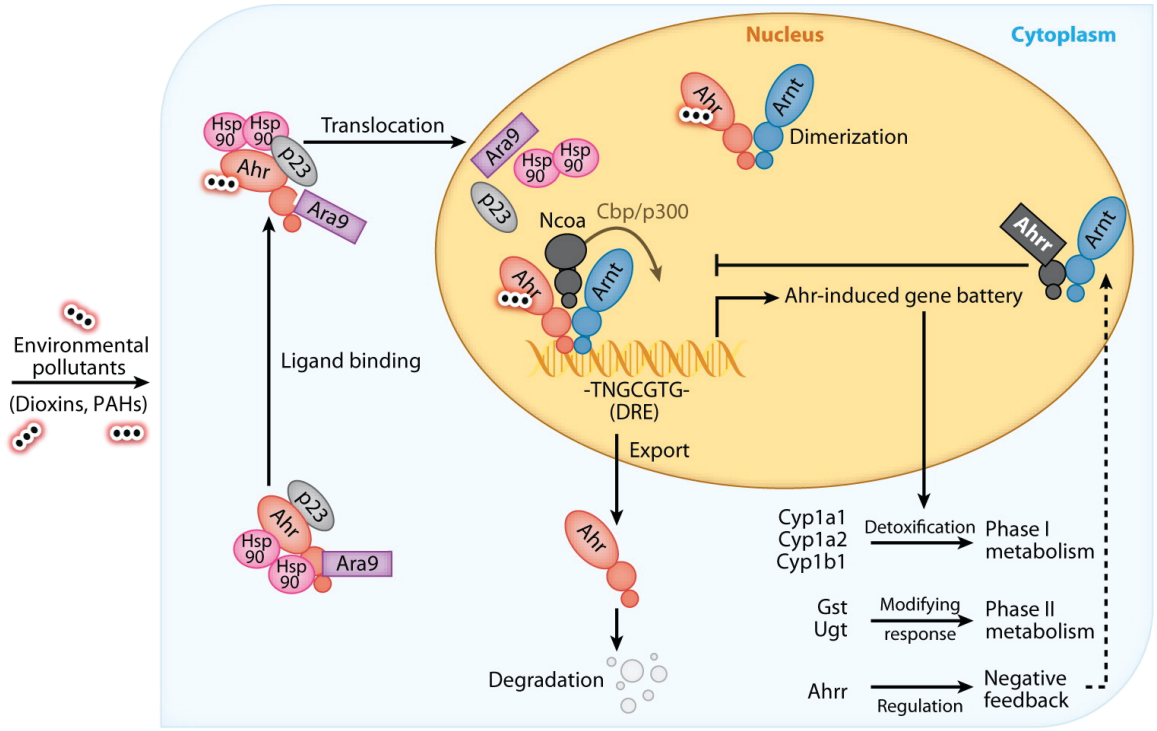

Figure 2.1. Ligand binding of the AhR induces a signaling pathway resulting in the upregulation of AhR specific gene targets. Upon ligand binding AhR dissociates from its cytoplasmic chaperone complex and binds the aryl hydrocarbon nuclear translocator (ARNT). This reveals a nuclear localization sequence that allows AhR/ARNT/ligand to enter the nucleus and bind to dioxin response elements (DRE), which results in the upregulation of gene expression of gene targets necessary for the metabolism of toxins. *McIntosh, BE, et al. Annu. Rev. Physiol. (2010) 72:625-645.*

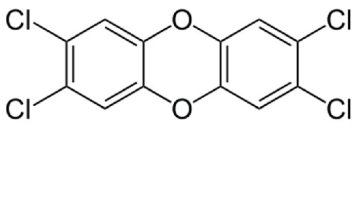

Polychlorinated dibenzodioxins
Dioxin, also known as TCDD

Polycyclic aromatic hydrocarbons
(PAH)

Polychlorinated biphenyls
(PCB)

Figure 2.2. Environmental toxins known to be AhR ligands. A common example of a polychlorinated dibenzodioxins is dioxin, also known as TCCD. Polycyclic aromatic hydrocarbons (PAH) can be found in atmospheric pollutants. Widely used as dielectric and coolant fluids in transformers, capacitors and electric motors, polychlorinated biphenyls (PCBs) are now banned in the United States.

The aryl hydrocarbon receptor: non-environmental roles

Several studies demonstrate that the AhR *contributes to regulation of* autoimmune responses[197,198,200–203,205], inflammation[203,206], cell growth[207], cell migration[208–210], apoptosis[211–214] and cancer progression[215–219]. Specifically with regard to hematopoietic cells, studies demonstrate that the AhR regulates development of Th17 cells, regulatory T cells subsets, and gut-associated T cells[197–204,220]. Importantly, recent breakthrough studies suggest that the AhR plays a critical role in nominal HSC growth and differentiation[160,221]. For example, $AhR^{-/-}$ mice are characterized by an increased number of bone marrow HSCs[221] and a commensurate increased propensity to develop lymphomas[222]. These insights led to the hypothesis that the AhR, activated by endogenous ligands, regulates stem cell growth and/or differentiation[223]. Despite these early results, little is known about the effects of AhR modulation on the development of Mk- or erythroid-lineage cells from bipotential progenitors. Involvement of AhR in this process is suggested by decreased numbers of erythrocytes and platelets in young $AhR^{-/-}$ mice and the

skewing of the blood cell repertoire towards myeloid and B lineage cells as $AhR^{-/-}$ mice age[221,224,225].

Development of blood lineages from a stem cell

The differentiation of HSCs into all eight blood cell lineages is a critical and tightly regulated physiological process[6]. Disruption of this regulation can have a profound downstream effect on multiple hematopoietic cell types, potentially leading to a myriad of blood cell disorders from leukemia to stem cell exhaustion[221,226,227]. However, definition of the molecular mechanisms that control specification of primary human blood cells has been hampered by the lack of a model system in which sufficient numbers of stem or progenitor cells can be grown and the absence of practical and efficient techniques for directing differentiation of hematologic progenitors into end stage cells. For example, several teams have published proof-of-principle examples of the derivation of megakaryocytes (Mk)[133,228,229] and erythroid-lineage cells[171,173,228] from embryonic stem cells (ESC) and induced pluripotent stem cells (iPSC). Many of the attempted methodologies have resulted in technically difficult protocols that produce insufficient yields for extensive studies. Development of a model system which results in robust expansion of these cell populations and with which molecular signals driving cell differentiation can readily be studied is needed.

Our conceptual approach to addressing this need was to mimic *in vitro* the natural sequences of blood cell development *in vivo* to derive the number and range of cells types needed for the creation of a genetically tractable iPSC-based platform. Key components of this new platform, as shown here, include the definition of feeder-free, chemically defined conditions under which megakaryocyte-erythroid progenitor cells (HPs) can be established and a stimulus (aryl hydrocarbon receptor/AhR hyper-activation) which results in a dramatic expansion of the HP population and the production of virtually unlimited numbers of Mk- and erythroid-lineage

cells from iPSCs. The *in vitro* system described herein allows the capture in culture and expansion of pure populations of HPs that exist transiently during *in vivo* development of end stage megakaryocytes and red blood cells. This platform allows unprecedented efficiency and consistency in the derivation of bipotential hematopoietic progenitors and their progeny from pluripotent stem cells using AhR modulation and reveals that AhR activity can drive bipotential progenitor cell fate, establishing the AhR as a key player in hematopoietic differentiation. In addition to demonstrating a critical role for the AhR in HP, Mk, and RBC development, the platform provides an important and genetically tractable system for studying blood cell differentiation at multiple, defined stages of development. The platform presented here represents a significant step towards the *in vitro* production of virtually unlimited numbers of therapeutic, patient-specific RBCs and platelets.

Materials and Methods

iPSC derivation and culture: iPSC derivation was achieved using the hSTEMCCA lentiviral vector as previously described[130,143].

Directed differentiation of iPSCs into hematopoietic cells: iPSCs were plated onto matrigel coated 6-well plates in iPSC media conditioned on iMEFs for 24 hours and supplemented with 2 ng/mL Rho Kinase Inhibitor and 20 ng/mL bFGF. After two days, iPSC media was replaced with media cocktails designed to initiate hematopoietic specification: *D0-1 media:* RPMI (Invitrogen A1049101) supplemented with 5 ng/mL hBMP-4 (R&D 314-BP-010), 50 ng/mL hVEGF (R&D 293-VE-010), 25 ng/mL hWnt3a (R&D 287-TC-500) and 10% KOSR; *D2 media:* RPMI supplemented with 5 ng/mL hBMP-4, 50 ng/mL hVEGF, 20 ng/mL bFGF and 10% KOSR; *D3 media:* StemPro 34 (Invitrogen 10639011), 5 ng/mL hBMP-4, 50 ng/mL hVEGF, and 20 ng/mL

bFGF; *D4-5 media:* StemPro 34, 15 ng/mL hVEGF, and 5 ng/mL bFGF; *D6 media:* 74% IMDM (Invitrogen 12330061), 24% Hams F12 (Mediatech 10-080-CV), 1% B27 supplement (Invitrogen 12587-010), 0.5% N2-supplement (Invitrogen 17502-048), 0.5% BSA (Sigma A3059), 50 ng/mL hVEGF, 100 ng/mL bFGF, 100 ng/mL hSCF (R&D 255-SC-010), 25 ng/mL hFlt3 Ligand (R&D 308-FKN-005); *D7 media:* 74% IMDM, 24% Hams F12, 1% B27 supplement, 0.5% N2-supplement, 0.5% BSA, 50 ng/mL hVEGF, 100 ng/mL bFGF, 100 ng/mL hSCF, 25 ng/mL hFlt3 Ligand, 50 ng/mL hTPO (Genentech G140BT), 10 ng/mL IL-6 (R&D 206-IL-010), 0.5 U/mL hEPOgen (Amgen) and 0.2 μM 6-formylindolo[3,2-b]carbazole (FICZ) (Santa Cruz SC300019). After Day 7, 0.5ml of Day 7 media was added to the culture daily without aspirating the media from the previous day. All base media mixes included 2 mM L-Glutamine (Invitrogen 25030081), $4x10^{-4}$ M Monothioglycerol (Sigma M1753), 100 mg/mL Primocin, and 50 μg/mL Ascorbic Acid. Cells in suspension were collected and assayed at Days 10-15 or split for long-term culture.

Methylcellulose assays: Non-adherent day 15 HPs were collected and plated in methylcult H4034 Optimum (Stem Cell Technologies, 4034) at a density of 56,000 cells per 3 mL of methylcult. The methylcult and cell mixture was plated in 35 mm culture dishes as per manufacture's instructions. Resultant colonies were scored on day 12 and classified as mixed, myeloid, or erythroid in origin.

Mass spectrometry analyses: Whole blood was diluted 1:500 in ESI buffer and analyzed directly. iPSC-derived erythroid-lineage cells were lysed with the addition of formic acid (0.8%) and the resulting solution was passed through a C18 spin column. Proteins were eluted with 60% acetonitrile/0.3% formic acid/water and assayed.

Megakaryocyte- and erythroid-lineage specification of HPs: Mk-lineage cells were generated from Day 15 HPs by first washing the cells and placing them in Mk specification media containing IMDM, 0.5% BSA, 10 mg/mL NTPs and dNTPs (Invitrogen), 40mg/mL LDL (Sigma L8292), 200 mg/mL human holo-transferrin (Sigma T0665), 10 mg/mL human insulin (Sigma I3536), 50 mM 2 ME, and 100 ng/mL human TPO. Erythroid-lineage cells were generated from Day 15 HPs by first washing the cells and placing them in erythroid specification media containing IMDM, 10% Plasmanate (Talecris Biotherapeutics Inc. NC27709), and 3 U/mL human EPO.

Lentiviral vector generation and application: PCR primers were designed to amplify the MMTV-DRE (mouse mammary tumor virus / dioxin response element region from the murine CY1A1 gene) promoter region from AHR activity reporter construct pGudLuc1.1, with integrated SpeI and NotI cut sites at the 5' and 3' ends respectively. The restriction enzyme digested PCR product was then inserted into the pHAGE2 lentiviral Ef1α-dsRed(NLS)-IRES-ZsGreen plasmid and the pHAGE2 lentiviral Ef1α-destabilized ZsGreen by excision of the Ef1α promoter and ligation of the SpeI and NotI digested MMTV-DRE. Additionally, the AHR repressor was cloned into the pHAGE2 lentiviral Ef1α-dsRed(NLS)-IRES-ZsGreen. Primers were designed to amplify the f.heteroclitus AHRR coding region from an HPV422-based construct, with NotI / BamHI cut sites incorporated at the 5' and 3' sites respectively. VSV-G pseudotyped lentivirus was packaged and concentrated as previously described. Cells were infected overnight and subsequent dsRed and ZsGreen gene expression was monitored by fluorescence microscopy and flow cytometry as indicated in the text.

AHR small molecule competition assays: 6-formylindolo[3,2-b]carbazole (FICZ), an AHR small molecule agonist, and CH223191, an AhR competitive inhibitor, were provided by David Sherr's laboratory. CH223191 was added to cultures at Day 6 at 5 mM (1x) and 2.5 mM (0.5x). 0.2 mM FICZ was added to cultures at Day 7 and media was added daily. DMSO was used as a vehicle control.

Quantitative RT-PCR: RNA was extracted using the RNeasy kit (Qiagen) according to the manufacturer's instructions and DNase treated using the DNA-free kit (Ambion AM1906). Reverse transcription into cDNA was performed using the High Capacity cDNA Reverse Transcription Kit (Applied Biosystems 4368814). Quantitative (real time) PCR amplification of cDNA was performed using Taqman probes for AHR (Hs00169233_m1), CYP1B1 (Hs002382916_s1), HBA (Hs00361191_g1), HBB (Hs00758889_s1), HBG (Hs01629437_s1), vWF (Hs00169795_m1), PF4 (Hs00427220_g1), NF-E2 (Hs00232351_m1) and CD62P (Hs00927900_m1) and run on the Applied Biosystems StepOne machine. Relative gene expression was normalized to B-actin (Hs99999903_m1).

Flow Cytometry: Roughly 10^5 cells were collected, spun, and re-suspended in 0.5% BSA in PBS. Samples were incubated for 30 minutes at ambient temperature with human antibodies including CD41a-FITC (BD 555466), CD235-PE (BD 555570), CD71-FITC (BD 555536), washed and spun at 3300 rpm for 7 minutes, and re-suspended in 0.5% BSA in PBS with 1 mg/mL Propidium Iodide. Samples were run on a BD FACScalibur using Cellquest Pro software and analyzed via FloJo 8.7. For ploidy analysis, cells were treated with 1.5% NP-40 (Boston Bioproducts P-872) and 62.5 mg/mL Propidium Iodide in PBS immediately before FACScalibur interrogation. For murine bone marrow, samples were first incubated for 5 minutes at ambient temperature with

murine conjugated antibody CD16/32 (BD 553142) before a 30-minute incubation with c-Kit-PE (BD 553355), CD41a-FITC (BD 553848), Ter119-PE (BD 553673). For cell viability assays, 2-3 x 10^5 cells were collected and resuspended in 8.8 mg/mL Hoechst 33342 in PBS supplemented with 5% FBS. Samples were then incubated in the dark at 37°C for 15 minutes, washed, and re-suspended in 1 mg/mL Propidium Iodide in 5% FBS. Samples were run on an LSR-II machine with FACSDiva software and analyzed via FloJo 8.7.

Gene expression analysis: The data analyzed correspond to the RMA-processed, batch-normalized, Affymetrix expression profiles downloaded from the dMap website (www.broadinstitute.org/dmap). This includes the expression levels of 8968 Entrez-annotated genes across 212 experiments representing 15 distinct populations (38 sub-populations) of hematopoietic cells. The data was projected onto the space of 37 manually curated AhR targets, plus AhR itself, and 72 experiments corresponding to 5 populations (11 sub-populations), defining the HSC-to-Mk/erythroid differentiation path. The genes were sorted based on hierarchical clustering with 1-Pearson correlation as the distance metric, and average linkage as the agglomeration rule[230] (Figure 1A). The normalized expression level of AhR within each cell population (sub-population) was computed and visualized by means of box-and-whiskers plots (Figure 1B). For each population, the plot reports the median (thick mid line), the middle half (the box), and the Interquartile Range (IQR, the distance between the "whiskers") of the distribution of AhR values. The difference in the expression level of AhR among cell populations was tested by standard analysis-of-variance (anova)[231].

Statistical Analysis: Results are presented as the mean ± the standard deviation of experiments performed in triplicate. Statistical significance was confirmed using the Student's t-test.

Results

Analysis of human hematopoietic cell differentiation genomic mapping (dMap) data suggests a role for AhR in normal hematopoietic specification

As a guide for assessing the possible role of the AhR receptor in hematopoietic cells, we analyzed the "dMap" dataset (www.broadinstitute.org/dmap)[232] a publicly available compendium of expression profiles from 71 distinct purified populations of human hematopoietic cells. For our purposes, we focused on the HSC-to-Mk/erythroid differentiation path and we analyzed the expression of a manually curated list of putative AhR target genes. Hierarchical clustering was carried out to evaluate the co-expression patterns of *AHR* and these genes. This analysis revealed up-regulated *AHR* mRNA expression in HSCs and MEPs **(Figure 2.3)**. Erythroid cells clustered into 2 groups. Earlier phase erythroid cells maintain elevated expression of the *AHR* and genes upregulated in MEPs. Later phase erythroid cells exhibited a largely reciprocal pattern. *AHR* levels were consistently upregulated in Mks. The levels of 21 genes, including several of considerable import to stem cells (e.g., *c-Myc*, *EGR1*, *ALDHA1*) were significantly correlated with *AHR* levels (false discovery rate $\leq$0.004). Other important hematopoietic-specific genes such as NFE2, a critical regulator of both the erythroid and

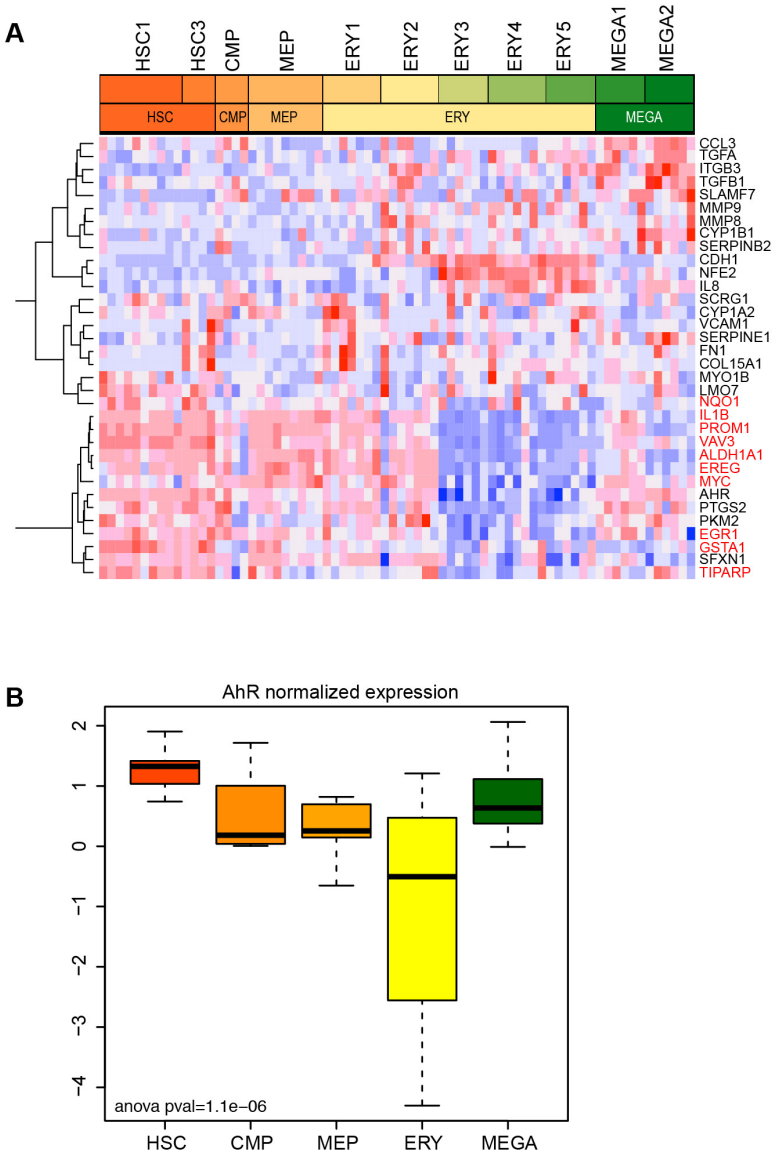

Figure 2.3. Analysis of human hematopoietic cell differentiation genomic mapping (dMap) data reveals a role for AhR in normal hematopoietic specification. (A) Computational analysis of comprehensive microarray data obtained through the Broad Institute's Differential Map Portal (dMAP). The genes were sorted based on hierarchical clustering with 1-Pearson correlation as the distance metric, and average linkage as the agglomeration rule[230]. (B) The normalized expression level of *AHR* within each cell population (sub-population) was computed and visualized by means of box-and-whiskers plots. For each population, the plot reports the median (thick mid line), the middle half (the box), and the Interquartile Range (IQR, the distance between the "whiskers") of the distribution of *AHR* values. The difference in the expression level of *AHR* among cell populations was tested by standard analysis-of-variance (anova)[231]. S. Monti contributed this figure.

Mk lineages were negatively correlated with *Ahr* expression. These results indicate that *Ahr* expression is evident in hematopoietic progenitor cells and suggest that the AhR may play

The aryl hydrocarbon receptor (AhR) agonist 6-formylindolo[3,2-b]carbazole (FICZ) allows for the exponential expansion of iPSC-derived HPs.

The clinical translation of iPSC-based technologies will require many modifications to improve the efficiency of generation and the safety profile of iPSC-derived cells. Using a novel, feeder cell-free, chemically-defined system for the production of hematopoietic progenitor cells from human iPSCs that is not beholden to the use of stromal cell lines or xenogeneic agents, our primary goal was the production of large numbers of clinically relevant, high purity hematopoietic cells. Our approach follows the roadmap provided by the developing embryo. Since ESC and iPSC resemble pluripotent, undifferentiated cells of the early blastocyst embryo, the signals active in the early embryo were harnessed to direct the differentiation of iPSC *in vitro*. Due to the known variability in the formation of human embryoid bodies[229], this protocol utilizes a 2D culture system optimized to produce bipotential hematopoietic progenitor cells within 10-15 days **(Figure 2.4A)**. Because of the expression of *AHR* mRNA early in the HP differentiation process **(Figure 2.3)**, a strong AhR agonist, FICZ, was added on Day 7.

In this system, differentiating iPSC produce an endothelial-like adherent layer from which non-adherent $CD45^+$ hematopoietic cells emerge beginning at Day 7 (data not shown). Days 7-15 are characterized by the rapid outgrowth of non-adherent cells **(Figure 2.4A and 2.5A)**. As judged by immunophenotyping at Day 15, greater than 50%

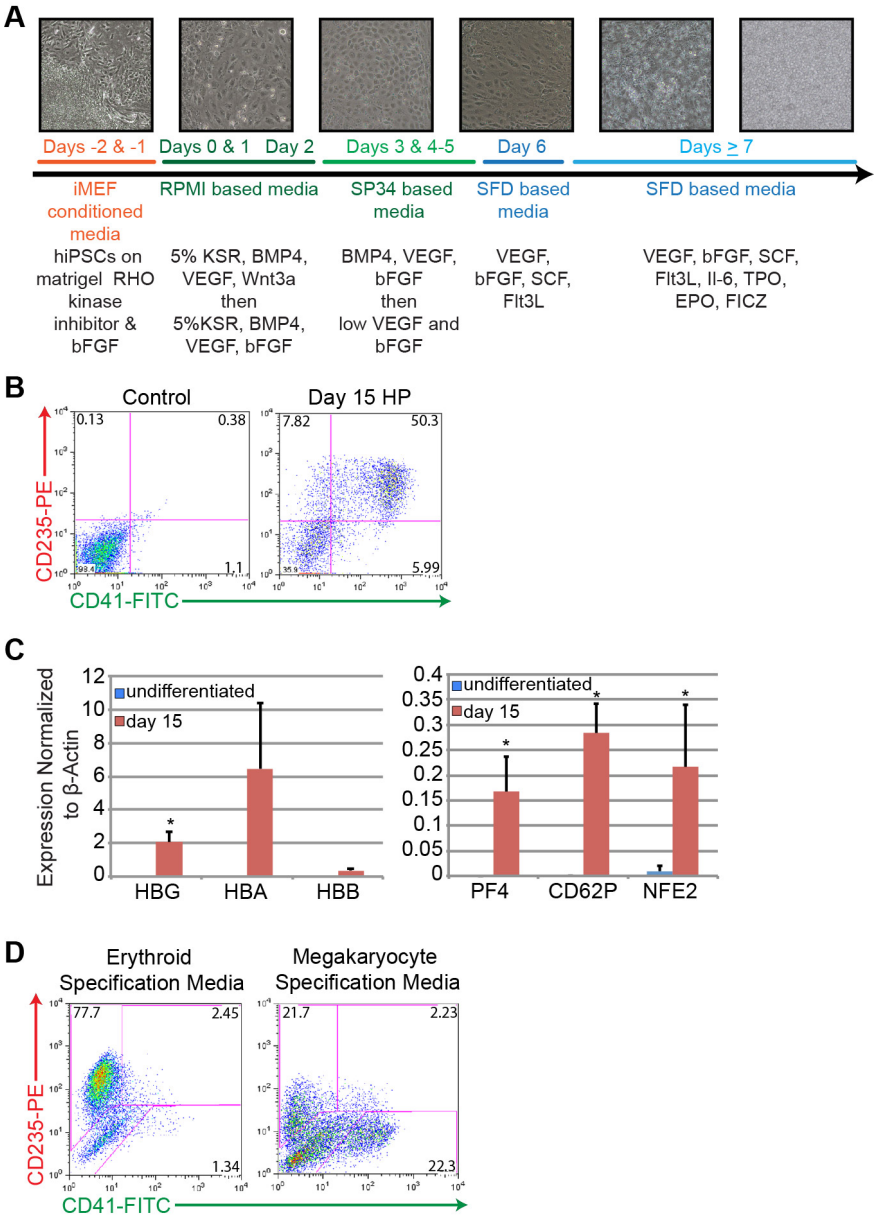

Figure 2.4. The feeder-free, chemically defined production of hematopoietic progenitor cells (HPs) from iPSCs produces populations of cells that express markers of both megakaryocyte and erythroid lineages. (A) Differentiation strategy from iPSC to HP stage. Phase contrast images (10x) of cultures depicting morphological changes and the production of both an initial adherent layer followed by non-adherent HPs. (B) Representative FACS analysis of Day 15 HPs that co-express CD235-PE (red cells) and CD41-FITC (megakaryocytes). (C) qPCR analysis of undifferentiated iPSCs vs. Day 15 HPs. Relative gene expression was normalized to β-actin. Data is the average of 3 independent experiments + SD. *P<.05. (D) Representative FACS analysis of Day 15 HPs that have been exposed to either erythroid- or megakaryocyte-specific specification media for 5 days. Results shown represent work done by both S. Rozelle (A, B, C) and B. Smith (D).

of these cells co-express CD235-glycophorin A (erythroid lineage) and CD41-integrin aIIb (Mk lineage) suggesting that bipotential HPs had been generated **(Figure 2.4B)**. When placed in colony forming assays, this total, unsorted population of cells produced roughly equal numbers of mixed, myeloid- and erythroid-lineage colonies suggesting the presence of bipotential HPs, as well as committed Mk- and erythroid-lineage cells **(Figure 2.5B)**. In comparison to undifferentiated iPSCs, these cells also significantly upregulate globin genes characteristic of erythroid-lineage cells and *PF4*, *CD62P*, and *NFE2* genes characteristic of Mk-lineage cells **(Figure 2.4C)**. Note that the timeframe to generate what phenotypically appear to be HPs is significantly shorter than that noted in previously described protocols[171,173] and that no fractionation or further manipulation of the cells is required. Importantly, maintenance of HP cultures in erythroid specification media containing EPO, or Mk specification media containing TPO, resulted in a final fate choice leading to the appearance of distinct populations of $CD235^+$ /$CD41^-$ erythroid- or $CD41^+$/$CD235^-$ Mk-lineage cells respectively **(Figure 2.4D)**. These results are consistent with the presence of functionally bipotential HPs.

A crucial roadblock in the translation of iPSC technology is the ability to produce sufficient, clinically relevant quantities of cells. Even for basic research studies, the numbers and quality of hematopoietic cells that can be produced through the directed differentiation of iPSC can be limiting[233]. With the outgrowth of HPs by day 15 of culture, we were presented with the possibility that ongoing AhR activation could continue to drive HP expansion. Here, we demonstrate that the AhR agonist FICZ has the ability to allow for the exponential expansion of iPSC-derived HPs. In comparison to

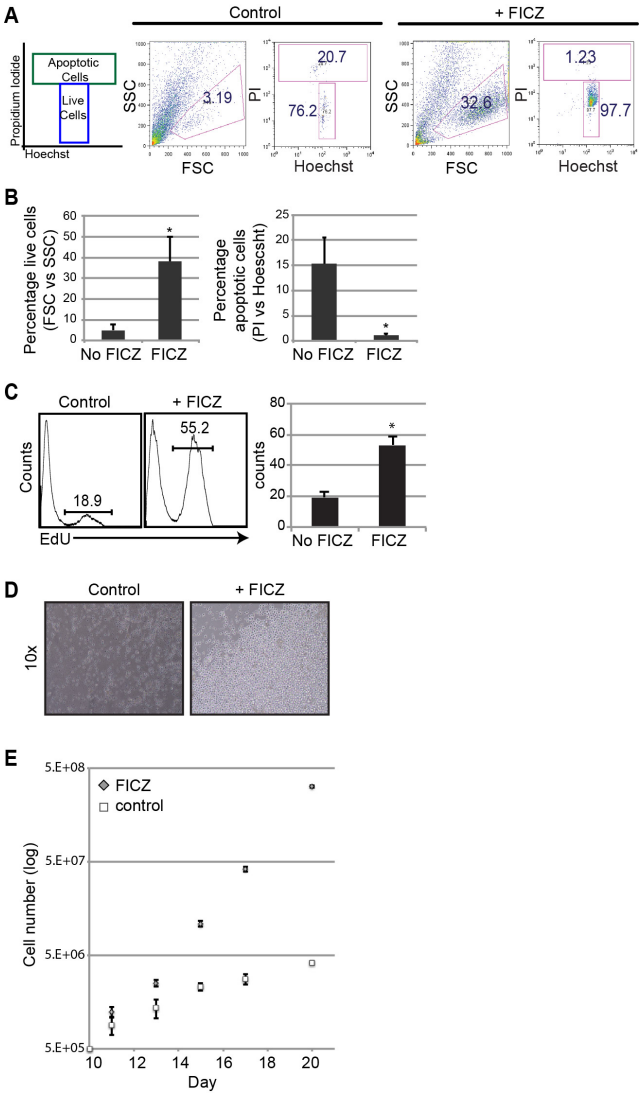

Figure 2.5. The aryl hydrocarbon receptor (AhR) agonist FICZ inhibits apoptosis and allows for the exponential expansion of iPSC-derived HPs. (A) Representative FACS analysis of live versus dead or dying cells (PI vs. Hoechst) from D15 HPs + FICZ. Plots were gated first in FSC vs. SSC and then from that population for PI+ and PI- Hoechst+. (B) FICZ increases the population of live cells as delineated by FSC and SSC and decreases the number of compromised or apoptotic cells. For the live cell gate, data is the average of 3 independent experiments + SD: *P<.01; For the apoptotic cell gate, data is the average of 3 independent experiments + SD: *P<.02. (C) EdU (5-ethynyl-2'-deoxyuridine) proliferation assay comparing D15 HPs + FICZ. Following FICZ stimulation at day 7, EdU incorporation into treated HPs was significantly increased compared to untreated controls indicative of increased proliferation. Data is the average of 3 independent experiments + SD. *P<.01. (D) Representative phase contrast images of HP population + FICZ. (E) Growth curve of D15 HPs + 0.2mm FICZ. Cells were counted manually using trypan blue exclusion. Graphical data and the associated statistics are the result of 3 independent experiments per group. Results shown represent work done by S. Rozelle (D, E), A. Leung (A, B), and G. Murphy (C, E).

untreated control samples, FICZ-treated HPs demonstrate significantly less cell death as judged by propidium iodide and Hoechst dye exclusion **(Figures 2.6A&B)**. In contrast to untreated cells in which 500,000 HPs yielded 4 million cells (8 fold increase), FICZ-treated day 15 HPs demonstrated logarithmic expansion such that FICZ treatment of 500,000 HPs yielded 300 million cells (600 fold increase) within 10 days **(Figure 2.6C)**.

AhR mediates the expansion and specification of bipotential hematopoietic progenitors

The results presented above strongly suggest that AhR hyper-activation drives human HP expansion. To further test this hypothesis, AhR expression and functionality in both undifferentiated iPSCs and differentiated HPs were investigated. Little or no AhR receptor protein was detected in human iPSC by Western blotting **(Figure 2.7A)**. However, a significant increase in expression of the prototypic AhR target gene, *CYP1B1* as seen by qPCR 72 hours after treatment with 0.2 μM FICZ suggesting that iPSC express AhR, but at levels below those detectable in Western blots **(Figure 2.7B)**. Similarly, AhR protein was not detected in day 15 HPs. However, treatment of day 15 HPs with FICZ significantly induced *CYP1B1* expression (**Figure 2.7B**). Similar data were obtained with two other AhR agonists, β-naphthoflavone (BNF) and the prototypic environmental AhR ligand, 2,3,7,8-tetrachlorodibenzo[p]dioxin (TCDD) **(Figure 2.8)**. In contrast to iPSCs or day 15 HPs, AhR was robustly expressed in day 30 and day 60 HPs **(Figure 2.7A)**.

To quantify baseline AhR transcriptional activity, presumably enforced by an endogenous AhR ligand, we cloned a human AhR-driven promoter[234,235] into a lentivirus reporter vector that encodes for dsRed and ZsGreen **(Figure 2.9A)**. This dual gene AhR-

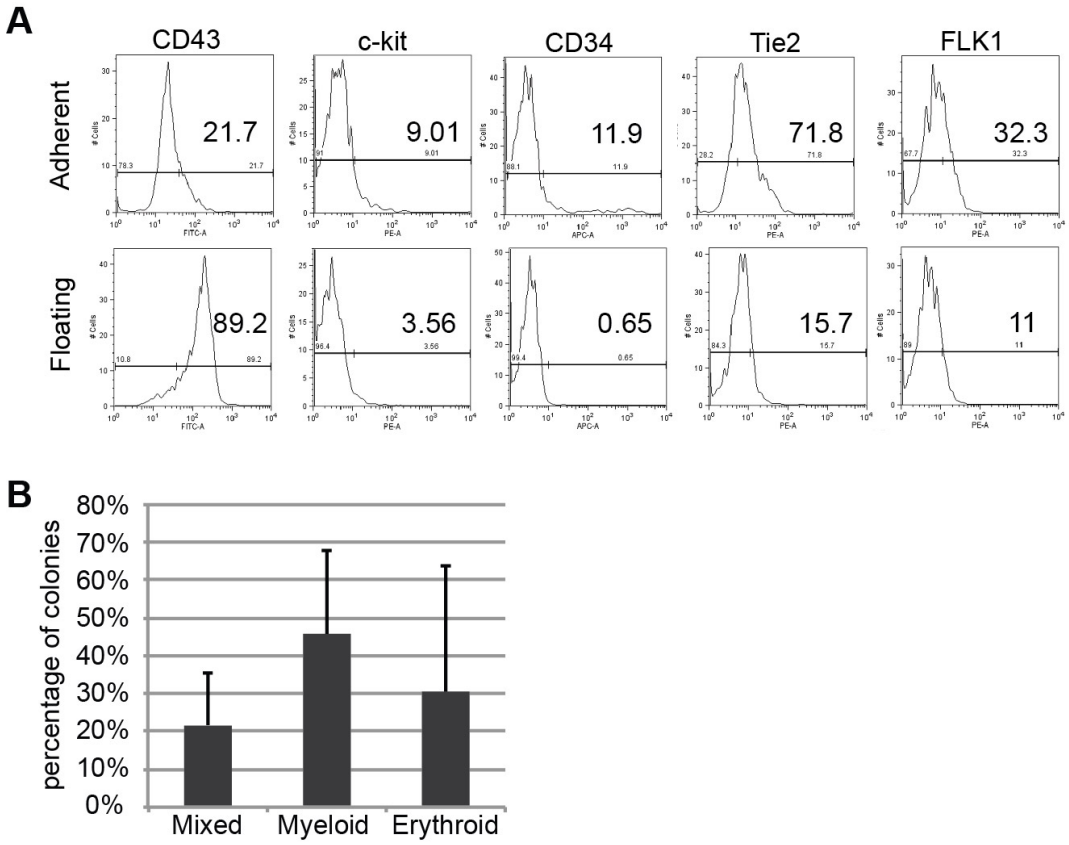

Figure 2.6. Characterization of early-stage iPSC-derived hematopoietic progenitor cells. (A) Flow cytometry characterization of adherent and floating cell populations in D12 hematopoietic cultures. The cells were examined for a panel of markers representing early-stage hematopoietic (CD43, c-kit, CD34) and endothelial markers (Tie2, KDR). These results indicate that floating cells are enriched for CD43 positivity, a marker of committed definitive hematopoietic progenitors, while the adherent layer contains a high proportion of cells positive for early hematopoietic markers c-kit and CD34, in addition to endothelial markers Tie2 and KDR. (B) Colony forming cell assays from unsorted D15 non-adherent cell populations in which 28,000 cells per assay were grown in methylcellulose with hematopoietic growth factors for 12 days. Data are averages of three independent experiments and graphed as a percentage of total colonies formed. (no statistical difference was noted between colony types). Results shown represent work done by A. Leung (A) and S. Rozelle (B).

driven reporter construct allowed for the normalization of transduction efficiency, correction for auto-florescence, and the quantification of baseline or FICZ-induced AhR transcriptional activity without bias for specific gene targets. Day 30 HPs were transduced with AhR-driven reporter lentivirus or mock infected at a multiplicity of infection (MOI) of 10 and grown in basal medium containing 0.2 μM FICZ for 72 hours. HPs were then subjected to three different growth conditions in order to assess the activity of AhR in this cell population: 1) the steady state condition consisting of cells maintained in 0.2 μM FICZ, 2) exposure to an increased FICZ concentration of 0.4 μM, or 3) growth in 0.2 μM FICZ but also in the presence of 5μM of a known AhR inhibitor, CH223191[236]. In contrast to the mock-infected HPs, the AhR-driven reporter-infected HPs displayed a modest increase in dsRed expression suggesting that the AhR responsive elements (AhREs) in the reporter were being transactivated in the HPs **(Figure 2.9B)**. An increase in the FICZ concentration to 0.4 μM significantly increased DsRed expression **(Figure 2.9B)**. These results are consistent with the induction of *CYP1B1* expression in primary HPs after FICZ exposure **(Figure 2.7B)**. Importantly, a significant decrease in DsRed expression (below the level of expression in the mock-infected populations) was noted when the reporter virus-infected cells, maintained in a basal level of 0.2 μM FICZ, were treated with 5 μM of CH223191 **(Figure 2.9B)**. Similar results were obtained using a lentivirus encoding an AhR-driven luciferase or green-fluorescent reporter (data not shown). These studies confirm the presence of a functional, FICZ-responsive AhR in human HPs.

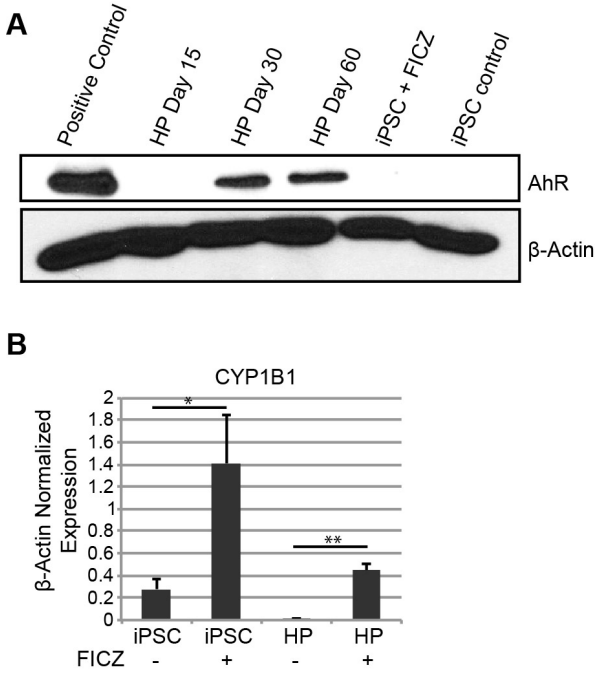

Figure 2.7. AhR agonist induces CYP1B1 target gene expression in human iPSCs and HPs. (A) Western blot analysis for AhR and β-actin protein expression in iPSCs and HPs. (B) qPCR data of iPSCs and Day 15 HPs with and without 0.2mm FICZ for 3 days. Expression is normalized to β-actin levels. Data is average of 3 independent experiments + SD. *P<.05, **P<.005. Results shown represent work done by J. Ubellacker and A. Parks (A) and B. Smith (B).

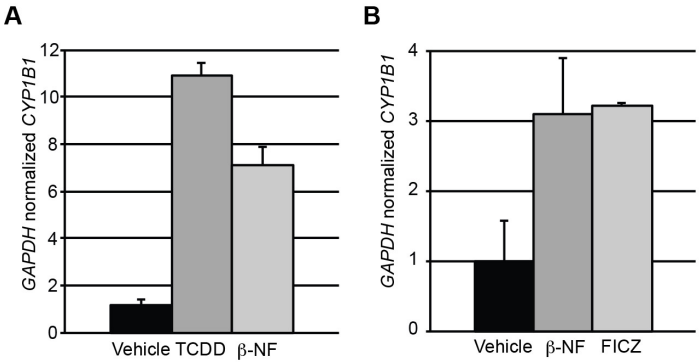

Figure 2.8. iPSCs and hematopoietic progenitor cells are responsive to a spectrum of AhR agonists. (A) RT-PCR analysis of CYP1B1 in iPSC treated with TCDD or β-NF for 4 days. Data are averages of duplicate wells + SE and values are normalized to GAPDH. (B) RT-PCR analysis of CYP1B1 in HP treated with β-NF or FICZ. Data are averages of two independent experiments + SE and values normalized to GAPDH. Results shown represent work done by J. Ubellacker and A. Parks.

In order to determine if FICZ-mediated transactivation of the AhR receptor was responsible for the exponential expansion of iPSC-derived HPs, the effect of AhR inhibition with CH223191 on cell viability and expansion of the HP population was tested. As previously shown in Figure 2, addition of 0.2 μM FICZ on day 7 of iPSC culture significantly increased the percentage of cells captured in the viable cell gate, as defined by forward and side scatter parameters (e.g., 15.5% vs. 8.09%) **(Figure 2.9C)**. However, treatment with 5 μM CH223191 one day prior to addition of FICZ completely blocked the increase in viable cells as measured either by forward and side scatter parameters or propidium iodide uptake. Furthermore, no significant expansion of HPs was seen in cultures treated with CH223191 plus FICZ (data not shown). These data indicate that AhR activation with FICZ mediates an increase in HP viability and drives expansion of HP populations. The efficacy of the CH223191 was confirmed by its ability to block *CYP1B1* induction as assayed by qRT-PCR **(Figure 2.9D)**.

Chronic AhR activation is permissive to erythroid cell maturation

Previous studies suggest that the AhR may play a critical role in hematopoietic cell development and function, possibly including the growth and differentiation of hematopoietic stem cells[160,189–191]. Having shown that AhR activation results in exponential expansion of HP populations **(Figure 2.6)**, and that the presence of EPO or TPO and FICZ generates either erythroid-lineage or Mk-lineage cells in the short term (**Figure 2.4D**), we then were in a position to determine if the AhR also contributes to HP differentiation into Mk- or erythroid-lineage cells over longer periods of time. To this end, HPs were cultured for extended periods of time (>120 days) in the presence of basal

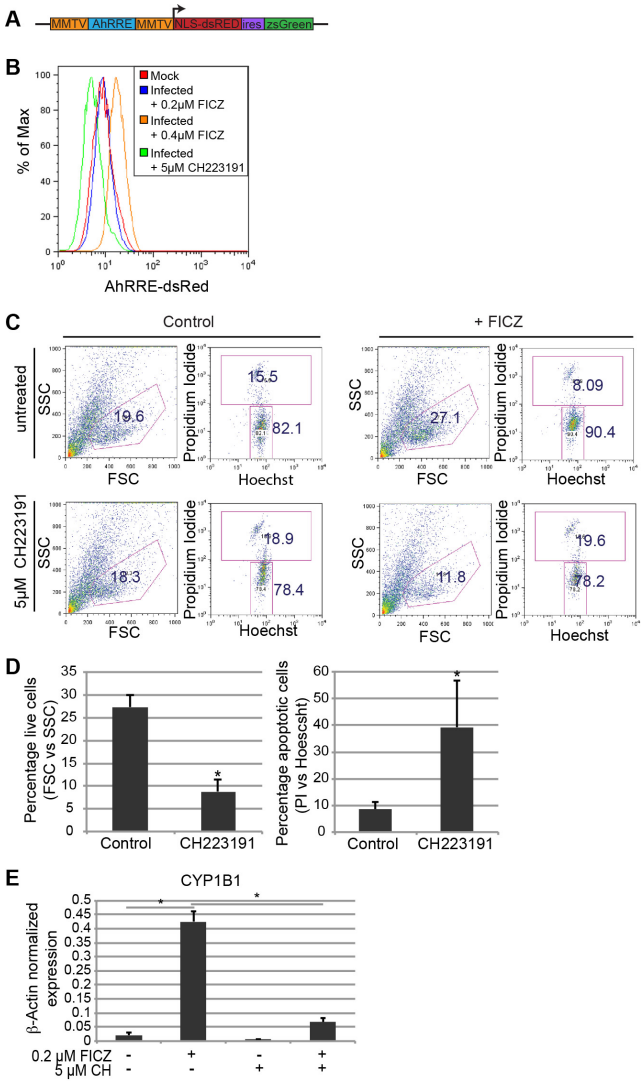

Figure 2.9. AhR mediates the expansion and specification of hematopoietic progenitor cells. (A) Schematic representation of pHAGE2 lentiviral reporter constructs that contain the mouse mammary tumor virus flanking the dioxin response element (MMTV-DRE-MMTV) driving the expression of NLS-dsRed (pHAGE2-MMTV-DRE-MMTV-NLS-dsRed-IRES-zsGreen) (B) Representative FACS analysis for DRE-dsRED in HPs infected with pHAGE2-MMTV-DRE-MMTV-NLS-dsRed-IRES-ZsGreen. Infected cells were untreated or treated with 5μM CH223191, or 0.4μM FICZ. (C) Representative flow cytometry dot plots of live versus dead cells (PI vs. Hoechst) from D15 HPs + FICZ and/or CH223191. For these experiments, HPs were pretreated with the known AhR inhibitor CH223191 at D6 before the addition of FICZ at D7. (D) Graphical representation of experiments performed in "C". For the live cell gate, data is the average of 3 independent experiments + SD: *P<.005; for the apoptotic cell gate, data is the average of 3 independent experiments + SD: *P<.04. (E) Expression of CYP1B1 as detected by qPCR of MEPs from "C". normalized to β-actin. Data is the average of three independent experiments + SD. *P<.005. Results shown represent work done by G. Murphy (B), A. Leung (A, B, C) and B. Smith (E) and S. Rozelle (B, E).

medium containing 0.2mM FICZ. Immunophenotyping of cell cultures maintained in these feeder-free conditions over a 60-day period revealed a progressive erythroid specification and maturation. As demonstrated in **Figure 2.10A**, the majority of early passage (Day 13) iPSC-derived HPs expressed CD71 (transferrin receptor) with a portion of the cells also expressing CD235 (glycophorin A) suggesting an immature erythroid cell phenotype. Under prolonged exposure to FICZ (30 days), these cells begin to downregulate CD71 and a larger percentage of cells express CD235 suggesting a more mature phenotype **(Figure 2.10A)**. By day 60 most (~70%) of the cells are $CD235^{+}/CD41^{-}$ indicating specification to the erythroid lineage under our basal growth conditions **(Figure 2.10B)**. These populations of iPSC-derived erythroid-lineage cells demonstrate functional maturity as assessed by their ability to respond to hypoxia **(Figure 2.10C)**. For example, when cultured under low oxygen concentrations (5% O_2) to simulate stress erythropoiesis, cells display hallmark characteristics of maturing erythroblasts including a reduction in cell size and the condensation of chromatin within the nuclei of the cells **(Figure 2.10C)**. More strikingly, when cells are centrifuged, bright red pellets can be seen indicating the production of hemoglobin **(Figure 2.10D)**. In contrast to peripheral blood cells, which only express α-globin and β-globin (forming the most common form of hemoglobin in adult humans), iPSC-derived erythroid-lineage cells express α-globin, γ-globin (fetal), as well as two embryonic globins (ζ- and ε-globin) as judged by mass spectrometry analysis **(Figure 2.11)**. These results, as well as the lack of adult β-globin in this population suggest that iPSC-derived erythroid-lineage cells are at an embryonic/fetal developmental stage.

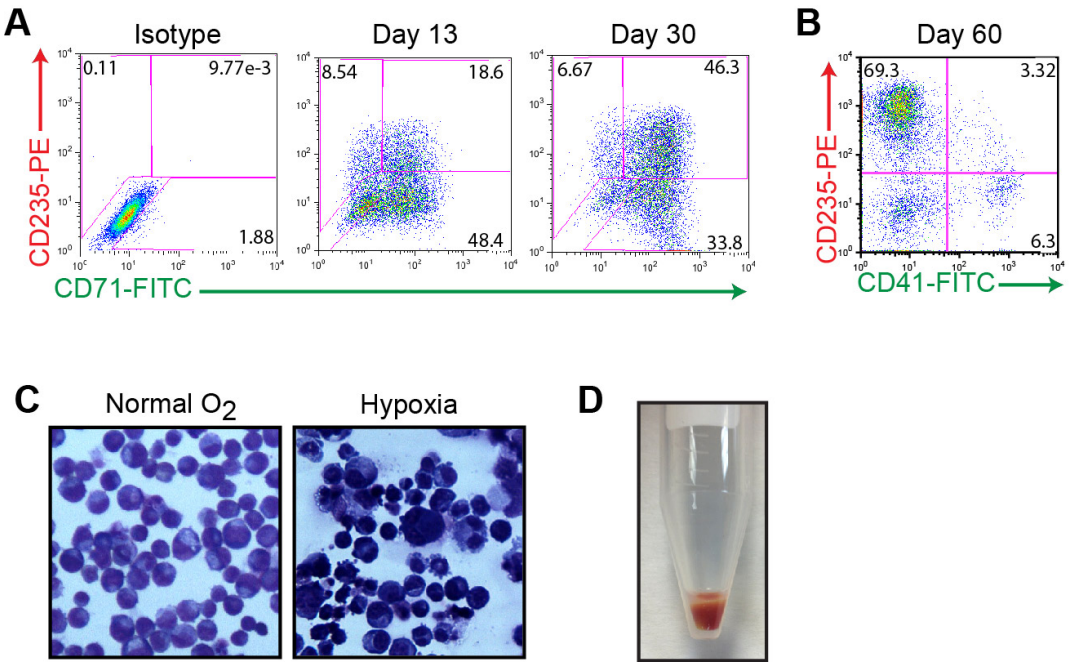

Figure 2.10. Continuous AhR activation is permissive to erythroid cell maturation. (A) Representative FACS analysis of cells co-expressing two hallmark markers of the erythroid lineage: CD71-FITC (transferrin receptor, early) and CD235-PE (glycophorin a, late) at days 15 and 30 of specification. (B) Representative FACS analysis of cells co-expressing CD235-PE and CD41-FITC demonstrating that by day 60, virtually all of the cells are committed to the erythroid lineage. (C) Wright-Giemsa staining of D30 erythroid-lineage cells pre- and post-exposure to hypoxic conditions demonstrating decreased size and condensed chromatin under low oxygen conditions. (D) Hemoglobin expressing cell pellet of iPSC-derived erythroid-lineage cells. Results shown represent work done by S. Rozelle.

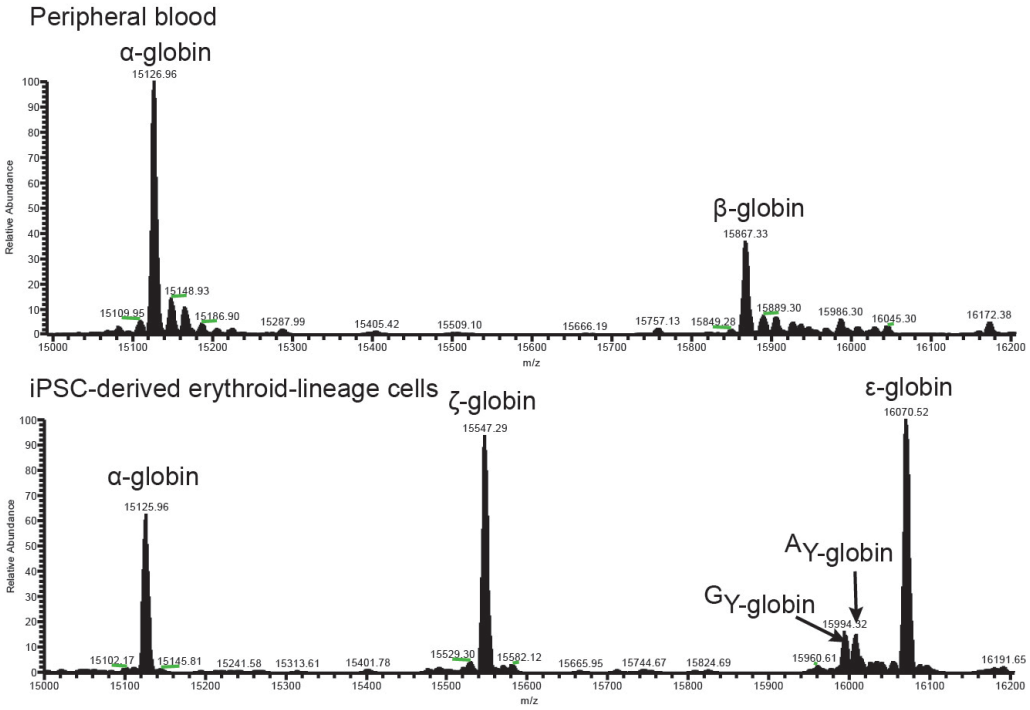

Figure 2.11. iPSC-derived erythroid-lineage cells express a spectrum of embryonic and fetal globins. (A) Mass Spectrometry analysis of human peripheral blood in comparison to D30 iPSC-derived erythroid-lineage cells. In contrast to peripheral blood cells, which only express a-globin and b-globin (forming the most common form of hemoglobin in adult humans), iPSC-derived erythroid-lineage cells express α-globin, γ-globin (fetal), as well as two embryonic globins (ζ- and εε-globin). These results, as well as the lack of adult globin (β-globin) in this population suggest that iPSC-derived erythroid-lineage cells are at an embryonic/fetal developmental stage. Results shown represent work done by S. Rozelle and analyzed by R. Théberge.

AhR repression promotes megakaryocyte specification

As the default pathway in our system seemed to allow for the specification and maturation of iPSC-derived HPs into the red cell lineage under chronic AhR agonism, we hypothesized that AhR downregulation in these long-term cultures might allow for the emergence of the alternative lineage, megakaryocytes. To test this hypothesis, we evaluated the effects of AhR inhibition with ectopic expression of an AhR reporter plasmid previously shown to block human AhR transcriptional activity[237,238]. We constructed and utilized a lentiviral vector that encoded an AhR

repressor element (AhRR) along with a ZsGreen reporter **(Figure 2.12A)**. This AhRR element potently and specifically inhibits either baseline or AhR agonist-induced AhR transcriptional activity[237,238]. In contrast to cells transduced with a control ZsGreen reporter, cells infected with the AhRR-ZsGreen lentivirus and cultured for 5 days produce a significantly higher number of large, $CD41^+$ Mk-lineage cells **(Figure 2.12C&D)**. Interestingly, while the AhRR-transduced populations were capable of producing Mk-lineage cells, they also contained fewer $CD235^+$ cells, suggesting that AhR antagonism initiates a transcriptional switch from erythroid to megakaryocyte lineage specification **(Figure 2.12C)**.

To further study the Mk-lineage cells produced via AhR antagonism, a discontinuous BSA gradient (0, 1.5, 3%) was used to isolate mature Mks from AhRR-ZsGreen-transduced populations. In contrast to the ZsGreen-$AhRR^-$ population, the majority of the ZsGreen-$AhRR^+$ population was positive for a combination of two hallmark Mk lineage markers, CD41a and CD42b **(Figure 2.12D)**. These cells also demonstrated hallmark characteristics of mature Mks including lobular nuclei and membrane blebbing at the surface of the cells **(Figure 2.13A)** and the ability to endoreplicate to 8N and 16N **(Figure 2.13B)**. Quantitative PCR analysis of these cells also revealed robust upregulation of a spectrum of Mk-related genes including GPV, GPIIb, PF4, and CD62P **(Figure 2.13C)**. Functionality of iPSC-derived Mks was assessed by their ability to produce platelets. Mature Mks were grown on an OP9 stromal layer for 3-5 days to allow for terminal Mk differentiation and platelet production.

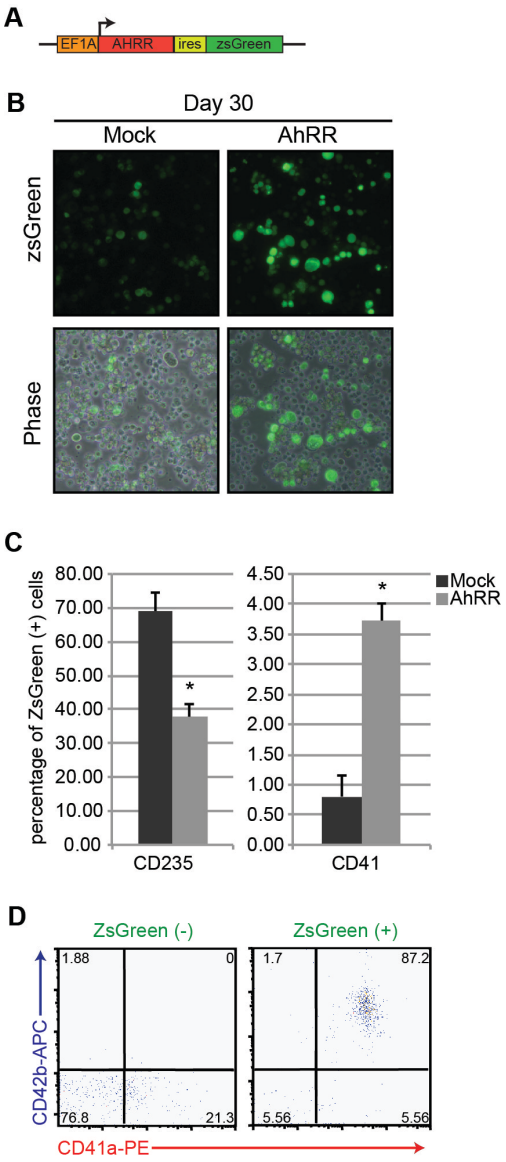

Figure 2.12. AhR repression promotes megakaryocyte specification. (A) Schematic representation of a pHAGE2 lentiviral reporter construct containing the AhR repressor (AHRR) and ZsGreen under the control of the constitutive promoter Ef1α (pHAGE2-Ef1α-AHRR-IRES-ZsGreen). (B) Phase and fluorescent images of D30 HPs following infection with a constitutively active ZsGreen control virus or pHAGE2-Ef1α-AHRR-IRES-ZsGreen. Large cells (megakaryocytes) are noted in the populations infected with the AHRR. (C) Graphical representation of the percentage of ZsGreen+ cells that express CD235 (erythroid lineage) or CD41 (Mk lineage) following mock or AhRR infection. Data are presented as means of three independent experiments + SD. *P<.005. (D) FACS analysis of AhRR-ZsGreen negative vs. positive fractions for hallmark megakaryocyte markers CD41a/CD42b. Results shown represent work done by G. Murphy and B. Smith.

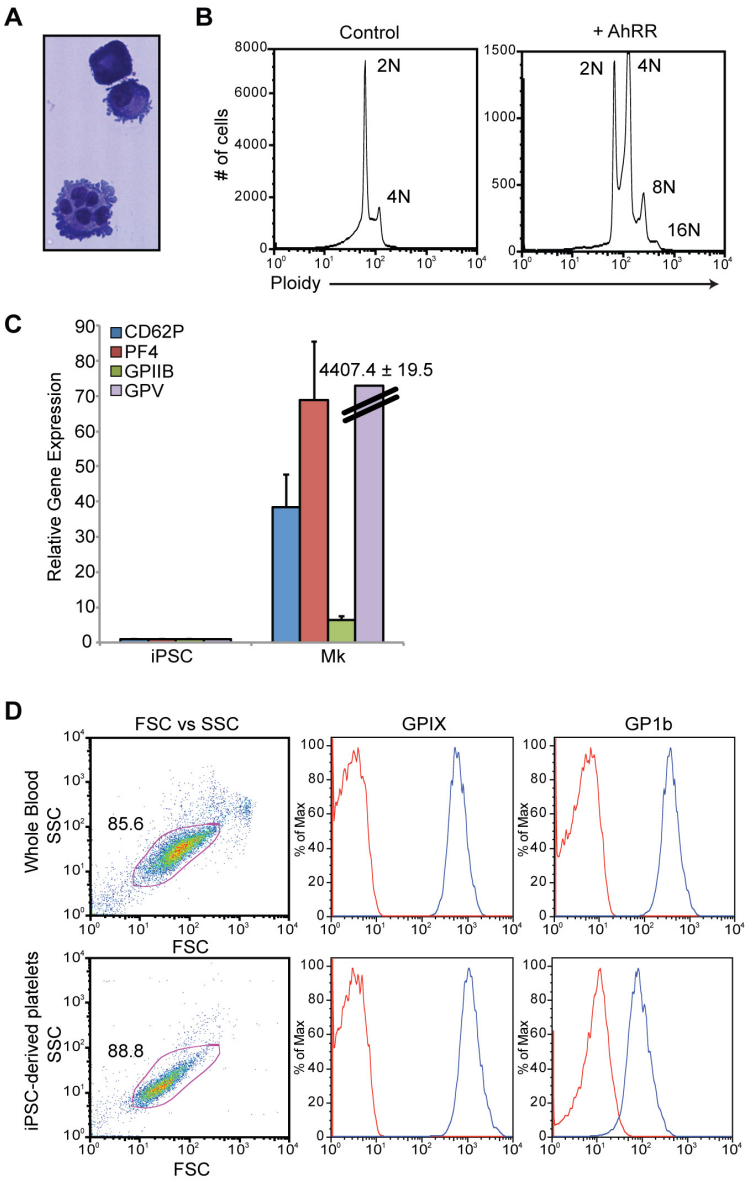

Figure 2.13. Characterization and functional analyses of iPSC-derived Mk-lineage cells. (A) Wright-Giemsa stain of megakaryocytes produced via AhR antagonism. (B) Ploidy analysis of iPSC-derived megakaryocytes demonstrating endoreplication. (C) qPCR analysis comparing undifferentiated iPSCs and iPSC-derived Mks for a spectrum of Mk-specific markers. Expression is normalized to β-actin levels. Data is average of 3 independent experiments + SD. (D) FACS analysis comparing platelets in whole blood to iPSC Mk-derived platelets. Mature Mks were grown on an OP9 stromal layer for 3-5 days to allow for terminal Mk differentiation and platelet production. Cultures were initially gated using GPIIb (CD41a) expression and demonstrated that iPSC Mk-derived platelets were similar to platelet populations from whole blood with respect to size (FSC), granularity (SSC), as well as the expression of GPIX and GP1b, two subunits of the GPIb/V/IX complex, that are characteristic of platelets. Results shown represent work done by B. Smith.

Cultures were initially gated using GPIIb (CD41a) expression and demonstrated that iPSC Mk-derived platelets were similar to platelet populations from whole blood with respect to size (FSC), granularity (SSC), as well as the expression of GPIX and GP1b, two subunits of the GPIb/V/IX complex, which are characteristic of platelets **(Figure 2.13D)**.

AhR agonism promotes HP production and expansion in murine bone marrow

To determine if AhR agonism would result in HP production and expansion from bone marrow precursors in a murine system, red cell-depleted, bone marrow from C57BL/6 mice was cultured for 3 days in the presence or absence of vehicle or 0.2 mM FICZ. Remarkably, in contrast to vehicle-treated controls, distinct populations of primary, $Ter119^+$ erythroid-lineage cells and $CD41^+/Ter119^+$ HPs were noted in the cultures following just 3 days of FICZ treatment **(Figure 2.14A)**. Interestingly, a statistically significant decrease in $cKit^+$ progenitor cells was noted in FICZ treated populations along with highly statistically significant increases in erythroid-lineage cells and HPs **(Figure 2.14B)**.

The AhR agonist FICZ is active in vivo and results in increased platelet counts in normal mice

It is possible that FICZ, a photo-metabolite of tryptophan, plays a role in regulating hematopoiesis *in vivo*. To determine if FICZ treatment on whole animals would affect

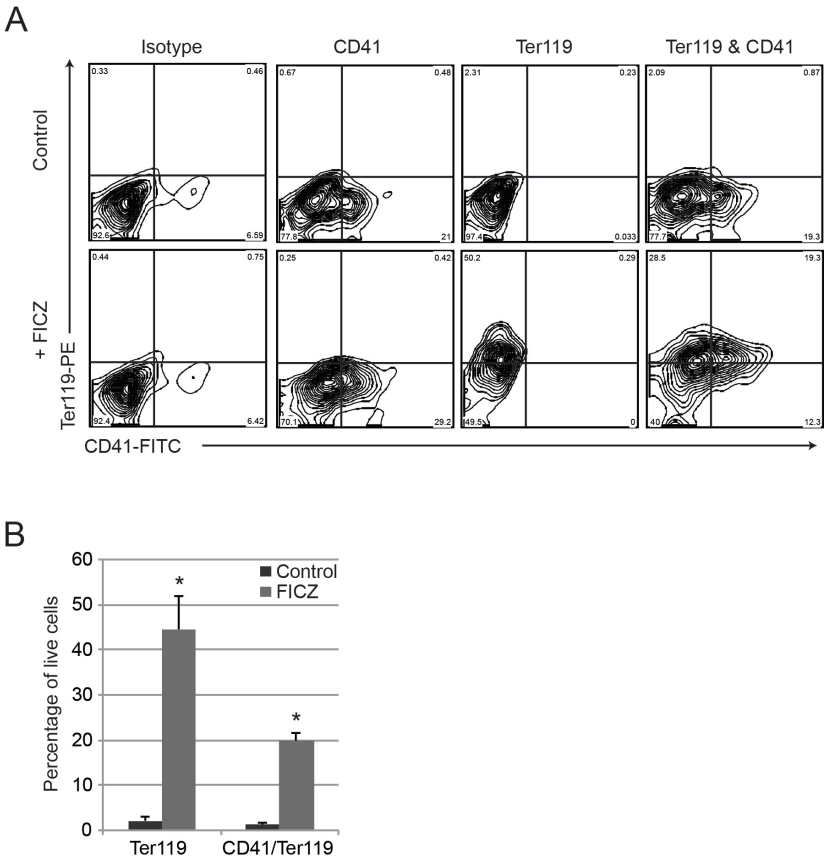

Figure 2.14. AhR agonism decreases c-kit expression in murine MEPs. (A) Representative FACS analysis of red cell depleted C57B6 bone marrow grown for 3 days under basal murine growth conditions +/- 0.2 mM FICZ. 1 x 10^5 cells were initially treated with CD16/32 Fc receptor block, followed by a directly conjugated monoclonal antibodies for cKit. (B) Graphical interpretation of FACS analysis for cKit (p=0.009) with or without the addition of 0.2 mM FICZ. Results are representative of three independent experiments + SD. Results shown represent work done by G. Murphy.

RBC or platelet production, C57Bl6 mice were injected daily intraperitoneally with FICZ suspended in vegetable oil using a weekly dose escalation scheme (Week 1: 1mg/kg; Week 2: 2mg/kg; Week 3: 4mg/kg). In contrast to mock-injected mice or mice injected with vehicle only, mice injected with FICZ showed increased platelet counts, as assayed by Hemavet quantification of peripheral blood bleeds, at all 3 time points (Day 7, 14, and 21) **(Figure 2.15A)**. Interestingly, a mouse that was immediately exposed to higher doses of FICZ (4 mg/kg) and did not undergo week 1 escalation demonstrated a more immediate and prolific platelet response. None of the mice in the study showed significant variations in either white blood cell (WBC) or red blood cell (RBC) counts (not shown). Following the 3-week time point, mice were sacrificed and livers and spleens harvested. Quantitative RT-PCR analyses for *CYP1B1* target gene expression revealed robust upregulation in the liver and spleen of FICZ treated animals confirming that we had reached biologically meaningful FICZ doses *in vivo* **(Figure 2.15)**. While agonism in an *in vitro* system promotes erythroid cells development, *in vivo,* AhR may interact with other factors affecting different signaling pathways than *in vivo*, allowing for an increase in platelets instead.

Collectively, the *in vitro* data suggest that production of erythroid-lineage cells is the default *in vitro* pathway of HPs chronically stimulated with an AhR ligand. Inhibition of that default pathway results in an increase in the percentage of Mk-lineage cells, an outcome that could reflect either a switch in cell fate decision to favor Mk production or the maintenance of a small population of Mks during a decrease in the production of AhR-dependent erythroid-lineage cells **(Figure 2.16)**.

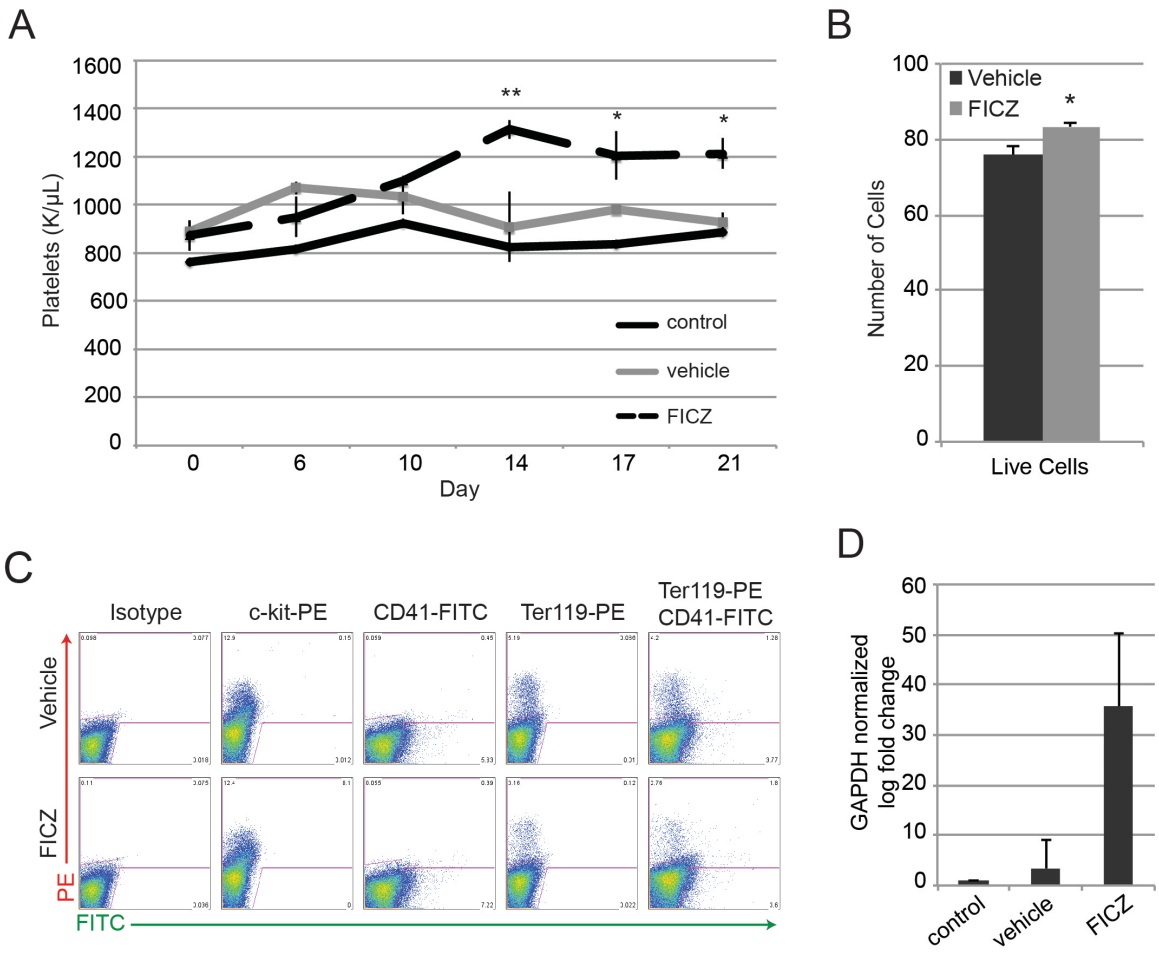

Figure 2.15. The AhR agonist FICZ is active *in vivo* and increases platelet counts in normal mice. (A) C57B6 mice were injected daily intraperitoneally with FICZ suspended in vegetable oil at a dosage of 4mg/kg. In contrast to mock-injected mice or mice injected with vehicle only, mice injected with FICZ showed increased platelet counts, as assayed by Hemavet quantification of peripheral blood bleeds, with statistically significant increases seen at days 14 (P=.002), 17 (P=.02), and 21 (P=.01) (B) Bone marrow from all mice was harvested at day 21, and following red blood cell depletion, samples were analyzed for viability (via propidium iodine staining) and immunophenotyped. In contrast to vehicle treated mice, the bone marrow cells of FICZ treated mice displayed a statistically significant increase in cell viability (P=.03) (C) Representative immunophenotyping of the bone marrow of all mice using a panel of hematopoietic markers revealing no noticeable differences between FICZ treated mice and vehicle treated controls. (D) Livers were harvested from sacrificed mice to confirm AhR activity in vivo. Quantitative RT-PCR analyses for CYP1B1 target gene expression normalized to GAPDH revealed robust upregulation in the livers of FICZ treated animals. Results shown represent work done by G. Murphy and S. Rozelle.

Discussion

Our results suggest that that AhR has a physiological and functional role in normal hematopoietic development, and that modulation of the receptor in bipotential hematopoietic progenitors can direct cell fate. We demonstrate a novel methodology for the directed differentiation of pluripotent stem cells in serum and feeder-free defined culture conditions into HPs capable of final specification into Mk- and/or erythroid-lineage cells.

As a starting point for these studies, we utilized human hematopoietic cell differentiation genomic (dMap) array data as a roadmap for assessing the possible role of AhR in hematopoietic cells. These analyses suggested that the AhR plays an important role in blood cell development and were consistent with previous studies[160,221,224,239].

In our studies, we have found that the use of a non-toxic aryl hydrocarbon receptor agonist in a directed differentiation scheme dramatically increases the number of HPs and resultant cells. This is an important finding in that traditionally, the evolutionarily conserved AhR has been studied for its role in environmental chemical-induced toxicity, and in our system it is shown to be involved in the growth and the differentiation of at least two crucial blood cell types. Following the addition of the potent AhR ligand FICZ to our cultures, we observed exponential expansion of HPs from a few thousand to 100 million cells in fewer than two weeks. Importantly, the role of AhR in the HP population was confirmed using a highly specific AhR inhibitor. This logarithmic expansion of cells appears to be a function of decreased cell death and is consistent with previous studies which suggest that the AhR can control apoptosis[211–213].

It is important to note that these results can be contrasted with work performed by Gasciewicz *et al*. in which AhR activation leads to exhaustion of the HSC pool as opposed to hematopoietic cell expansion. This apparent contradiction could reflect different stages in hematopoiesis (HSCs vs. HPs) or the nature of the ligand. Interestingly, while the exposure of

murine bone marrow to AhR agonism resulted in increased numbers of erythroid-lineage cells and HPs, a decrease in cKit^{+} progenitor cells was also noted perhaps suggesting a preferential switch to bipotential progenitor fate. Considerable evidence also indicates that functional outcomes may differ when using different AhR ligands, for example TCDD vs. FICZ[208].

Interestingly, FICZ, the AhR ligand utilized throughout this work, is a photo-metabolite of tryptophan originally described by the Rannugs[240]. Based on previous

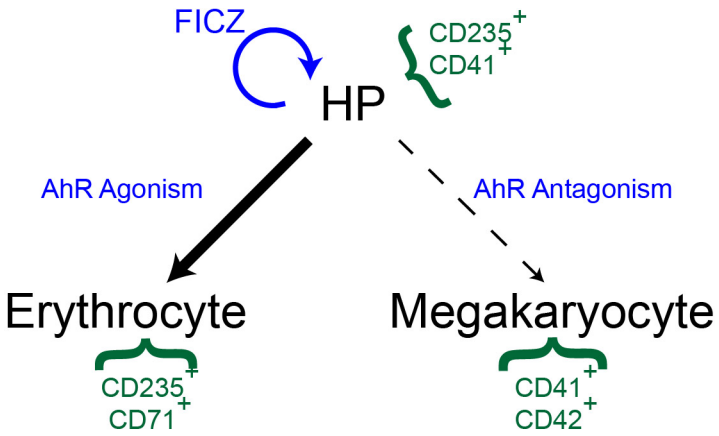

Figure 2.16. Mechanistic diagram of AhR involvement in normal hematopoietic development. The AhR agonist FICZ allows for the production and exponential expansion of hematopoietic progenitor cells (HPs). Continued AhR agonism is permissive to erythroid-lineage cell maturation whereas AhR antagonism elicits a transcriptional switch, which preferentially directs HPs to become megakaryocytes.

studies demonstrating the ubiquity of FICZ[241] and taken together with our data demonstrating the activity of this ligand, it is possible that FICZ plays a role in regulating hematopoiesis *in vivo*, possibly with other endogenous AhR ligands. In our *in vitro* system this leads to the expansion of erythroid lineage cells. *In vivo*, FICZ's interactions with other AhR ligands may explain the increase in platelets seen in mice injected with FICZ. The ability to expand HPs *in vitro* with an AhR ligand also suggests that blood cell development may be affected by a variety of environmental ligands[224,242].

In addition to allowing for the exponential expansion of HPs, our results indicate that AhR modulation is also involved in the further specification of both the erythroid and Mk lineages with AhR agonism permissive to the differentiation of erythroblasts and antagonism or downregulation of AhR leading to Mk specification. Although erythropoietin (EPO) and thrombopoietin (TPO) are the major drivers in RBC and platelet development, AhR may play a cytokine-independent role in the development and specification of these lineages and warrants further study in this capacity.

During the course of our studies, we derived putative progenitors known to express markers of both the Mk and erythroid lineages. A particularly striking outcome of our experiments is the development of a simple protocol for the rapid and highly efficient derivation of putative HPs, which expand exponentially under AhR agonism. In addition to the ability to answer basic biological questions concerning hematopoietic development, a useful outcome for this work will be the utilization of this *in vitro* platform for the production of blood products as the combination of AhR modulation with a completely chemically defined and xenobiotic agent-free differentiation scheme makes good manufacturing practice production and clinical translation feasible. Blood transfusion is an indispensable cell therapy, and the safety and adequacy of the blood supply are of national and international concern. An iPSC-based system, such as the one

described here in which large numbers of cells can be produced, could allow for red blood cell and platelet transfusion without problems related to immunogenicity, contamination, or supply. Furthermore, the ability to produce both populations of cells from a single source, and the fact that both platelets and mature RBCs contain no nuclear genetic material decreases safety concerns with the use of iPSC-derived cells and paves the way for clinical translation.

CHAPTER 3:

IN VITRO AND *IN VIVO* MODELS OF ERYTHROPOIESIS

Introduction

Erythropoiesis: from HSC to erythrocyte

Erythrocytes, or red blood cells (RBCs), can be classified as primitive or definitive depending on the origin of the cell. Primitive erythropoiesis occurs early in embryonic and fetal development in the yolk sac. Primitive RBCs, while very similar to definitive RBCs, can complete their maturation, including enucleation, in the bloodstream, but express a panel of embryonic and fetal hemoglobins[7]. When hematopoiesis moves to the bone marrow, all definitive hematopoietic cells are produced from the hematopoietic stem cell (HSC). Erythropoiesis from the HSC requires a series of cell fate decisions that rely on transcription factor expression to direct which type of mature hematopoietic cell a progenitor will become. Daughter cells of the HSC undergo specification to the common myeloid progenitor and then towards the megakaryocyte erythroid progenitor (MEP) due in part to upregulation of GATA1, in contrast to the persistent signaling from PU.1 in the lymphoid pathway[38,243–245]. The MEP, a short-lived progenitor, receives the last signals required for erythroid specification from erythropoietin and the upregulation of erythroid specific transcription factors[246]. The final stages of erythroid differentiation involve maturation steps, which alter morphology and cell surface markers, and increases hemoglobin production **(Figure 3.1)**.

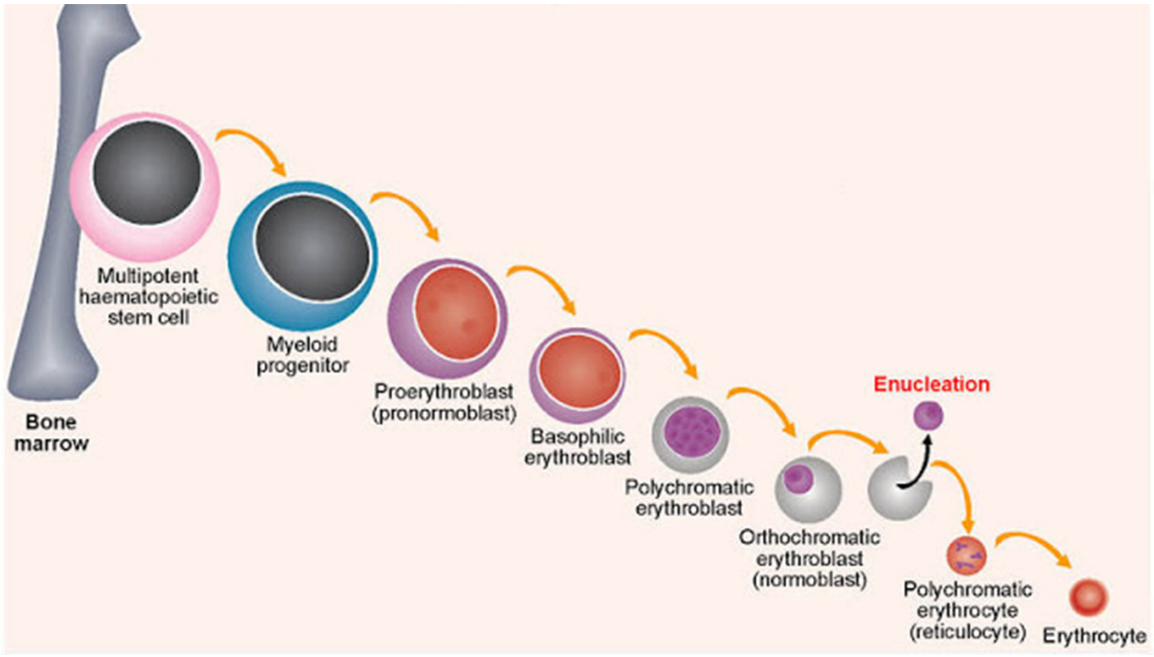

Figure 3.1 Erythroid development takes place in the bone marrow through a series of intermediate cell types. *Adapted from http://nephrotube-anemia-ckd.blogspot.com/p/erythropoiesis-rbcs-formation.html*

Erythropoiesis: Morphological changes during maturation

Under normal levels of EPO, RBCs develop within weeks progressing through multiple steps of maturation. The individual cell types are characterized morphologically based on size, hemoglobin content, and the size and appearance of the nucleus. The first erythroid specific precursor produced under EPO stimulation is the pro-erythroblast, which has a large nucleus and limited hemoglobin in the large cytoplasm[247]. The basophilic erythroblast contains a slightly smaller nucleus and is more basophilic than the pro-erythroblast due the ribosome content in the cytoplasm as hemoglobin production escalates. The last erythroid lineage cell capable of mitosis is the polychromatophilic erythroblast. The cytoplasm of polychromatophilic erythroblasts stains more grey than blue, as the increased amounts of hemoglobin in the cytoplasm are more acidophilic. The normoblast is the smallest nucleate cell in the erythroid lineage. The chromatin in the nucleus has condensed, showing up as a very dark compact structure. After the nucleus is extruded, the cell is known as a reticulocyte. Nuclear extrusion, or the process of expelling the nucleus from the cell, takes place in erythroblastic islands consisting of a central macrophage surrounded with differentiating and enucleating erythroblasts within the bone marrow[63–65]. Upon signals from the macrophage, an RBC releases its nucleus, which is promptly phagocytosed by the macrophage, leaving an anuclear cell behind. Even after nuclear extrusion there is sufficient mRNA to continue hemoglobin production for 1-3 days. Within 24 hours of reticulocytes escaping into the circulation, the cells take on their characteristic biconcave shape due to membrane loss and remodeling that allows RBCs to have increased surface area for optimal oxygen exchange and the deformability to navigate the fine vascular structures of the microcirculation[66] **(Figure 3.2)**.

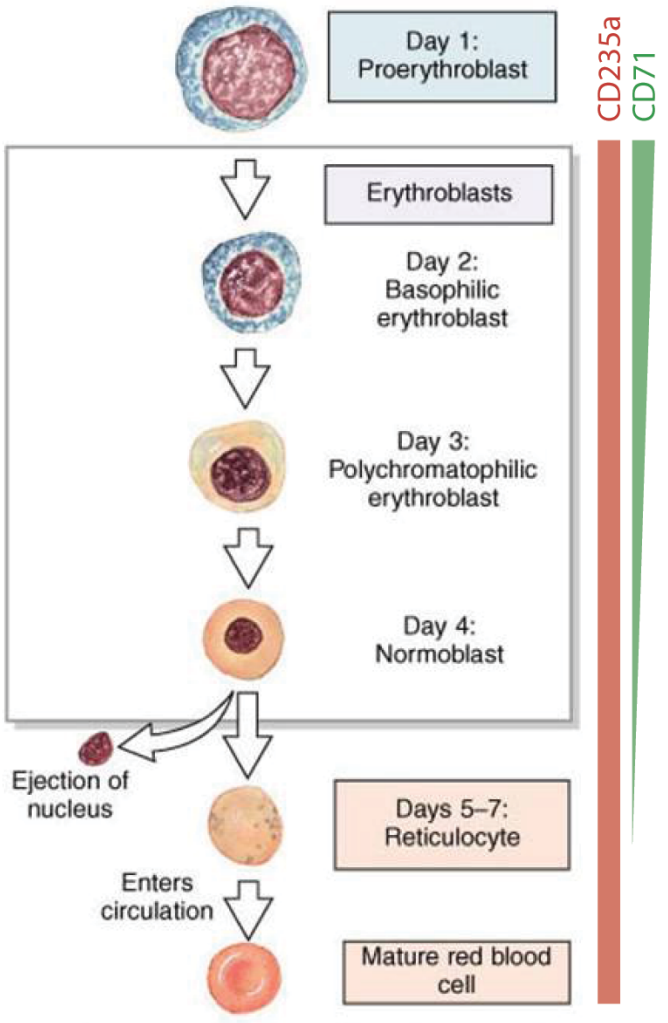

Figure 3.2. Morphology and surface markers of erythroid maturation. Maturation of erythroid cells can be visualized by size, morphology, as well as color, from stains such as Wright-Giemsa. During the erythroblast stages the cell is accumulating hemoglobin and reducing other proteins in the cytoplasm followed by condensation of the chromatin and exclusion of the nucleus. Once in circulation the cell will become a biconcave disc. *Modified from Marieb and Hoehn*[248].

Erythropoiesis: Cell surface markers identify RBC maturation state

The most commonly used cell surface markers used for identification of erythroid lineage cells are glycophorin A and the transferrin receptor. Glycophorin A, also known as human CD235a, or its counterpart, murine Ter119, is expressed on the cell surface of hematopoietic cells with erythroid potential[249,250]. It is expressed ubiquitously throughout erythroid development with similar levels on pro-erythroblasts and erythrocytes[251,252]. And while it is useful for locating erythroid cells, its constitutive expression makes it unable to discern maturation differences. The transferrin receptor, CD71, in conjunction with CD235a can to identify specific stages of erythroid development[253–255]. CD71 is required early in erythroid development for the uptake of transferrin, and thus allows for the transport of iron needed for hemoglobin production[256,257]. Reduction in hemoglobin synthesis and removal of non-essential proteins during the final stages of maturation results in loss of CD71 expression [251,252,258]. Complete loss of CD71 occurs at the reticulocyte stage allowing reticulocytes to be identified as anuclear cells with $CD235a^{+}CD71^{low/neg}$ surface markers **(Figure 3.2)**.

Hemoglobin Expression: A site-specific oscillation through development

Hemoglobin expression, while dependent on erythropoiesis, is not regulated by erythroid maturation. The site of hematopoiesis plays a larger role in the regulation of which hemoglobin molecules are expressed, rather than the maturation state of the cells. This is due to the variety of transcription factors involved in hemoglobin expression and their time/site specific expression.

Human hemoglobin, made up of a dimer of dimers has 6 distinct normal variants. During early human embryonic development the embryo relies on the yolk sac for nutrients. It is here, in the yolk sac blood islands, that that the first primitive RBCs are derived[7,61]. These early RBCs express embryonic globins zeta (*HBZ*) and epsilon (*HBE*). These hemoglobins have been

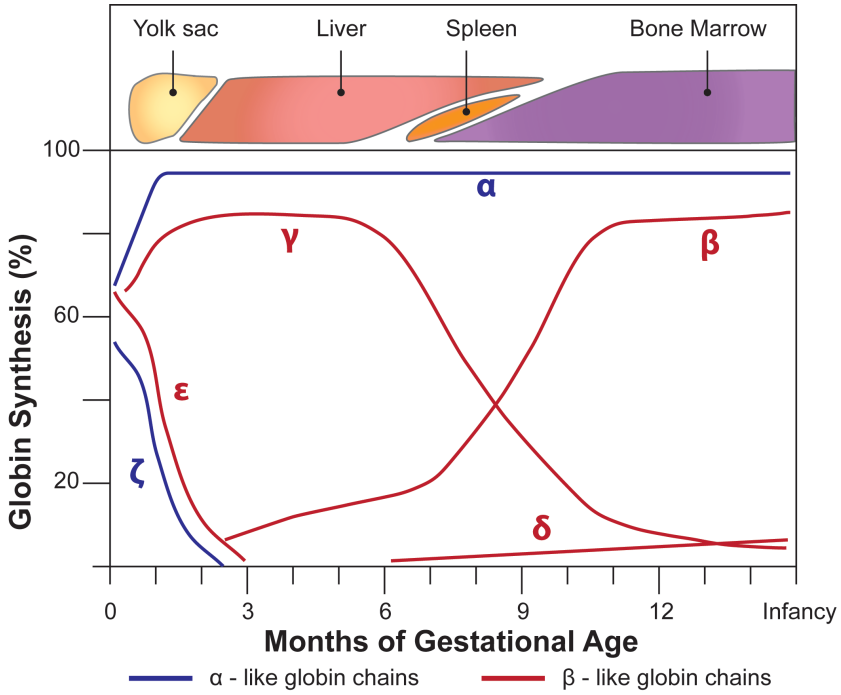

Figure 3.3 Hemoglobin expression varies as a result of the site of hematopoiesis. Hemoglobin expression changes as the site of hematopoiesis moves from the yolk sac to the bone marrow. This results in down regulation of embryonic (ε) and fetal (γ) and upregulation of beta (β), while alpha (α) is expressed throughout. *Modeled after Sankaran and Nathan*[58]**.**

found to make up a variety of tetramers including $\zeta_2\varepsilon_2$ (Gower1), small amounts of $\alpha_2\varepsilon_2$ (Gower2) and $\zeta_2\gamma_2$ (Portland1). As the embryo develops, the site of hematopoiesis moves from the yolk sac to the aorta-gonad-mesonephros (AGM) region and then to the fetal liver. This allows for the increase in the number of hematopoietic cells required to support the growing fetus. RBCs in the fetal liver produce alpha (*HBA2* and *HBA1*) and gamma (*HBG2* and *HBG1*) globins to make fetal hemoglobin: $\alpha_2\gamma_2$ (HbF). HbF is required at this stage of development when fetus is taking oxygen from the mother[62]. HbF has higher oxygen binding affinity, allowing for oxygen to be removed from the maternal blood system and transported to the fetus[259]. Towards the mid stages of gestation, hematopoiesis moves to the bone marrow, where it will reside for the adult life of

the individual. The HSC, which resides in the bone marrow, is the source of all definitive hematopoiesis. Commonly referred to as hemoglobin switching, this time only the gamma chain, expression is downregulated, switching to high expression of beta globin, *HBB*. This final form of hemoglobin, $\alpha_2\beta_2$ or HbA, makes up 97-99% of the hemoglobin expressed in the adult with <1% HbF[62] **(Figure 3.3)**.

Mouse Models for the study of in vivo hematopoiesis

The *in vitro* study of human erythropoiesis is extremely difficult and humanized mice have aided this quest. Humanized mice have been injected with human cells for the study of cellular potential, maturation, and hemoglobin switching. This is a common method for observing bone marrow reconstitution [260,261], defects in hematopoiesis[262,263], HSC and progenitor cell potential[11,160,264,265], progenitors from iPSC sources[266] and erythropoiesis[267].

Humanizing a mouse, in which the human cells are the sole focus, requires the removal or depletion of the murine component and the addition of human cells as the replacement[268]. To maintain these cells for study the mice must be altered by compromising their immune system Nod-SCID (NOD.CB17-*Prkdc*^{scid}/J) mice are one example of an immunocompromised mouse[269–271]. However, NSG (NOD.Cg-*Prkdc*^{scid} *Il2rgtm1Wjl*/SzJ) mice are more receptive to human cells than their Nod-SCID counterparts due to the deletion of IL2Rgamma [272–276]. To increase dependence on the human hematopoietic cells NSG mice can be sub-lethally irradiated[182]. This will cause apoptosis in murine hematopoietic cells in the mouse. When human cells are injected into the mice, they replace the cells that are lost, creating an environment in which the mouse is dependent on the human cells. Human hematopoietic cells can reconstitute the mouse with continued production of all hematopoietic lineages for months[182,272,273,277]. The advancements in

humanized mouse models offer stem cell biologists valuable tools to study the development and differentiation of cells created *in vitro* in an *in vivo* environment.

Materials and Methods

Cell generation and culture: Hematopoietic progenitors (HP) were generated from iPSCs using our previously published protocol[278]. Cells were kept in D7 media unless otherwise noted, 74% IMDM, 24% Hams F12, 1% B27 supplement, 0.5% N2-supplement, 0.5% BSA, 50ng/ml hVEGF, 100ng/ml bFGF, 100ng/ml hSCF, 25ng/ml hFlt3 Ligand, 50ng/ml hTPO (Genentech G140BT), 10ng/ml IL-6 (R&D 206-IL-010), 0.5U/ml hEPOgen (Amgen) and 0.2 μM 6-formylindolo[3,2-b]carbazole (FICZ) (Santa Cruz SC300019). Mitomyocin-C treated OP9 stromal layer was plated on gelatin coated well in DMEM, FBS, 2mM L-Glutamine (Invitrogen 25030081), and 100 mg/ml Primocin.

Staining: Cells were cytospun onto glass slides and stained with either Wright-Giemsa or Benzidine stains. Wright-Giemsa stains were performed with the Hema 3 Stat Pack (Fisher 23-123869). Benzidine stains were performed using DAB Peroxidase Substrate Kit, 3,3'-diaminobenzidine (Vector Labs SK-4100) according to manufactures instructions. Slides were imaged on a Nikon Eclipse Ti and images processed and quantified with ImageJ software.

Sorting and Microarray: HPs on day 15 and day 30 that were non-adherent cells were collected, washed into PBS-0.5% BSA, and stained for 45 minutes on ice with human CD235a-FITC (BD 559943). Cells were washed and resuspended in PBS-0.5% BSA with 1 μg/mL Propidium Iodide. The Beckman Coulter MoFlo Legacy at Boston University's Flow Cytometry Core Facility was used to collect 100,000-200,000 CD235+ cells. Following the sort cells were pelleted and

resuspended in 200 uL QIAzol Lysis Reagent (Qiagen 79306). RNA extraction of samples and running of the Illumina gene expression microarray was completed by the Baldwin Lab at Boston University and Paola Sebastiani of Boston University School of Public Health completed analysis of the microarray data in consultation with the Murphy Lab.

Maturation media: Cells were washed and then grown as a non-adherent culture in either Day 7 media or SFD (74% IMDM (Invitrogen 12330061), 24% Hams F12 (Mediatech 10-080-CV), 0.5% N2 supplement (Invitrogen 17502-048), 1% B27 supplement (Invitrogen 12587-010), 0.5% BSA in PBS (Sigma A1470, Cohn analog)), 5% Plasmanate, 10^{-7}M FICZ (Santa Cruz, SC300019-S, and 3U/mL hEPOgen, for 3 days. Cells grown in EMM1 were washed and then grown as a non-adherent culture in IMDM, 5% Plasmanate, 5% protein free hybridoma media II, PFHII (Life Technologies 12040-077), 2 U/mL hEPOgen (Amgen NDC55513-144-01) for 7-9 days. Cells grown in EMM2 were washed and then grown as a non-adherent culture in IMDM, 5% Plasmanate (Talecris Biotherapeutics Inc. NC27709), 5% PFHII, 2 U/mL hEPOgen, and 300 ug/mL transferrin (Sigma T0665) for 9 days. All medias contained 2mM L-Glutamine (Invitrogen 25030081), 4x10^-4 M Monothioglycerol (Sigma M1753), 50ug/ml Ascorbic Acid, and 100 mg/ml Primocin.

Humanized Mouse Models: Nude (J:NU Tyr^{c}/Tyr^{c}, Jax #007850) and NSG (NOD.Cg-*Prkdc*^{scid} *Il2rgtm1Wjl*/SzJ, Jax #005557) mice from Jackson Laboratories were housed in Boston University's Animal Facility according to National Institutes of Health and Institutional guidelines for the care and use of animals in research. Mice were anesthetized and numbered using ear punches. Sub-lethal irradiation of 2.5 Gy [182] was performed under semi-sterile conditions using a cesium-137 source. Cells were washed into PBS+ and 7-10, 50 or 100 million

approximately day 30 erythroid lineage cells were injected intraperitoneally 24 hours post irradiation. Retro-orbital bleeds were performed into EDTA coated vials and peripheral blood used for FACS and luciferase analysis.

Generation of lentivirus and infection of hematopoietic progenitors: The pHAGE2-Ef1α-luciferase plasmid was a gift from the Wilson Lab. VSV-G pseudotyped lentivirus was packaged and concentrated as previously described. On day 20 HPs were infected with lentiviruses containing Ef1α-luciferase or Ef1α-ZsGreen at an MOI of 1 to 10 with the addition of polybrene (5 μg/ml) to D7 media. After 24 hours cells were pelleted and resuspended in fresh D7 media for expansion.

In vivo imaging: Luciferase activity was detected with 200 μL of 30 mg/mL D-Luciferin Injection Ready Substrate (System Biosciences BLIV800A-1) per mouse or 200 μL of 30 mg/mL D-Luciferin in PBS (Perkin and Elmer 122796). Mice were imaged with a 3 min exposure on a Xenogen Spectrum *In Vivo* Imaging System 100 (IVIS) after 30 minutes incubation. Images were processed and signal quantified using Xenogen's Living Image Acquisition/Analysis Software. Luciferase imaging for cells, peripheral blood, and spleen homogenates was performed in a 96-well plate following a 2-minute incubation with 22.5 μg D-Luciferin.

Flow cytometry: Roughly 10^5 cells were collected, spun, and re-suspended in 0.5% BSA in PBS. Samples were incubated for 30 min at ambient temperature with human antibodies including CD41a-FITC (BD 555466), CD235-PE (BD 555570), CD71-FITC (BD 555536), CD71-APC (BD 341028) washed and spun at 3300 rpm for 7 minutes, and re-suspended in 0.5%

BSA in PBS with 1 mg/ml Propidium Iodide. Samples were run on a BD FACScalibur using Cellquest Pro software and analyzed via FloJo 8.7.

Results

The *in vitro* modeling of erythropoiesis from stem cells is a difficult task. While many methods have been attempted they usually require cell purification step, co-culture with stromal layers, or technically difficult embryoid body formation[233]. Very few mature cells are produced and only two have demonstrated the production of cells with primarily HBB expression[165,169]. Given that our HP differentiation protocol *(see chapter 2)* robustly generates progenitors capable of erythroid specification, we hypothesized that these cells were capable of both erythroid maturation and switching, which will ultimately allow me to observe differences between wildtype and SCD-derived cells.

Directed differentiation to HPs causes upregulation of erythroid specific genes.

As cells specify to a particular lineage their gene expression changes. This results in an increase in lineage specific genes with a concordant decrease in other lineages. To test the ability of the iPSC-derived HPs to specify towards the erythroid lineage we conducted a microarray gene expression of sorted CD235+ cells in comparison to undifferentiated samples. This was done with sorted 100-200,000 day 15 and 30 cells and unsorted day 60 cells **(Figure 3.4A)**. Day 60 was unsorted as at this time point 80% of the cells express CD235 (**Figure 2.10**). Three cells lines were used to examine differences between control and sickle cell disease-specific iPSC used in differentiations. There is no observable differences between the lines, indicating that sickle cell disease-specific iPSC have the same potential to upregulate erythroid lineage genes as wild type

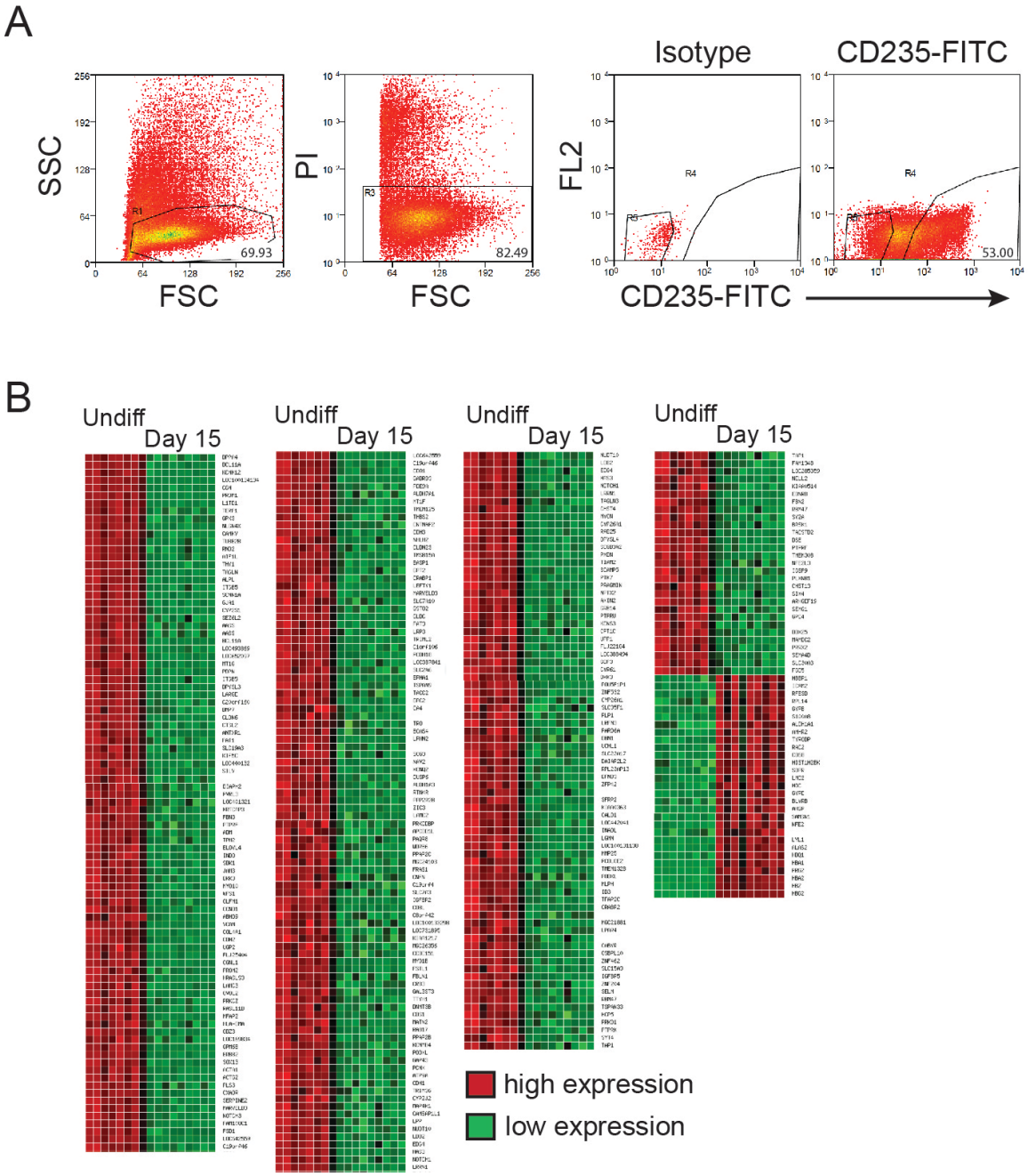

Figure 3.4. Differential gene expression of undifferentiated cells and erythroid-lineage cells. A) Sorting of D15 and D30 cells was done by FSC vs. SSC, propidium iodide for live cells and then for hCD235-FITC+. B) Differentially expressed genes seen between undifferentiated (undiff) and day 15 cells with Illumina microarray. Results shown represent work done by S. Rozelle (A), Baldwin Lab and P. Sebastiani (B).

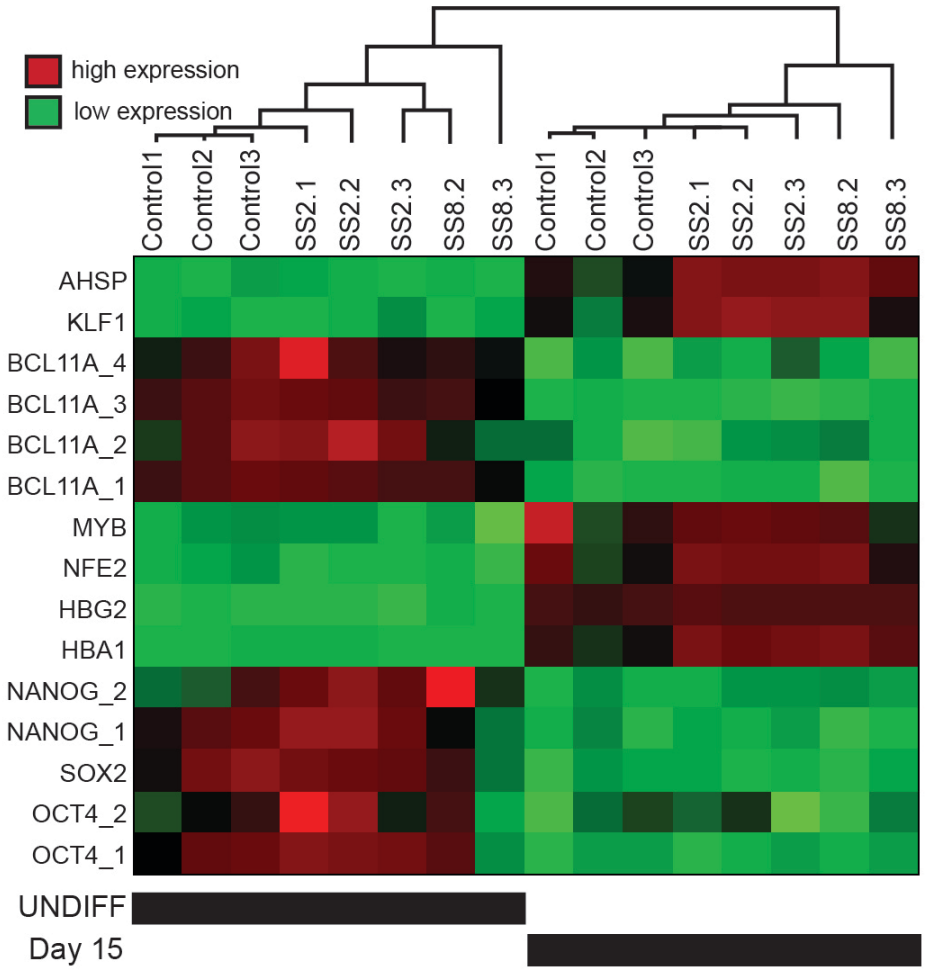

Figure 3.5. Clustering analysis for erythroid specific genes. Clustering analysis of erythroid specific genes comparing undifferentiated (undiff) and day 15 cells for control cells and two sickle disease specific lines. Results shown represent work done by S. Rozelle and the Baldwin Lab and analyzed by P. Sebastiani.

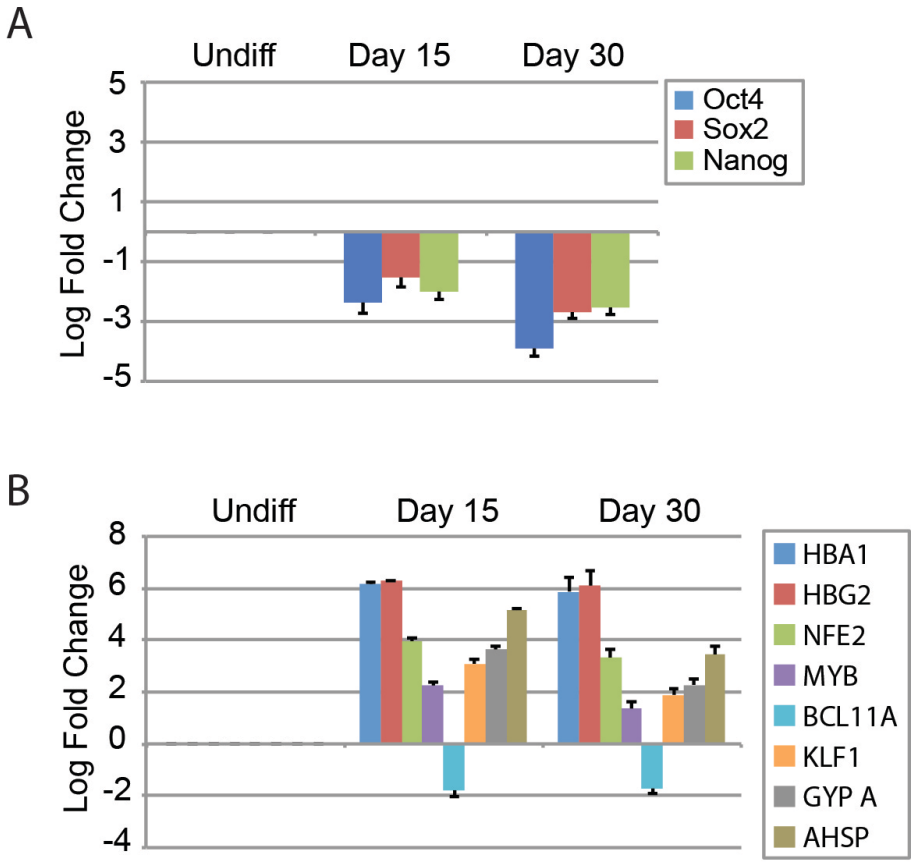

Figure 3.6. Graphical representation of pluripotency and erythroid specific gene expression during differentiation. Bar graphs showing log fold change for pluripotency (A) and erythroid specific (B) gene expression in undifferentiated (undiff), day 15, and day 30 cells from the microarray. Results shown represent work done by S. Rozelle and the Baldwin Lab and analyzed by S. Rozelle and P. Sebastiani.

control cells. Clustering demonstrates a large number of genes downregulated with differentiation with only a small subset upregulated **(Figure 3.4B)**. Closer analysis of erythroid and pluripotency genes shows loss of pluripotency as the cells go through differentiation, and upon day 15, as a hematopoietic progenitor (HP) there is upregulation of erythroid specific genes **(Figure 3.5)**. Graphical representation of gene expression over time of a subset of genes confirms shows 3 fold upregulation erythroid specification and 1.5 fold decrease in of pluripotency factors Oct4, Sox2, Nanog expression **(Figure 3.6)**. *BCl11,* a gene that plays a key role in silencing *HBG* expression is down regulated early in erythropoiesis and upregulated after hemoglobin switching.

Maturation medias cause morphological and cell surface marker expression changes consistent with erythroid maturation.

Historically, erythroid lineage cells are made to mature to the point of enucleation through co-culturing and/or maturation medias[233,279]. The use of co-culturing eliminates the ability of the produced cells to be used clinically, as there is no guarantee cross-contamination will not occur. This is even more critical when the stromal layer utilized is murine instead of human. Therefore, is it important to create an environment in which the cells can mature in a chemically dependent manner. When cells persist in the HP production media, Day 7, they are capable of limited maturation as seen by CD235 and CD71 expression as well as the ability of the cells to respond to low oxygen conditions (**Figure 2.10**). This media is designed for the production of HPs, and therefore contains cytokines that signal for hematopoietic progenitor specification and proliferation. Removal of these cytokines allows further specification to the erythroid lineage. Plasmanate, a human plasma-mimetic, was used to mimic the environment in which erythroid cells are known to mature. Plasmanate contains albumin and globulins, and other normal blood proteins which aid in creating an environment conducive for RBC maturation[280]. A maturation

media using plasmanate demonstrates the ability of a heterogeneous HP population to increase CD235+ CD71+ from 54.6% to 72.7%. There is also an increase in CD235+ from 7.5% to 18.4%, suggesting these cells are capable of full maturation **(Figure 3.7A)**. While this condition allow for surface marker changes, little to no changes in cellular size were noted **(Figure 3.7B)**. To verify that the cells are capable of enucleation cells were cultured with an OP9 human bone marrow stromal layer. FACS results for CD235 and CD71 show that the presence of OP9s also allows for generation of a more homogenous population of cells. Co-culture with OP9s dramatically increased the number of solely CD235+ cells in Day 7 media. The number of CD235+ cells increases from 37.5% to 46.3% when the cells are cultured in a maturation media containing IMDM, 5% PFHMII, 5% Plasmanate, and 2 U/mL of EPO, also known as EMM1 **(Figure 3.8)**. Serum-free protein free hybridoma media (PFHMII) was added to the maturation media to help support the cells in suspension culture[179]. Cells grown on OP9s in EMM1 enucleate in very small amounts, less than 1% **(Figure 3.8, red arrow)** While EMM1 is useful to mature HPs to enucleated erythroid cells, it is not sufficient for extended propagation of the cells off the OP9 stromal layer. Additions to EMM1 including transferrin, ascorbic acid, and α-monothiol glycerol to create EMM2 were sufficient to generate a homogenous population of erythroid lineage cells with 35.2% CD235+ without a stromal layer **(Figure 3.9)**. Cells cultured in EMM2 in a spin culture demonstrated more enucleation than static cultures (data not shown) and increased their hemoglobin content 1.5-5 fold depending on the cell line, as seen with benzidine staining **(Figures 3.10 & 3.11)**.

While erythroid cells capable of maturation and enucleation can be generated from human normal and sickle iPSCs, hemoglobin switching *in vitro* does not occur. To examine hemoglobin switching it we next turned to an *in vivo* model.

Chimerism of iPSC-derived erythroid cells in humanized NSG mice

While limited maturation can be achieved, *in vitro* hemoglobin switching rarely occurs in the laboratory. In 2012, Kobari et al. demonstrated with HPLC that iPSC derived erythroid-lineage cells injected into NOD/SCID-LtSz-scid/scid (NSG) mice were capable of producing not only beta globin, but the sickle cell isoform as well[182]. While this study was promising there were so few RBCs produced that only HPLC analysis was performed. This study suggested that should large quantities of human erythroid lineage cells be used, hemoglobin switching might be observed. Accordingly NSG mice (NOD.Cg-*Prkdc*^{scid} *Il2rgtm1Wjl*/SzJ), were sub-lethally irradiated with 2.5 Gγ and the following day 10, 50 or 100 million erythroid lineage cells were injected intraperitoneally. Both retro-orbital bleeds and bone marrow harvesting were performed to detect the presence of the human cells. CD235-FITC antibody separates human erythroid cells from murine erythroid cells allowing the detection of human cells in the bone marrow on Day 14 as 34.6% of the total population **(Figure 3.12B)**. One week later, on D21, 0.1% of the peripheral blood population was human cells **(Figure 3.12C)**. As the spleen is a primary the site of hematopoiesis in the mouse, as well as the site of RBC destruction, histological sections were made from each mouse spleen. H&E staining revealed the presence of RBCs in the spleen in higher quantities than the control mouse **(Figure 3.13)**. Interestingly, there appears to be more RBCs in the spleens of the mice who received 10 million cells from SCD-specific iPSC than the mouse who received 50 million control cells (**Figure 3.13**). Based on these results we hypothesize that the SCD-specific cells have matured to the point in which they have sickled and accumulated in the spleen awaiting destruction by splenic macrophages.

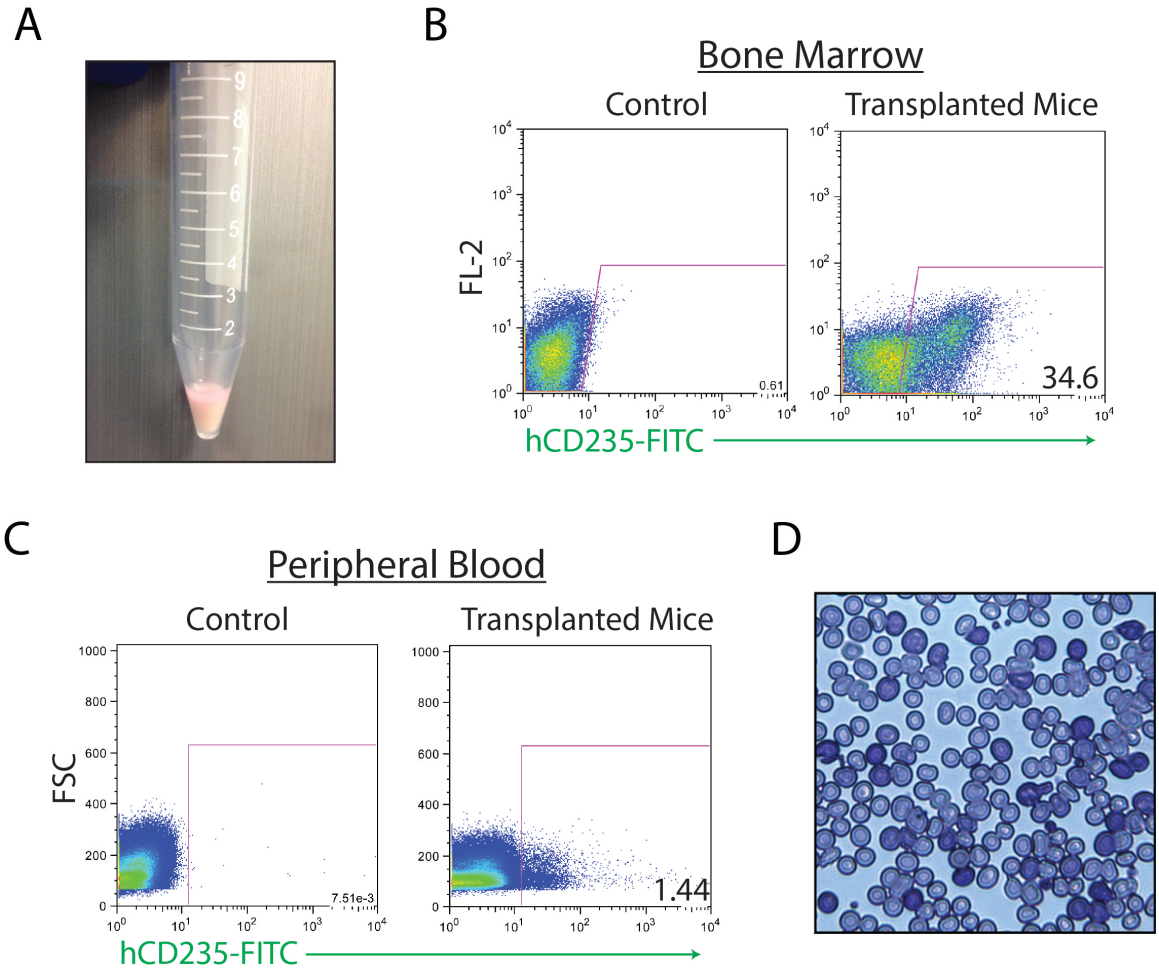

Figure 3.12. Human cells demonstrate chimerism in NSG-mouse model. A) Large scale production of HPs from WT iPSC for intraperitoneal injection into mice. B & C) FACS of human CD235 expression demonstrates chimerism in bone marrow after 14 days and peripheral blood after 21 days. D) Wright-Giemsa stain of Day 21 murine peripheral blood.

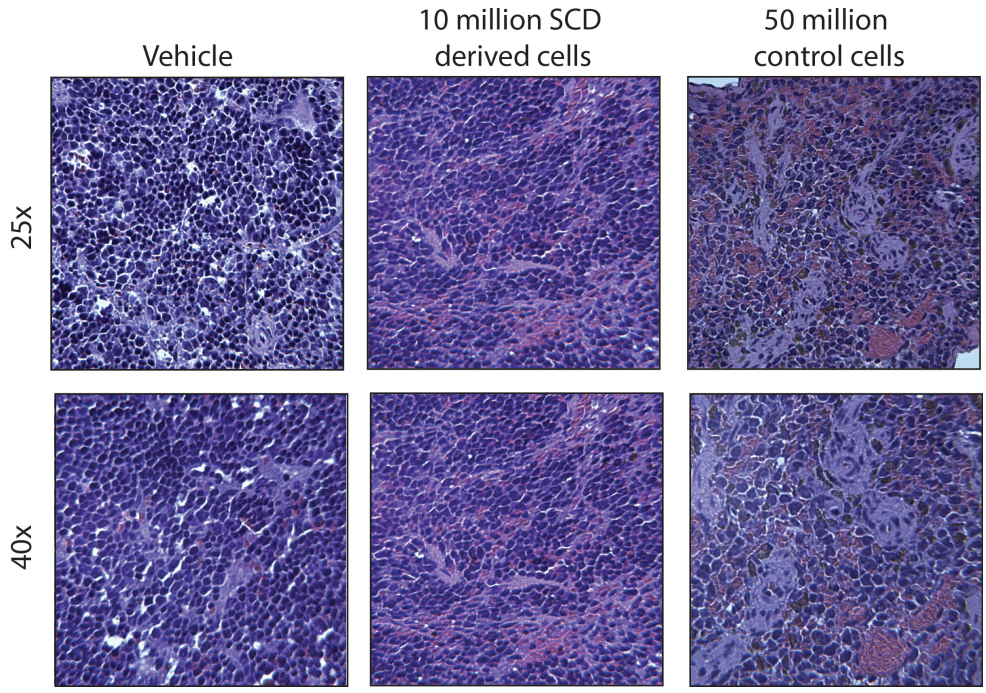

Figure 3.13. H&E stains of spleens from humanized NSG mice. Large amounts of RBCs accumulate in the spleens of humanized mice, more so when cells are derived from SCD-specific iPSC.

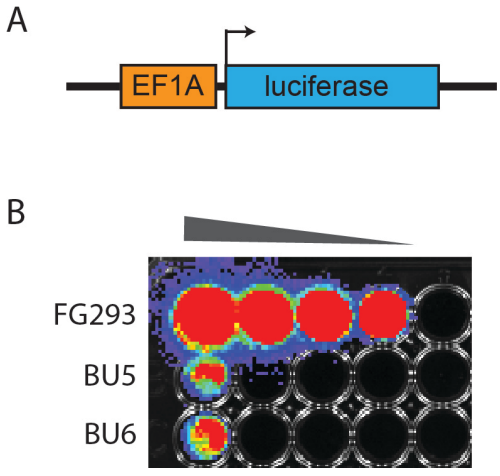

Figure 3.14. HPs can be infected with luciferase expressing lentivirus. A) Model of vector with a constitutive promoter, Ef1α, driving luciferase expression. B) IVIS image of multiple cell lines infected with 100 uL of virus expressing luciferase.

In vivo visualization of human erythroid lineage cells in mice using constitutive luciferase expression

To map the presence of the human cells in the mouse over time, erythroid lineage cells were infected with constitutively expressed luciferase **(Figure 3.14)**. When the cells are exposed to exogenous D-luciferin the luciferase within the cells catalyzes a chemical reaction that results in the emission of light that can be detected at 560 nm on an *In Vivo* Imaging System (IVIS). Initially these experiments were done in Nude mice for optimal visualization of the cells. 8-10 million cells infected with a lentivirus containing Ef1a-luciferase were injected intraperitoneally and anesthetized mice imaged every other day starting 24 hours after injection of the cells. Eight million FG293 cells were also infected with Ef1a-luciferase and injected into a mouse as a control for infectivity of the cells and location of the signal, as these cells are incapable entering the lymphatic system and ultimately the peripheral blood as seen with hematopoietic stem cell transplants. While the signal varies from day to day, it persists for 21 days **(Figure 3.15)**. There appears to be foci of signal in the lower quadrants of the mice and some near the upper right quadrant, possibly in the spleen, suggesting that these cells are capable of homing to the bone marrow and entering the peripheral blood **(Figures 3.16 & 3.17)**. Cells expressing Ef1a-luciferase were put in maturation media for 9 days and the signal analyzed on the IVIS **(Figure 3.18)**. While nude mice are optimal for imaging purposes, they contain an intact immune system

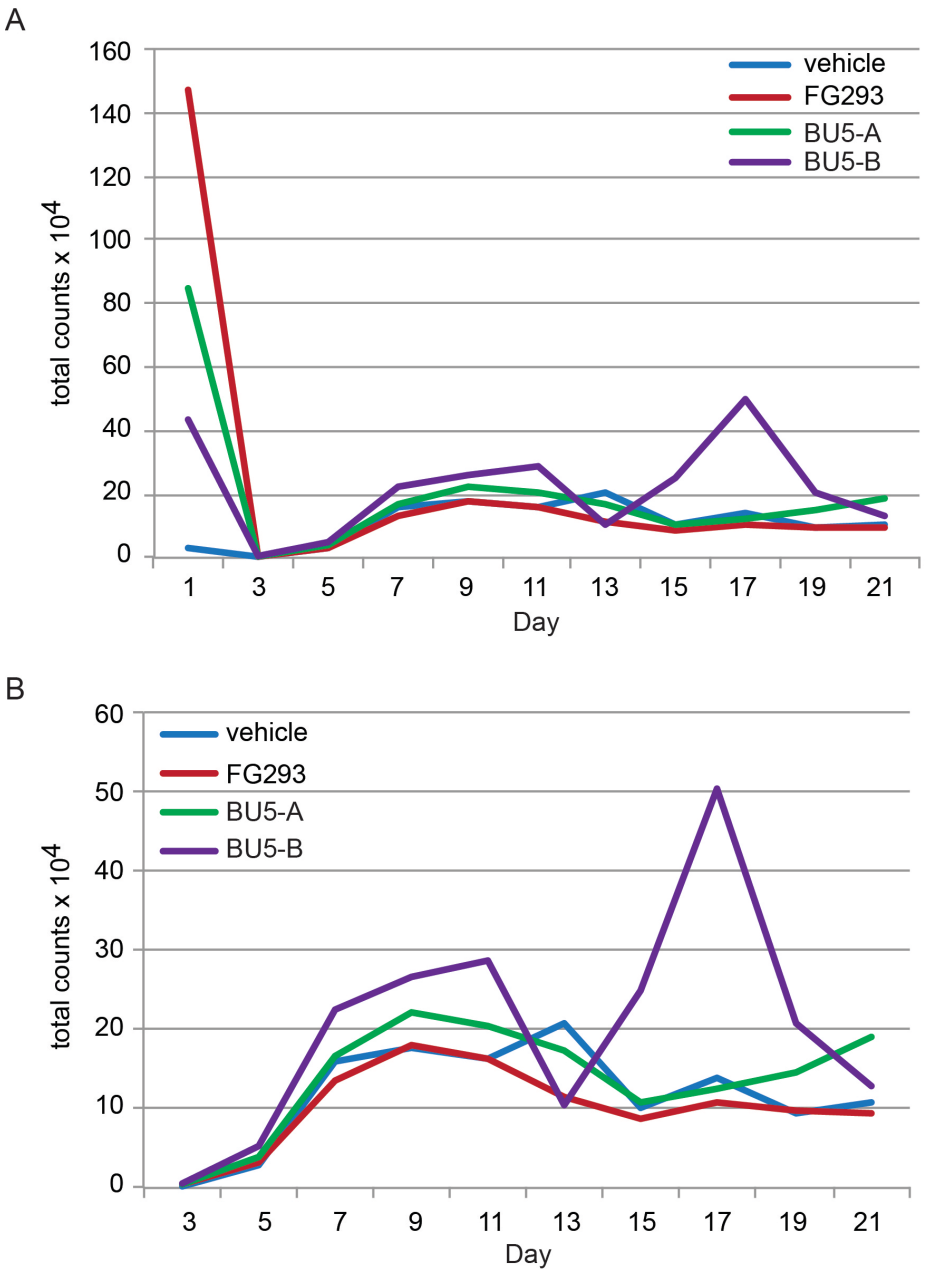

Figure 3.15. Quantification of luciferase signal in region of interests denoted in Figures 3.16 and 3.17. A) Line graph showing total counts x 10^4 for days 1-21. B) Line graph for days 3-21 displaying total counts x 10^4.

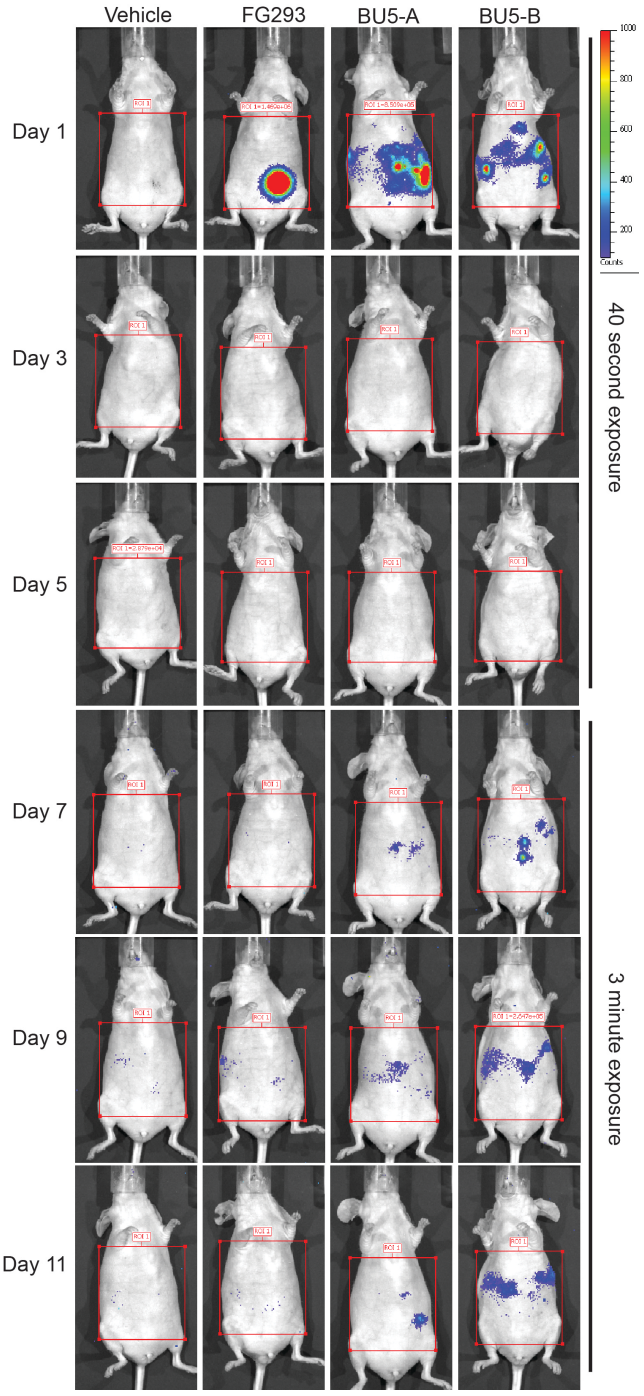

Figure 3.16. IVIS luciferase images of days 1-11 of nude mice injected with 10 million human cells expressing luciferase. Cells appear as colored pixels in the mice with the color blue indicating low amounts of cells and red high amounts of cells. Red boxes indicate defined regions of interest used for quantification of the signal. Initial exposures were too short and a time course was done to determine 3 minutes the optimal exposure time.

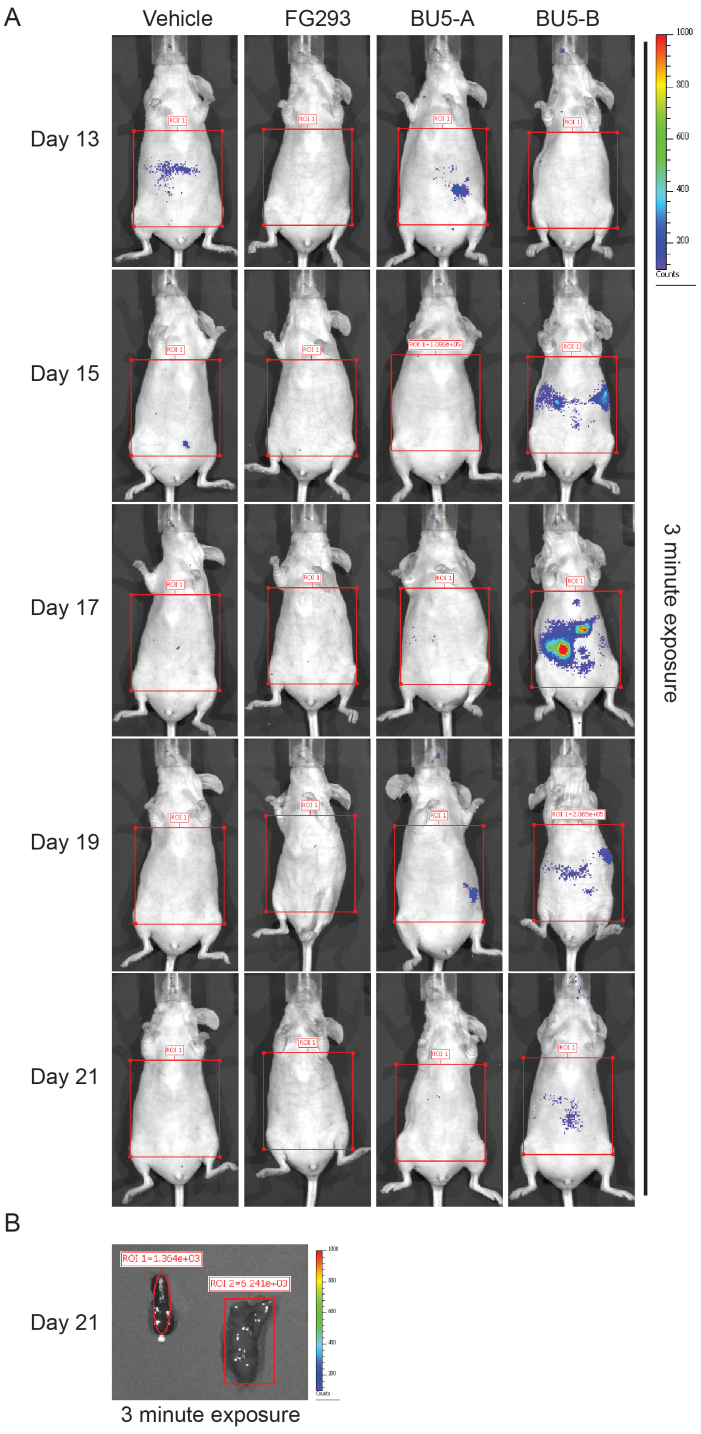

Figure 3.17. IVIS luciferase images of nude mice injected with 10 million human cells expressing luciferase. A) Cell appears a colored pixels in images for days 13-21. Blue color indicates few cells, red many. B) Luciferase IVIS image of the BU5-B mouse spleen (left) and liver (left).

that can attack the human cells and reduce survival. Therefore it was important to return to using NSG mice. NSG mice were irradiated as before, 8-10 million cells infected with Ef1a-luciferase injected intraperitoneally, and anesthetized mice imaged every 3 days starting 24 hours after injection of the cells. Days 1-7 show high amounts of signal as the cells are near the surface of the mouse, but as the majority of the cells enter the lymphatic system and ultimately the peripheral blood the signal diminishes **(Figures 3.19 & 3.20).** Variation in signal intensity from day to day was thought to be due to variation in purchased D-luciferin batches used and therefore all subsequent experiments utilized the same batch of D-luciferin made in the laboratory. The signal in this experiment diminished much more quickly than previous experiments **(Figure 3.20)**, which raised the question if these mice still had the capacity to remove the human cells from circulation. In NSG mice the remaining immune cell that could be clearing the human cells from circulation is the macrophage [272].

Depletion of macrophages in humanized Nod-SCID Gamma (NSG) mouse model does not increase viability of mice or injected human erythroid cells

Macrophage depletion can be obtained in a site-specific manner through the use of liposomal delivery of clodronate[281]. Clodronate, dichloromethylene diphosphonate CL2MDP, in the cytosol of cells can be mistakenly identified as a pyrophosphate and is used to generate an ATP analog. This non-hydrolyzable ATP analog can enter the mitochondria outer membrane and by irreversibly binding to ATP transporters disrupt the polarization of the mitochondrial membrane, leading to apoptosis[282]. As clodronate is toxic to cells, targeted delivery using liposomes, clodrosomes, allows for uptake by cells that phagocytosis foreign objects, mainly macrophages. While clodrosomes can be delivered directly to the site in which depletion is desired[283,284], intraperitoneal injections has been demonstrated to target macrophages in the spleen, liver and

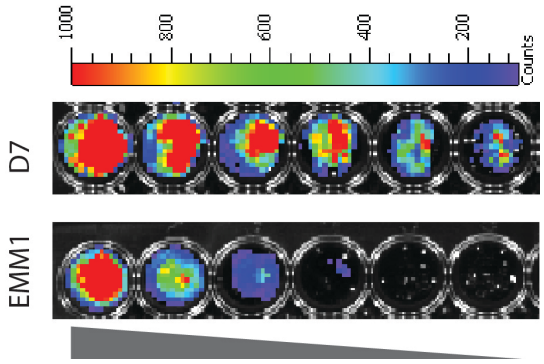

Figure 3.18. IVIS images of luciferase signal of cells in day 7 media or erythroid maturation media 1 for 7 days. Cells appear as colored pixels with the color blue indicating low amounts of signal and red high amounts of signal.

peritoneum[285,286]. Previous experiments suggested that it takes five-seven days to fully deplete the macrophage population and therefore multiple treatments of clodrosomes were necessary[287].

Depletion of macrophages was attempted twice, under differing conditions, but with similar results. Initially, macrophages were depleted post- irradiation and injection of the 10 million human cells expressing Ef1a-luciferase and Ef1a-ZsGreen **(Figure 3.21A)**. ZsGreen was to be used as a method for identifying human cells without having to undergo a staining protocol, which could have resulted in variable results. Unfortunately, treatment with 200 µg of clodrosomes resulted in low viability for the treated mice and no conclusions regarding the persistence of the human cells could be made **(Figure 21B)**. Analysis of the spleens by imaging or spleen homogenates with additional D-luciferin treatment revealed no luciferase or ZsGreen expression. This was also confirmed using a peripheral blood from retro-orbital bleeds **(Figure 3.22B)**. Due to the early death of the mice, the protocol was adjusted.

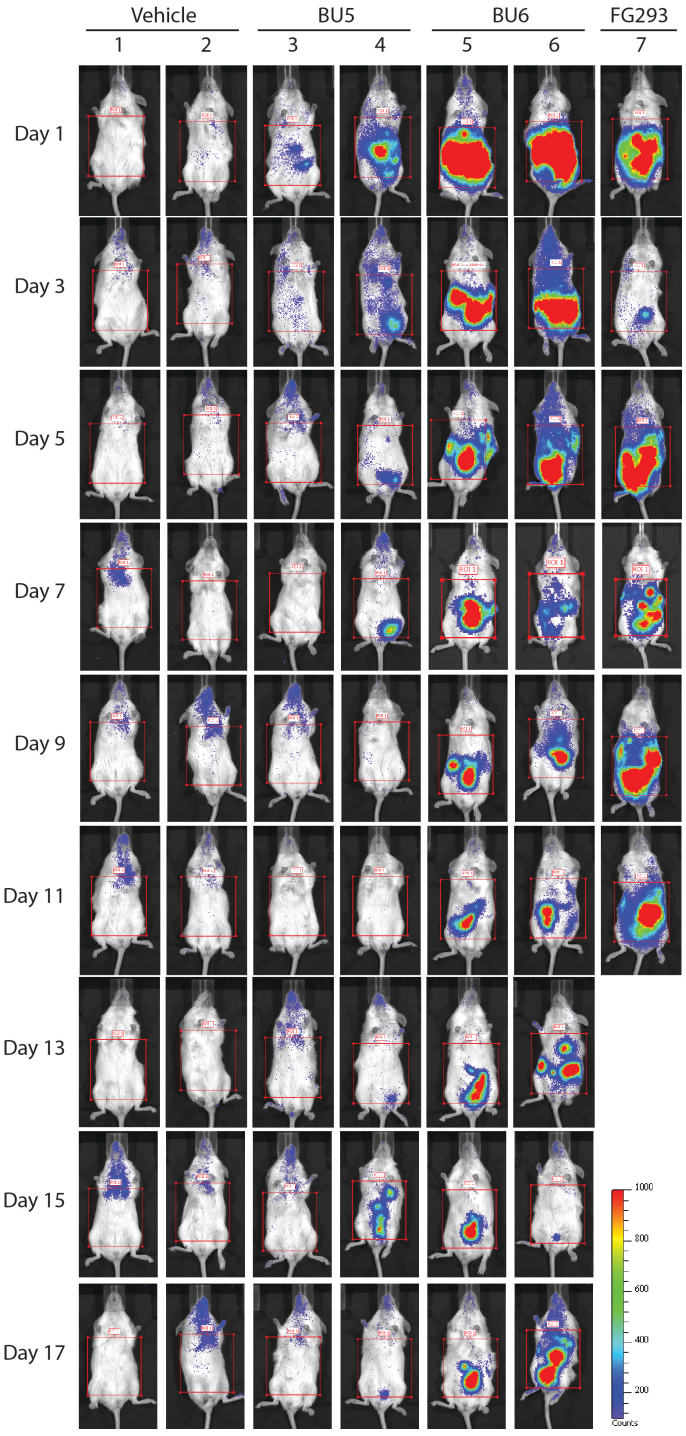

Figure 3.19. IVIS luciferase images of days 1-17 of humanized NSG mice with two luciferase expressing control cell lines BU5 and BU6. Cells appear as colored pixels in the mice with the color blue indicating low amounts of cells and red high amounts of cells. Red boxes indicate defined regions of interest used for quantification of the signal.

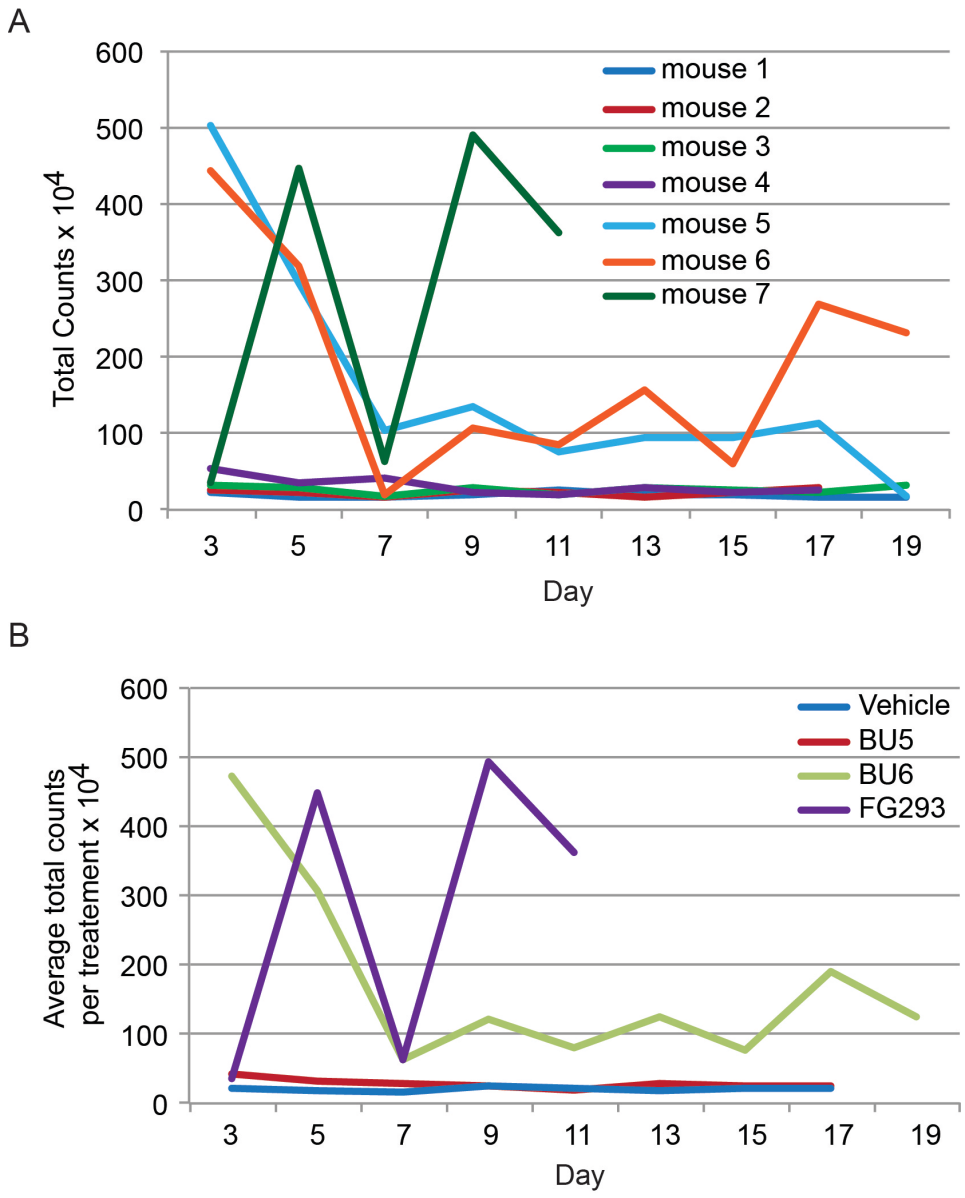

Figure 3.20. Quantification of luciferase signal in region of interests denoted in figure 3.19. A) Line graph showing total counts x 10^4 for days 3-19 of individual mice. B) Line graph for days 3-21 displaying the average total counts x 10^4 per treatment group.

Macrophage depletion with a lower concentration of clodronate, 100 μg, began prior to irradiation, under the assumption that there would be better human cell survival and bone marrow reconstitution if there were fewer macrophages present when the human cells were initially injected into the mice **(Figure 3.23A)**. This experiment also limited the handling and anesthetizing of the mice by combining the injections of clodrosomes to the days in which the mice were imaged. Unfortunately there was no improvement in mouse viability following this protocol and conclusions about human cell viability could not be made **(Figures 3.23B & C**). While this method of macrophage depletion is robust, others have also noted that these experiments required an increased number of mice, compared to traditional experiments, to account for the premature death of the mice[287].

Discussion

Erythropoiesis has been studied extensively in xenopus, zebrafish, rats, chickens, mice, and humans. Yet with all we understand about the process of making RBCs, to do so efficiently *in vitro* has eluded researchers for years. An even more difficult process is making RBCs that have matured to produce enucleated RBCs with expression of HbA. Researchers have invested years trying to make this a reality[233]. By using erythroid progenitors derived from iPSCs large numbers of cells can be obtained for studies into the steps of maturation and hemoglobin switching. With our method of producing HPs millions of cells to test maturation and *in vivo* models could be obtained.

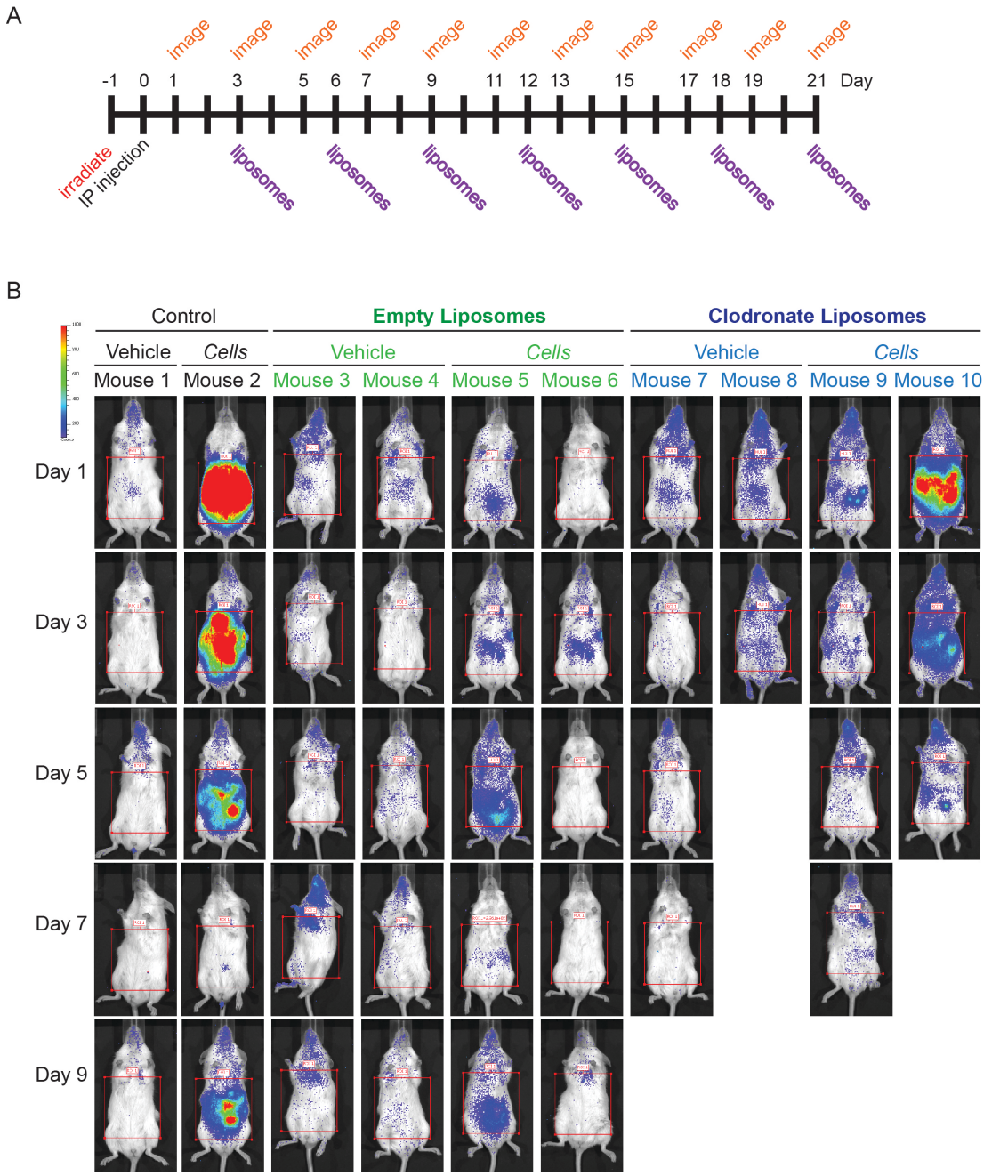

Figure 3.21. Clodronate treatment of humanized NSG mice. A) Experimental diagram indication time points for either empty or 200-µg clodronate filled liposome injections. B) IVIS luciferase images of mice that received nothing, empty liposomes, or clodronate liposomes with and without cells. Cells appear as colored pixels in the mice with the color blue indicating low amounts of cells and red high amounts of cells. Red boxes indicate defined regions of interest used for quantification of the signal.

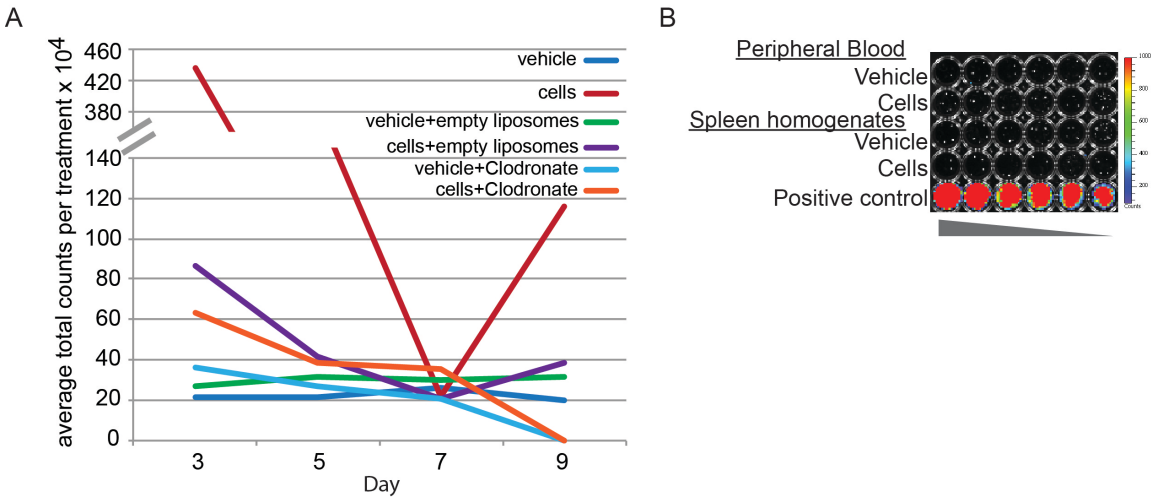

Figure 3.22. Analysis of luciferase signal. A) Line graph displaying the average total counts x 10^4 per treatment group for days 3-9 B) IVIS image of luciferase expression in peripheral blood or spleen homogenates from mice 1, vehicle, and 2, cells.

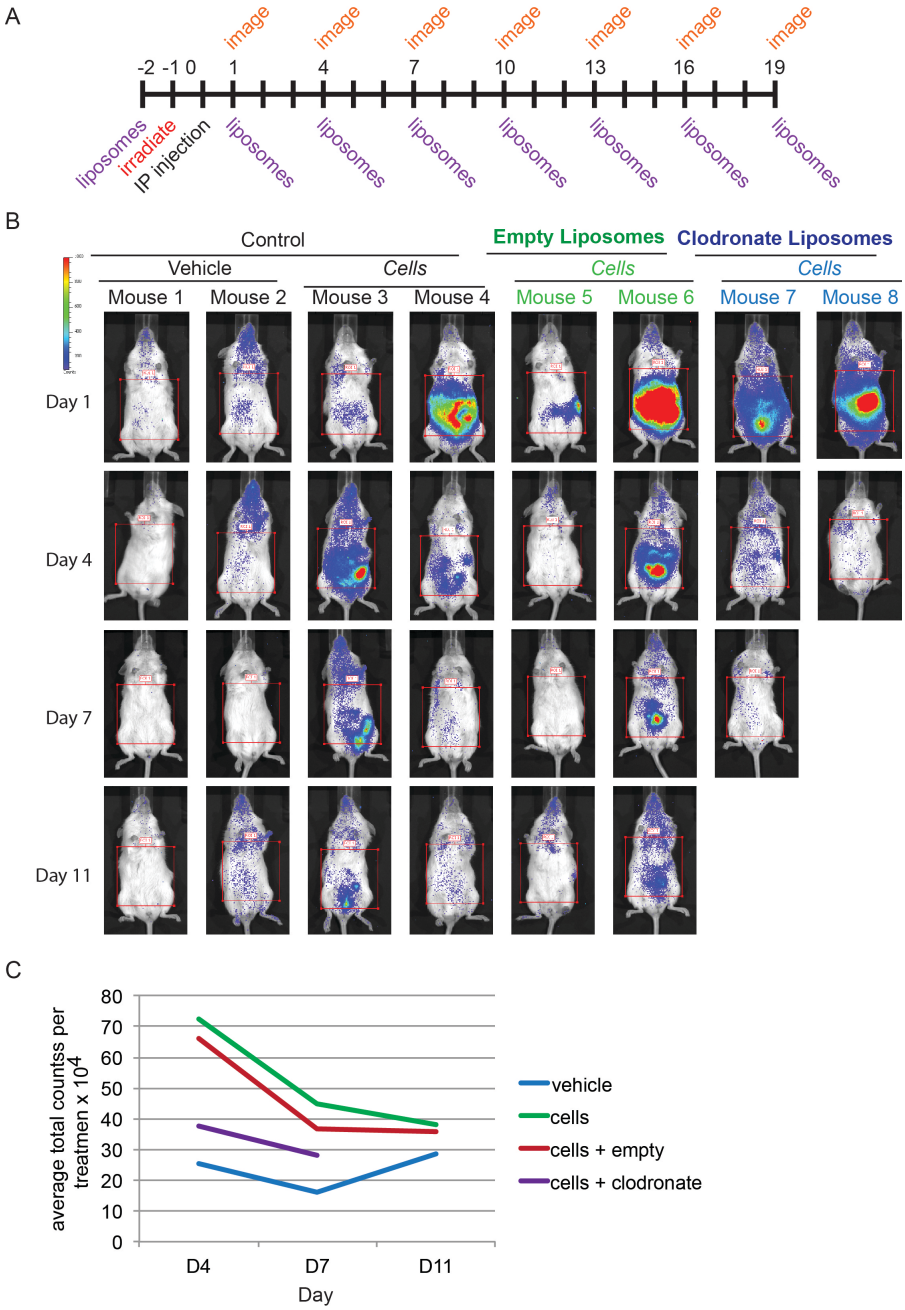

Figure 3.23. Humanized NSG mice treated with 100 µg of clodrosomes. A) Experimental diagram indication time points for liposome injections. B) IVIS luciferase images of mice that received nothing, empty liposomes, or clodronate liposomes with and without cells. C) Line graph of average luciferase counts x 10^4 per treatment group.

Erythroid maturation occurs most reliably on stromal layers such as murine fetal liver or human bone marrow stroma, OP9. Co-culturing creates opportunities for contamination of the produced cells, limiting their clinical applications. I set out to demonstrate that our cells are capable of maturation, and then to do so in a chemically defined manner. The microarray data verified that our differentiation protocol to HPs create a transcriptional environment conducive to the maturation of erythroid lineage cells **(Figures 3.5 & 3.6)**. It also showed that crucial erythroid lineage and hemoglobin regulators such as *KLF1* and *BCLl11A* were regulated as expected.

Limited maturation occurs in our HP production media, Day 7, as seen by surface expression of CD235, glycophorin A, and CD71, transferrin receptor. This media, while good for production and expansion of HPs contains cytokines that block further maturation. Removal of the cytokines with addition of plasmanate, and EPO creates a uniform population of 72% CD235+CD71+ cells **(Figure 3.7)**. However it took additions to the media and an OP9 stromal layer to see minimal enucleation occur **(Figure 3.8)** and further media changes to get increases in hemoglobin content **(Figures 3.10 & 3.11)**, and 35% of cells solely CD235+ in EMM2 **(Figure 3.9)**.

While maturation is important, maturation can occur without hemoglobin switching. This is common during development when cells are produced by the AGM. All hemoglobin expression seen with our cells *in vitro* demonstrates that our cells are embryonic and fetal in nature. They express *HBE, HBZ, HBA*, and *HBG*, but not *HBB* (**Figure 2.11**). It is not yet possible to reliably generate large quantities of *HBB* expressing cells from an embryonic source such as hES or iPSC[233]. In 2012, Kobari et al. published that erythroid cells produced from iPSC were capable of hemoglobin switching when put into NSG mice[182]. While no one has been able to replicate Kobari's results, however, the logic behind the experiment was valid. The bone marrow niche is extremely complex, consisting of many cell types from multiple cell lineages. To replicate that in

a dish without co-culturing is very difficult. To show that iPSC derived erythroid lineage cells are capable of switching would validate iPSC disease modeling. Therefore, putting them into an *in vivo* environment that can support them through switching and maturation is a logical idea. Preliminary experiments also suggested that it was possible, as I see increased accumulation of RBCs in the spleen when the erythroid lineage cells were derived from SCD-specific iPSCs **(Figure 3.13)**. This result launched many experiments designed to track erythroid lineage cells in the mice so that these cells could be isolated from murine cells and analyzed for hemoglobin content.

The number of human cells in the mouse is small and they are difficult to find either by FACS or by luciferase using an IVIS **(Figures 3.15-3.19)**. The macrophage is one of the remaining immune cells in NSG mice, and therefore the suspect in the destruction of the human cells. Although others have shown that the macrophage is responsible for the destruction of human erythroid cells in NSG mice and that clodronate can increase human chimerism this result could not be replicated[287] **(Figures 3.21 & 3.23)**. While titration of clodrosome dosage may increase viability in the mice, there are other methods to combat macrophage phagocytosis of human cells including preventing the macrophage from identifying the cells as foreign.

CD47, integrin-associating protein (IAP) is expressed on the surface of both human and mouse cells. It is most commonly interacts with thrombospondin to control angiogenesis and inflammation or with integrin $\alpha_4\beta_3$ to control cell adhesion and migration. When it interacts with signal-regulatory protein-α (SIRPα) on macrophages it allows macrophages to recognize cells as "self" or "foreign", with foreign cells being phagocytized. Expression of murine CD47 on human cells can prevent phagocytosis by changing the "eat me signal" to a "self" signal[288]. Others have adapted mice to express human CD47 as another method for preventing destruction of human cells in mice[288,289]. As our cells are easily transduced with lentivirus, perhaps a pHAGE

expression plasmid that contains murine CD47, can be infected into the human erythroid lineage cells and hinder their phagocytosis.

While this model is currently incomplete, much of the groundwork for the *in vivo* imaging and assays, as well as erythroid maturation experiments have been done. Cell morphology, Wright-Giemsa staining and FACS markers CD235 and CD71 can be used to determine the maturation state of iPSC-derived erythroid lineage cells. Hemoglobin switching, which ultimately will be determined by mass spectroscopy analysis of globin proteins,, could occur in the NSG mice. Conditions for sorting human cells from murine peripheral blood and spleen homogenates have been determined (data not shown), which will allow for a pure population of human cells to analyzed after maturing and switching *in vivo*. Even if hemoglobin switching never occurs in the mice, this model is important for determining the *in vivo* maturation, lifespan and splenic transport of iPSC-derived human cells.

CHAPTER 4:

CHARACTERIZATION OF HbF LEVELS IN SICKLE CELL DISEASE-SPECIFIC iPSC-DERIVED ERYTHROID LINEAGE CELLS

Introduction

Sickle cell disease: a brief description of pathophysiology

SCD comprises a group of disorders caused by the homozygosity or compound heterozygosity for the sickle hemoglobin (HbS; $\alpha_2\beta^S{}_2$) gene. This study focuses on the characterization of erythroid lineage cells derived from induced pluripotent stem cells (iPSC) from individuals who have sickle cell anemia. Sickle cell anemia is defined as homozygosity for β-globin gene (*HBB)* codon 6 GAG>G*T*G or glu6val mutation. Sickling diseases are prevalent in sub-Saharan Africa, Middle East, and the Indian subcontinent. Annually, 280,000 infants with sickle cell disease are born world-wide[290]. HbA, ($\alpha_2\beta_2$), is the normal adult hemoglobin. Eight percent of African Americans are carriers of the HbS mutation, and 1 in 600 newborns have sickle cell anemia. Nearly 100,000 sickle cell disease patients reside in the US. The clinical course of this disease is highly variable and affects many organs[79]. Upon deoxygenation, mutant β-globin polymerizes and forms a rigid structure, which is responsible for the characteristic change in erythroid cell shape, from a normal biconcave disc to a deformed sickle cell. This rigid β-globin polymer reduces cell flexibility, often resulting in vaso-occulusion and hemolysis. Vaso-occlusion, or the process of blocking blood vessels with sickled cells, is a predominant clinical manifestation of the SCD **(Figure 4.1)**. Occlusive episodes result in painful attacks often treated with opioid analgesics. Numerous episodes can result in ischemic injury and permanent organ damage. Despite the presence of HbS, individuals can present with a range in the severity of the disease phenotype. This indicates that

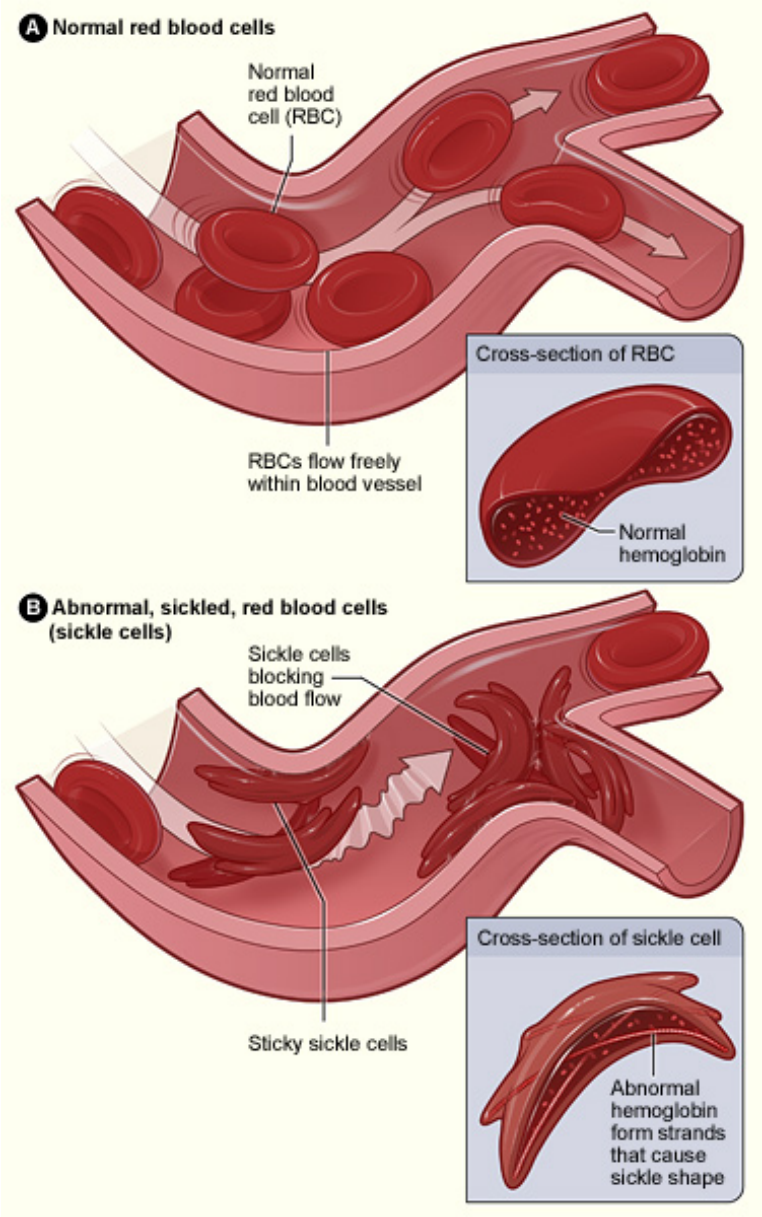

Figure 4.1. Diagram of HbS polymers altering red blood cell shape and blocking blood flow resulting in a vaso-occlusive episode. *http://www.nhlbi.nih.gov/health/health-topics/topics/sca/*

deoxyHbS polymerization is necessary, but insufficient alone to account for the marked heterogeneity of disease manifestations, which are genetically modulated and environmentally affected. Fetal hemoglobin (HbF $\alpha_2\gamma_2$) is predominant in the fetus and in infants, and individuals with sickle cell anemia have less severe disease when, HbF levels remain high as adults [72,74,83]. It is now understood that high amounts of HbF lower the concentration of HbS within a cell and also inhibits deoxyHbS polymerization[74].

Hemoglobin gene expression shifts during development from fetus to adult

Hemoglobin is a hetrotetramer made from two dimers, each a heterodimer containing one alpha-type globin and one beta-type globin. Alpha-type globins consist of alpha (α, *HBA2, HBA1*) and zeta (ζ, *HBZ*) types, with the later expressed solely embryonically. The beta-type globins are much more numerous and have specific temporal expression patterns related to development. They consist of epsilon (ε, *HBE*) in the embryo, gamma ($^{G}\gamma$, $^{A}\gamma$ *HBG2, HBG1*) in the fetus, with delta (δ*, HBD*) and beta (β, *HBB*) in the adult. In the developing embryo and the fetus, the majority of heterotetrameric consist of embryonic and fetal hemoglobin forms $\zeta_2\varepsilon_2$ (Gower1), $\zeta_2\gamma_2$ (Portland1), and $\alpha_2\gamma_2$ (HbF), with small amounts of $\alpha_2\varepsilon_2$ (Gower2). In adults this ratio is reversed, with 97% HbA, $\alpha_2\beta_2$, and only trace amounts of $\alpha_2\delta_2$ (2%) and $\alpha_2\gamma_2$ (<1%) **(Figure 4.2)**. It is not uncommon to see this ratio of hemoglobin expression altered in SCD patients, with HbF levels reported as high as 30% in adults.

Hemoglobin haplotype is associated with SCD severity and outcome

The persistence of HbF into adulthood has been extensively studied for its ameliorative effects on HbS polymerization, and has allowed for classification of patients based on genetic markers in and around the *HBB* gene cluster. Restriction site analysis has identified five distinct haplotypes

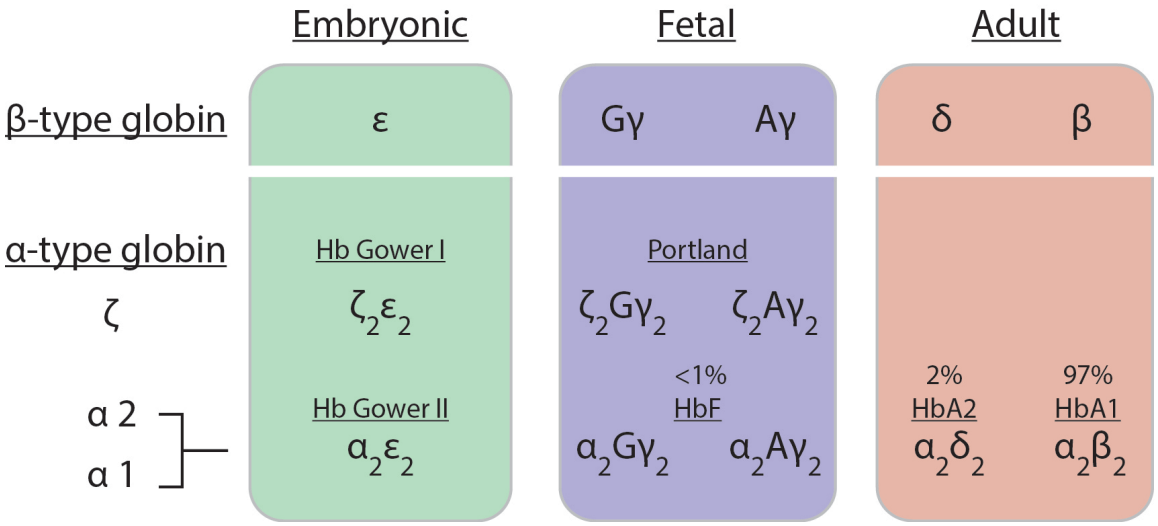

Figure 4.2. Tetrameric forms of hemoglobin present during embryonic, fetal, and adult stages of life. The predominant embryonic tetramers made of α, ζ paired with ε are Gower I and Gower II. Fetal tetramers are identified as Hb Portland and HbF with HbF the most abundant form in fetal development and present in small amounts in adults. The adult the tetrameric hemoglobin is HbA1, the most prevalent form, with minor amount of HbA2 formed from the α- and δ-globin proteins. Percentages indicate amounts typically present in adults. *Modeled after http://themedicalbiochemistrypage.org.*

linked to the sickle cell mutation: Senegal, Cameroon, Benin, Bantu (Central African Republic), and Arab-Indian[84,85]. A patient's haplotype has been associated with disease severity and outcome[86]. Individuals with the Bantu haplotype have been linked to a severe disease outcome due to high incidence of organ damage. Intermediate disease severity is typical with Benin haplotypes while the Senegal and Arab-Indian haplotypes have milder symptoms[86,87]. A mutation at -158 position in *HBG2* is related to higher HbF levels seen in the Senegalese and Arab-Indian haplotypes[87]. As HbF levels within each haplotype varies, it implies that factors other than elements linked to the *HBB* gene cluster affect HbF concentration.

Quantitative trait loci affect HbF expression in adulthood

Hereditary persistence of fetal hemoglobin was originally believed to be solely due to deletions in the *HBB* gene cluster or point mutations in promoters of the γ-globin genes. It is now understood that persistence of HbF into adulthood is inherited as a combination of quantitative genetic traits that are found throughout the genome. Studies performed on twins by Swee Lay Thein's group at Kings College London School of Medicine, demonstrated that quantitative genetic factors are responsible for 89% of HbF level variation[89]. These genetic factors are commonly known as quantitative trait loci (QTLs). QTLs are genetic loci that are associated with a quantifiable difference in HbF. The first QTL identified is a single nucleotide polymorphism at the -158 position of *HBG2*, found in 1985 by sequencing of the *HBG* genes[291]. The C-T polymorphism creates an Xmn1 restriction site hence it is sometimes termed the Xmn1-*HBG2* locus, and acts in cis. Other QTLs act in trans. Genome-wide linkage analysis in an extended Asian-Indian family identified a region on chromosome 6q23-q24[292,293] linked to higher percentage of HbF expressing cells. This region is now known as the *HBS1L-MYB* intergenic region (HMIP), for the two genes it lies between and accounts for 19% of the variation seen in HbF levels of Northern Europeans[93].

Furthermore, the advent of genome-wide association studies has led to the identification of SNPs in chromosome 2p16 through two separate studies[94,294]. These SNPs in intron 2 of the oncogene *BCL11A* are responsible for 15.1% of the HbF levels in Northern Europeans[94]. These three common QTLs only explain 44% of the variation in HbF expression levels in adults, suggesting that there are still unknown QTLs to be accounted for[293,295].

Hydroxyurea is an inducer of HbF and the only FDA approved treatment for SCD

Hydroxyurea (HU) is a ribonucleotide reductase inhibitor originally utilized as chemotherapy agent with potent effects on rapidly dividing cells in the bone marrow. It was approved for use as a treatment for SCD in February 1998 to reduce the frequency of pain crises and the need for blood transfusions in adult patients with recurrent moderate-to-severe painful crises (generally at least three during the preceding 12 months)[78,296,297]. While the efficacy of HU in the treatment of SCD is attributed to its ability to boost the levels of HbF, limited work on the genetic determinants of the HbF response to HU has been published[298]. Since HU's cytotoxic effect is most potent in rapidly dividing late erythroid precursors, their removal through stimulated apoptosis increases recruitment of early erythroid precursors that can produce HbF. Others have suggested that HU acts directly on late precursors to stimulate HbF expression. Alternatively, it may interrupt the transcription factors that selectively bind to promoter or enhancer regions around the globin genes, thereby altering the ratio of HbA to HbF[299]. HU might also have other mechanisms of action that account for its utility in SCD.

Patient response to HU treatment is highly variable with ten to twenty percent of patients having no clinically significant response. It has been hypothesized that the reason certain individuals do not respond to HU is due to the capacity of the patient's marrow to sustain the myelotoxicity encountered with HU[300]. Traditional methods for determining how and why certain

individuals respond to HU requires erythroid progenitor cells from many patients and the ability to study the bone marrow compartment of the same individuals. As this is technically difficult to do, iPSCs have the potential to grant researchers an unlimited supply of erythroid progenitors, which allows for the characterization of HU response and HbF levels. iPSC-derived erythroid cells also allow researchers to put these cells in mice to observe the *in vivo* role of the bone marrow compartment.

Materials and Methods

iPSC derivation and culture: iPSC derivation was achieved using the hSTEMCCA lentiviral vector as previously described[131]. Peripheral blood mononuclear cells (PBMCs) were used as source material for iPSC production[143]. Individual sample collection occurred at Boston Medical Center, Boston, MA or at King Saud University, Riyadh, Saudi Arabia Samples were centrifuged at 37°C for 25 minutes at 1800 rcf and the resulting buffy coat was collected in a 15ml Falcon tube. Cells were resuspended in 2 ml of expansion medium, consisting of QBSF-60 (Quality Biological 160-204-101), 50 ng/ml hSCF (R&D 255-SC-010), 10 ng/ml hIL-3 (R&D 203-IL-010), 2 U/ml hEPOgen (Amgen), 40 ng/ml hIGF-1 (R&D 291-GI-050), 50 mg/ml Ascorbic Acid (Sigma A4403), 100 mg/ml Primocin (Invivogen ant-pm-2) and 1 μM Dexamethasone (Sigma D4902). After 8-9 days, polybrene was added to the media (5 mg/ml) and the hSTEMCCA lentivirus was added to the culture at an MOI ranging from 1 to 10. After 24 hours, the inoculated culture was spun at 2250 g for 90 minutes and the polybrene media was discarded. The cells were then plated onto irradiated mouse embryonic fibroblasts (iMEFs) and cultured for roughly 15 days in "iPSC media" that includes DMEM F12 (Invitrogen 11330057) 10 ng/ml bFGF (R&D 233-FB-025) 1 ng/ml rho kinase inhibitor (Cayman Chemical 10005583) 20% knock-out replacement serum (KOSR) (Invitrogen 10828028) and 100 mg/ml Primocin. Clones were then picked and expanded for long-term culture. Hematopoietic progenitors were generated

from iPSCs using our previously published protocol[278]. Cells were kept in D7 media unless otherwise noted, 74% IMDM, 24% Hams F12, 1% B27 supplement, 0.5% N2-supplement, 0.5% BSA, 50ng/ml hVEGF, 100ng/ml bFGF, 100ng/ml hSCF, 25ng/ml hFlt3 Ligand, 50ng/ml hTPO (Genentech G140BT), 10ng/ml IL-6 (R&D 206-IL-010), 0.5U/ml hEPOgen (Amgen) and 0.2 mM 6-formylindolo[3,2-b]carbazole (FICZ) (Santa Cruz SC300019). Mitomyocin-C treated OP9 stromal layer was plated on gelatin coated well in DMEM, 10% FBS, 2mM L-Glutamine (Invitrogen 25030081), and 100 mg/ml Primocin.

Analysis of clinical records: De-identified and anonymized medical records were examined to extract desired information regarding HU usage, HbF levels, and disease pathophysiology. Statistical analysis and multidimensional plots comparing the above parameters were done.

Hydroxyurea treatment of iPSC-derived erythroid cells: A final concentration 0.5 μM of HU (Sigma H8627-1G), unless otherwise noted, was added to day 7 media. Cells were pelleted, washed and resuspended in day 7 media with and without HU. Cells were grown for 3-10 days with media additions every other day. The final concentration of HU was maintained throughout additions.

Quantitative RT-PCR: RNA was extracted using the RNeasy kit (Qiagen) according to the manufacturer's instructions and DNase treated using the DNA-free kit (Ambion AM1906). Reverse transcription into cDNA was performed using the High Capacity cDNA Reverse Transcription Kit (Applied Biosystems 4368814). Quantitative (real time) PCR amplification of cDNA was performed using Taqman probes for HBE (Hs00362216_m1) HBA

(Hs00361191_g1), HBB (Hs00758889_s1), HBG (Hs01629437_s1) on the Applied Biosystems StepOne machine. Relative gene expression was normalized to B-actin (Hs99999903_m1).

Intracellular flow cytometry*:* Roughly 10^5 cells, Fetalrol (Trillium Diagnostics, LLC FH101) or peripheral blood were collected, spun, and fixed in 0.05% glutaraldehyde (Sigma G5882)-0.1%BSA-PBS for 10 minutes. Cells were pelleted and washed three times with 0.1%BSA-PBS. Cells were permeabilized in 0.1% Triton (Life Technologies HFH10)-0.05%BSA-PBS for 3 minutes, 0.1%BSA-PBS added, and then cells were pelleted. Cells were re-suspended 0.1%BSA-PBS for staining. Samples were incubated for 30 min at ambient temperature with human antibodies including CD235-PE (BD 555570), and CD71-APC (BD 341028) or 15 minutes with HbF-FITC (Life Technologies MHFH01), washed and spun at 3300 rpm for 7 minutes, and re-suspended in 0.5% BSA in PBS. Samples were run on a BD FACScalibur using Cellquest Pro software and analyzed with FloJo 8.7.

Results

Analysis of clinical HbF readings demonstrated variation in HbF levels amongst individuals

Under an approved of Boston University School of Medicine IRB protocol for the collection of patient material for the creation of iPSC lines, consenting patients were

Sample	PB Draw	PB processing	Initial Freeze	Initial Thaw	Infection	Colonies Picked/(Frozen vials)	Pluripotency Staining
US-001	20110822	20110822	20110822		20111018	didn't get any clones	
US-002	20110822	20110822	20110822	20111222	20111018	3/3 each	yes
US-003	20110912	20110912	20110912		20110921	didn't get any clones	
US-004	20110912	20110912	20110912		20110921	3/3 each	yes
US-005	20110919	20110919	20110919		20110927	3/3 each	yes
US-006	20110926	20110926	20110926		20111004	3/3 each	yes
US-007	20110926	20110926	20110926	20111014			
US-008	20111017	20111017	20111017	20111222	20111025	3/3 each	yes
US-009	20111017	20111017	20111017		20111025	3/3 each	yes
US-010	20111024	20111024	did not process well and therefore discarded				
US-011	20111031	20111031	20111031		20111110	didn't get any clones	
US-012	20111031	20111031	20111031		20111110	3/3 each	yes
US-013	20111031	20111031	20111031		20111110	3/3 each	yes
US-014	20111107	20111107	20111107		20111117	3/3 each	yes
US-015	20111114	20111114	20111114	20111122	20111129	3/3 each	yes
US-016	20111114	20111114	20111114	20111122	20111129	3/3 each	yes
US-017	patient assigned ID but unable to draw blood						
US-018	20111121	20111121	20111121		20111129	3/3 each	yes
US-019	20111121	20111121	20111121		20111129	3/3 each	yes
US-020	20111128	20111128	20111128	did not expand enough to infect			
US-021	20111205	20111205	20111205		20111215	didn't get any clones	
US-022	20111219	20111219	20111219	did not expand enough to infect			
US-023	20111219	20111219	20111219	did not expand enough to infect			
US-024	20120109	20120109	20120109		20120118	3/3 each	yes
US-025	20120127	20120127	20120127		20120130	3/3 each	yes
US-026	20120127	20120127	20120127		20120130	didn't get any clones	
US-027	20120130	20120130	20120130	did not expand enough to infect			
US-028	20120130	20120130	20120130		20120207	3/3 each	yes
US-029	20120130	20120130	20120130		20120207	3/3 each	yes
US-030	20120206	20120206	20120206	did not expand enough to infect			
US-031	20120213	20120213	20120213		20120224	didn't get any clones	
US-032	20120227	20120227	20120227			2/3 each	yes
US-033	20120227	20120227	20120227			didn't get any clones	
US-034	20120305	20120305	did not process well and therefore discarded				
US-035	20120319	20120319	20120319		20120327	3/3 each	yes
US-036	20120326	20120326	20120326		20120403	3/3 each	yes
US-037	20120409	20120409	20120409		20120413	1/3	yes
US-038	20120430	20120430	20120430		20120508	3/3 each	yes
US-039	20120507	20120507	20120507		20120515	didn't get any clones	
US-040	20120810	20120810	20120810		20120824	didn't get any clones	
US-041	20121120	20121120	20121120		20121127	3 (10/3/3)	yes
US-042	20120917	20120917	20120917		20121001	didn't get any clones	
US-043	20121022	20121022	20121022		20121031	3 (10/10/10)	yes
US-044	20121022	20121022	20121022		20121031	3 (10/10/10)	yes
US-045	20121022	20121022	20121022		20121031	3 (10/3/3)	yes
US-046	20121112	20121112	20121112		20121120	didn't get any clones	
US-047	20121119	20121119	20121119		20121127	3 (10/3/3)	yes
US-048	20121126	20121126	20121126			2 (7/3)	yes
US-049	20121203	20121203	20121203		20121213	2 (10/3)	yes
US-050	20121203	20121203	20121203		20121213	didn't get any clones	
US-051	20130107	20130107	no buffy coat, tried processing, not enough cells to freeze or infect				

Table 4.1. BMC patient enrollment and iPSC generation. Information regarding ability to reprogram each patient sample displayed as year_month_day. Numbers of clones generated and how many vials were frozen of each clone is included. Grey boxes indicate an inability to generate iPSCs with that sample. Pluripotency staining for TRA1-81 was used for quality control. Production of iPSCs and staining was performed by S. Rozelle and A. Sommer.

Sample	Date Received	Initial Thaw	Infection	Colonies Picked/(Frozen vials)	Staining
SA 5	20120726	20121026	20121105	3 (10/3/3)	yes
SA 36	20120726	20130105	20130114	3 (5/3/3)	yes
SA 40	20120726	20121201	20121210	2 (10/3)	yes
SA 43	20120726	20120806	20120814	didn't get any clones	
SA 49	20120726	20120813	20120829	didn't get any clones	
SA 53	20120726	20130216	20130225	3 (10/3/3)	yes
SA 64	20120726	20130114	20130121	3 (5/3/3)	yes
SA 82	20120726	20130105	20130114	3 (10/3/3)	yes
SA 92	20120726	20120813	20120829	didn't get any clones	
SA 108	20120726	20130216	20130225	3 (10/3/3)	yes
SA 168	20120726	20120813	20120829	didn't get any clones	
SA 170	20120726	20121026	20121105	didn't get any clones	
SA 207	20120726	20130309	20130318	didn't get any clones	
SA 208	20120726	20130309	20130318	3 (3/3/3)	yes
SA 209	20120726	20130114	20130121	3 (10/3/3)	yes
SA 210	20120726	20130413	20130422	3 (10/3/3)	

Table 4.2. Saudi Arabian patient enrollment and iPSC generation. Information regarding ability to reprogram each patient sample displayed as year_month_day. Numbers of clones generated and how many vials were frozen of each clone is included. Grey boxes indicate an inability to generate iPSCs with that sample. Pluripotency staining for TRA1-81 was used as quality control for generated iPSC. Production of iPSCs and staining was performed by S. Rozelle and A. Sommer.

recommended to be part of the study through their clinician. Patient selection was voluntary and random at Boston Medical Center, Boston, MA and at King Saud University, Riyadh, Saudi Arabia. Not all samples from patients enrolled in the study were able to generate iPSCs **(Tables 4.1 & 4.2)**. Due to the fact that this is not a linear study, clinical information was gathered retroactively and therefore HbF levels, listed at a percentage of the total hemoglobin are limited to readings obtained in the course of regular clinical care **(Table 4.3, Figure 4.3A)**. Despite incomplete data the clinical information demonstrates that HbF levels vary in individuals over

SCD #	Age	Hydroxyurea	Hb F% 6m	1yr	2yr	3yr	4yr	5yr	6yr	7yr	8yr	9yr	10yr	20 yr	30yr	Lowest HbF >4yr	Avg HbF >7yr
5	9	no	24.3							8.5						8.5	8.5
40	20	no												4.1		4.1	4.1
43	6	no				36.9											
49	30	yes													20.4	20.4	20.4
53	14	no					24.9		16.1					12.6		12.6	14.4
63	26	yes											6.3	2.4		2.4	4.4
64	14	no								11.4	9		4.2			4.2	8.2
82	24	no								22.9	18.3	20.3	14.8	20.4		14.8	19.3
92	51	no														18.1	
108	9	no		53.6									29.6			29.6	29.6
168	16	no			36.2			25.3	24.3	17.7			18.4			17.7	22.2
170	3	no		34.2													
207	8	no					10.4				9.5					9.5	9.5
208	7	no					17.1									17.1	
209	12	no														transfused	
210	9	no							14.8							14.8	14.8

Table 4.3. HbF levels in Saudi Arabian patients as a factor of age. HbF% of the total hemoglobin content in the cells is noted for a range of ages. Lowest and average HbF% levels were calculated from readings taken after 4 and 7 years of age respectively.

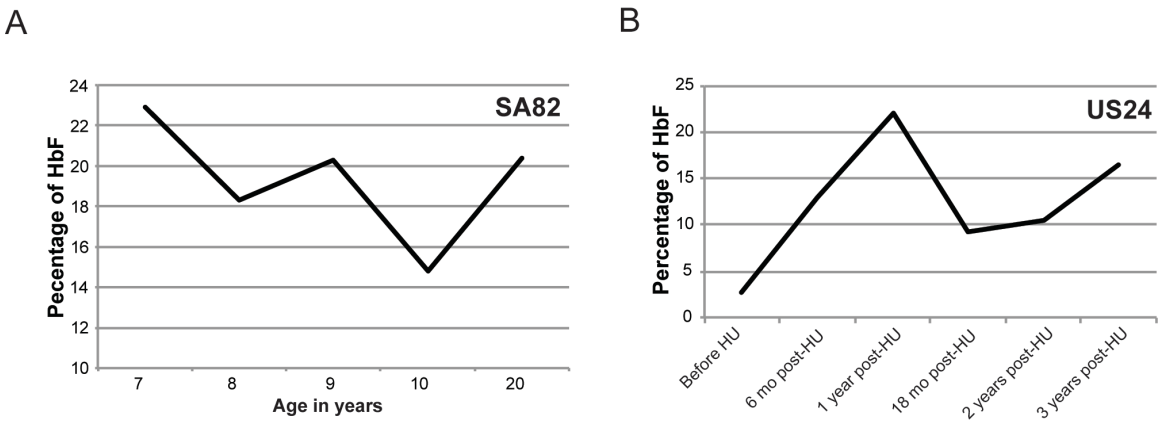

Figure 4.3. HbF levels plotted according to time with and without HU treatment. A) SA82 HbF% graphed in respect to age in years. B) US24 HbF% graphed in respect to time of HU treatment.

time irrespective of HU prescription. This could be a result of episodic blood transfusion or intermittent use of HU, information difficult to ascertain from available records.

iPSC-derived erythroid lineage cells respond to HU treatment

To determine if variations in HbF levels resulted from the differential ability of erythrocytes to respond to HU, I compared the response of patient-specific iPSC-derived erythroid cells to varying dosages of HU. To verify this response I planned to quantify changes in clinical HbF mRNA expression in response to HU treatment and determine if these changes correlated with changes induced in response to HU in erythroid lineage cells generated from patient-specific iPSCs.

Initial experiments were performed to verify the correct dosage and duration of treatment of iPSC-derived hematopoietic progenitor cells (HPs) based on information from previously published experiments using K562 cells. Initially I tested various dosages of HU for 5 days and saw a robust response in *HBG* mRNA levels when cells were treated with 0.5 μM HU **(Figure 4.4A)**. After determining the optimal concentration of HU, I conducted a time course and concluded that 10 days resulted in a greater than 2-fold increase in *HBG* expression **(Figure 4.4B)**. I compared the increase in *HBG* between control and SCD-specific derived HPs. I saw a difference in *HBG* expression following treatment with 0.5 μM HU for 10 days. When changes in *HBG* expression were quantified in SCD-specific cells, I found that the relative response to HU treatment was distinct for each cell line. US2.1 had an over 3-fold increase in *HBG* expression compared to SA82.1, whose *HBG* expression increased 1.3-fold **(Figure 4.4C)**. The level of *HBG* expression in untreated populations also varied significantly between cells lines, with SA82.1 having a starting amount of *HBG* expression 4 times higher than US2.1. This led me to question

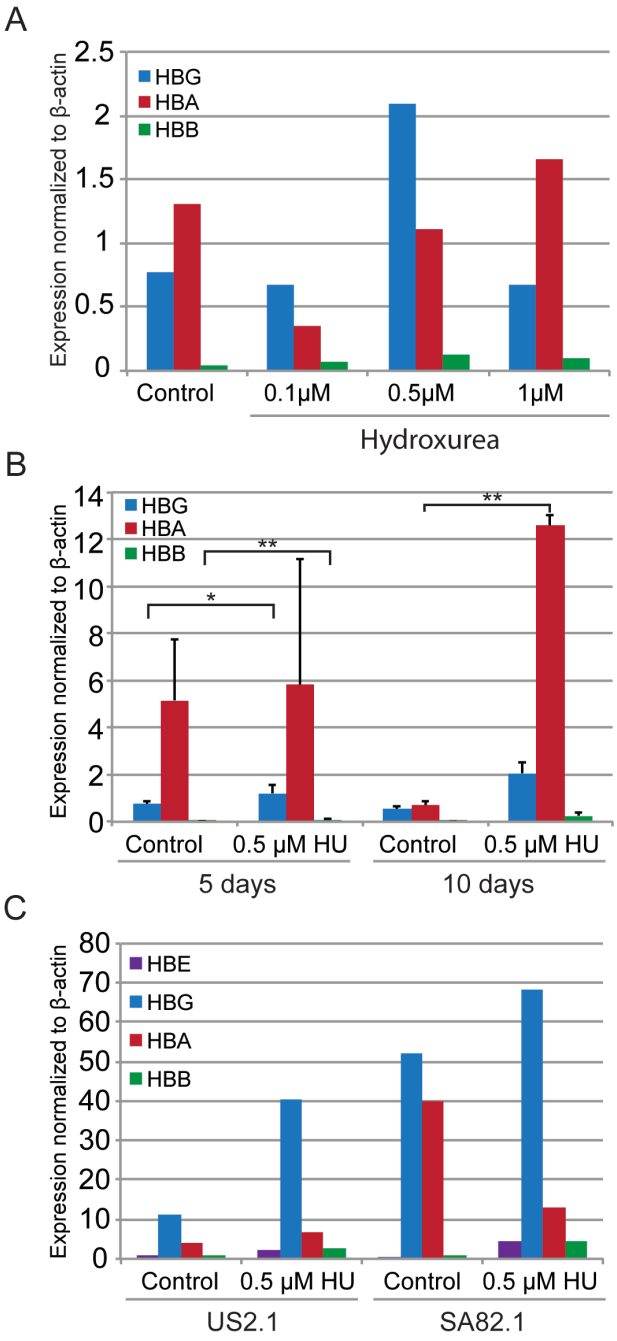

Figure 4.4. HBG levels increase following hydroxyurea treatment in erythroid lineage cells. A) RT-PCR for HBG, HBA, and HBB in wildtype cells treated with varying concentrations of HU for 5 days, n=1. Expression is normalized to β-actin. B) RT-PCR for HBG, HBA, and HBB in wildtype cells treated for 5 or 10 days with 0.5 μM HU, n = 3. Expression is normalized to β-actin. *P < .05, **P < .005. C) RT-PCR for HBG, HBA, and HBB in either SCD-specific US2.1 or SA82.1 cells treated with 0.5 μM HU for 10 days, n=1. Expression is normalized to β-actin.

whether baseline *HBG* expression, as well as the difference in response to HU, was reflective of what happened in the patients.

Determination of HU response in patients was complex due to variables in HU dosage and clinical management of the disease.

To test the hypothesis that patient-specific iPSC-derived erythroid lineage cells are capable of recapitulating an in vivo differential HU response, I first needed to determine how observe how HU usage affected HbF levels in the patient **(Table 4.4, Figure 4.3B)**. Patient treatment and response information was obtained from medical records. Initial inspection revealed highly variability among patients in dosage and timing of HU treatments, transfusion frequency, crisis history, age, gender and ethnicity, all of which could significantly affect the observed increases in HbF protein levels. This nullifies utilizing a simple percentage increase in HbF following initiation of HU as a way to determine responsiveness. To account for some of the variables in treatment, I decided to compare HbF% (percentage HbF of total hemoglobin) and HU dosage (mg) with respect to time. Data surrounding transfusions and crises was noted in an effort to reduce the number of variables **(Figure 4.5B)**. Mean corpuscular volume (MCV) values of the patient's RBCs was used as a surrogate to confirm compliance of HU use, as MCV should increase above baseline while taking HU[301]. Each individual had a unique profile based on his or her clinical history, which we used to categorize each as a responder versus a poor responder to HU **(Figure 4.5B)**. Individuals whom showed greater than a 5% increase in HbF levels with a corresponding increase above threshold in MCV were considered responders. Weak responders had variable increases and decreases in HbF levels with MCV increases above threshold. Those with no visible increase in HbF levels were considered non-responders. While the plots were visually informative as to HbF levels, there was additional important data to consider. Clinical

						HbF levels								
ID	taking HU at time of collection?	HbF reading at collection	Date of HU start	Earliest HU Prescription at BMC	HU stop date	2 years pre-earliest HU pres.	1 year pre HU	6 months pre-HU	At Commencement	6 months post HU	1 year post-HU	18 months post-HU	2 years post-HU	3 years post-HU
US-002	Yes		8/22/11						6.5					
US-004	Yes	9.2	Unknown	9/12/03			5.1		4.2	5.3				
US-005	Yes		2/14/11					3.6	2.5	5.2	7.6	12.5		
US-006	Yes	8.5	Unknown	8/31/04					16.6			17.1	16.7	
US-008	Yes	16.4	Unknown	1/7/02		18.1					8.9	4.6	15	
US-009	Yes		11/6/06										4.7	
US-011	Yes	4.5	Unknown	4/8/03				33.5	8.7				8	13.4
US-012	Yes	5.7	Unknown	11/21/01		12.3				8.3	5.1	3.7	6.4	6.7
US-013	Yes	0.9	2/16/07					1.9	1			2.3	2.6	1.2
US-014	Yes		Unknown	9/6/09								1.3	1.8	1.6
US-015	No		Unknown		06/31/1999									
US-016	No	15	Unknown	11/5/02	9/24/03		12							
US-018	Yes	5.2	9/26/05			0.9	1.7	1.4	2.1	9.7	5.4	4.5	3.2	1.2
US-019	Yes	7.1	Unknown	9/6/07								6.4		
US-021	Yes		10/14/07			3.6	2.8	4.7	3.2		7.3		5.1	
US-024	Yes	3.1	6/29/05						2.7	12.9	22.1	9.2	10.4	16.5
US-025	No	2	2/27/12	N/A	3/26/12									
US-026	Yes	20.3	Unknown	4/25/01					16.7	24.6	30.1		27.6	7.7
US-028														
US-029	Yes	5.9	6/24/05						4.7					4.3
US-031	Yes		2/9/07			8.1			2.4	0.9	3.5			
US-032	Yes	6.1	Unknown	12/8/08		8	7.1		9.3	10.1			13.8	
US-033	Yes	11.8	9/1/08	8/5/10		5.4			5.1	6.7				11.8
US-035	No	4.5		10/8/07	5/1/09				4.7					
US-036	Yes	20.4	12/3/04					8.8	3.8	21.4	25.3		19.7	18.4
US-037	Yes	8.9	4/27/09	9/30/05	10/2/07	6.9	3.6	1.2	2.2	8.5				8.9
US-038	Yes	3.9	Unknown	10/17/01		7.1	16.5				10.6			6
US-039	No	2	N/A	N/A	N/A									
US-040	No		N/A	N/A	N/A									
US-041	No		6/16/04		8/9/11		3		4.6	17.2	18.5	14.5	10	17.6

Table 4.4. HbF levels in BMC patients while taking hydroxyurea overtime. HbF% at the date of collection was obtained from an identical peripheral blood sample as the one for iPSC generation. If known, the initial prescription date or earliest BMC prescription date for HU is noted. HbF% of total hemoglobin in the cells is listed for time points before and after initiation of HU treatment.

notes for potential weak/non-responders revealed that many had been explicitly taken off of HU treatment (2 of 3 patients), while another was noted as noncompliant with regularly taking their medication. Once these individuals were excluded from the analysis, only robust responders remained. Having eliminated all potential for a comparison between *in vivo* clinical treatments and *in vitro* cell-based experiments, I focused the remainder of my research on identifying iPSC lines that represent the potential variety of HbF levels and haplotypes. This resulted in the use of six iPSC lines, three control and three SCD-specific lines. The SCD-specific lines consisted of one African-American (US2.1), one Arab-Indian (SA108.1), and one Benin haplotype (SA82.1) with average HbF levels ranging from 6.5%-29.9% **(Table 4.5)**. While there are many SCD-specific iPSC lines to study, characterization of HU response did not reveal any weak or non-

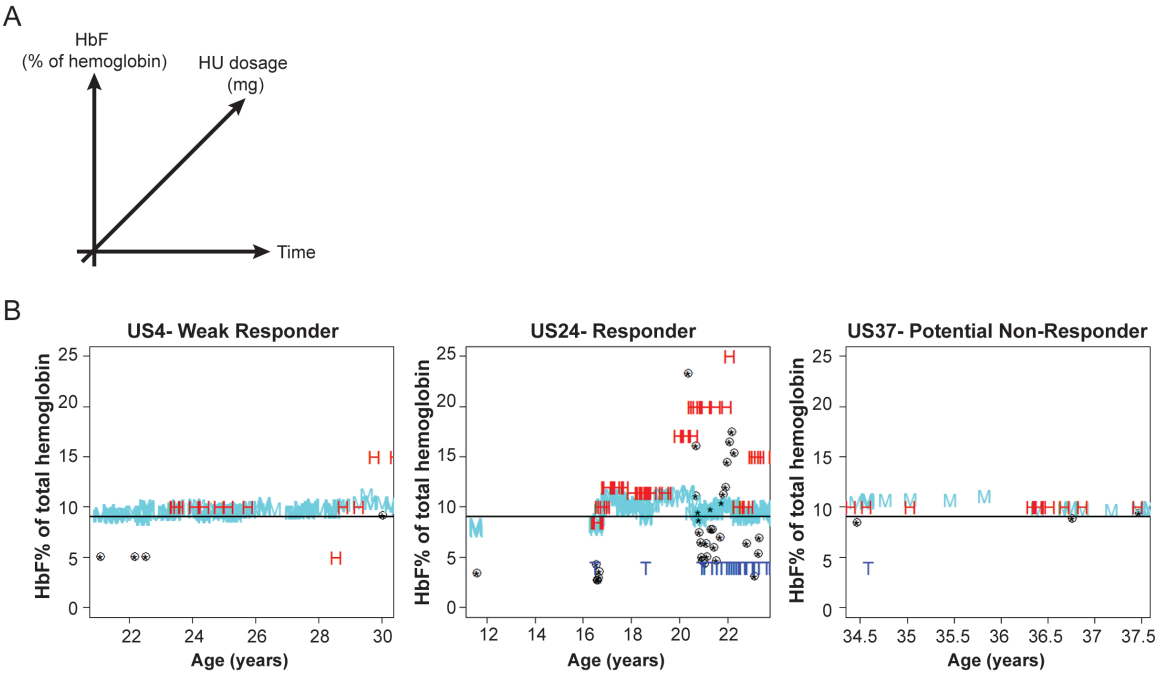

Figure 4.5 Analysis of HbF levels in respect to HU dosage and time. A) Diagram illustrating the goal of analyzing HbF% and HU dosage as a product of time. B) Plots of three individuals US4, 24, and 37 in which HbF% (red H), MCV (teal M), transfusions (blue T), and HU dosage (⊗) are plotted according to age of the patient in years. MCV is plotted as MCV/10 against a normal value of 90 fL (black line). HU is plotted as dose/100 mg in reference to the y-axis.

Cell Line	Phenotype	Collection Site	age	Gender	average % HbF	Rx HU
BU1	control	BMC	43	M		no
BU5	control	BMC	45	M		no
BU6	control	BMC	39	M		no
US2.1	HbSS	BMC	34	F	6.5	yes
SA82	Benin	Saudia Arabia	24	M	19.9	no
SA108	Arab	Saudia Arabia	9	M	29.6	no

Table 4.5. Cell lines used for analysis of HbF have various baseline HbF levels and phenotypes.

responders. Therefore, the focus of this project changed to recapitulating the *in vivo* variation in HbF levels in my *in vitro* system.

HBG and HBA globin gene expression increased in culture over time

To further understand why there are differences seen in *HBG* expression in our cultures, I performed a time course to test if culture maturation played a role in *HBG* expression. Cells were analyzed by RT-PCR on Day 15, 17 and 24, in which Day 0 is defined as the first day of the HP differentiation protocol[302]. On day 15 cells are isolated from the adherent layer from which they originated. I choose day 17 and 24 for the amount of time the cells were absent from the feeder layer, under the assumption that the change in culture environment affects the maturation capabilities of the cells. Both BU1 and SA82 cell lines showed trend of *HBG* and *HBA* expression increasing over time **(Figure 4.6)**. This is seen to a smaller lesser extent in SA108.1 as significant variability between experimental replications of SA108 masked the emergence of any consistent trends. Neither *HBB* nor *HBE* showed any significant changes in expression throughout the three time points.

Fetal hemoglobin protein levels showed variation between cell lines and decreased over time

While gene expression can be indicative of protein expression, it is not always correlative. In order to explore the protein levels of HbF, I adapted a clinical assay designed to detect fetal-maternal hemorrhage using flow cytometry. This assay allows the quantitative analysis of HbF at the single-cell level, which allows for a comparison of multiple time points and conditions. Fetalrol, peripheral blood spiked with various amounts of cord blood, was the positive control for the presence of HbF, while peripheral blood alone served as the negative control **(Figure 4.7)**. Consistent with mass spectrometry results **(Figure 2.11)**, erythroid lineage cells express high

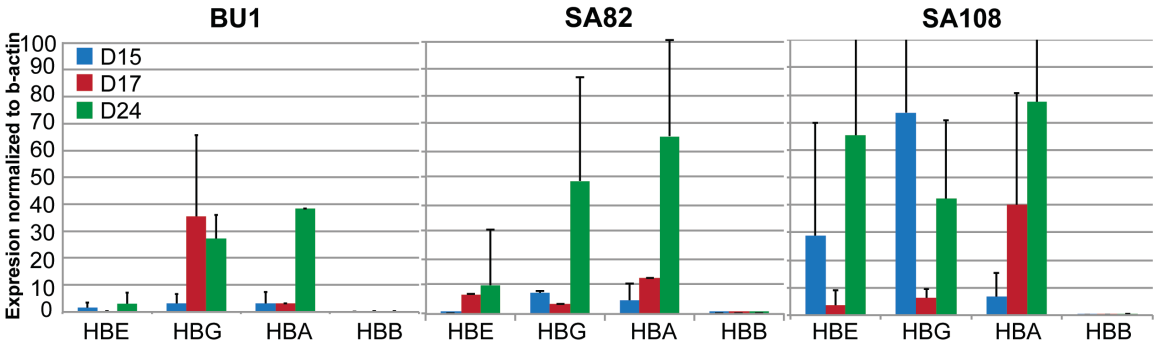

Figure 4.6. Globin expression in erythroid lineage cells over time. RT-PCR for HBE, HBG, HBA, and HBB on days 15, 17, and 24 in one wildtype, BU1, and two SCD lines SA82 and SA108, n=3. Expression is normalized to β-actin.

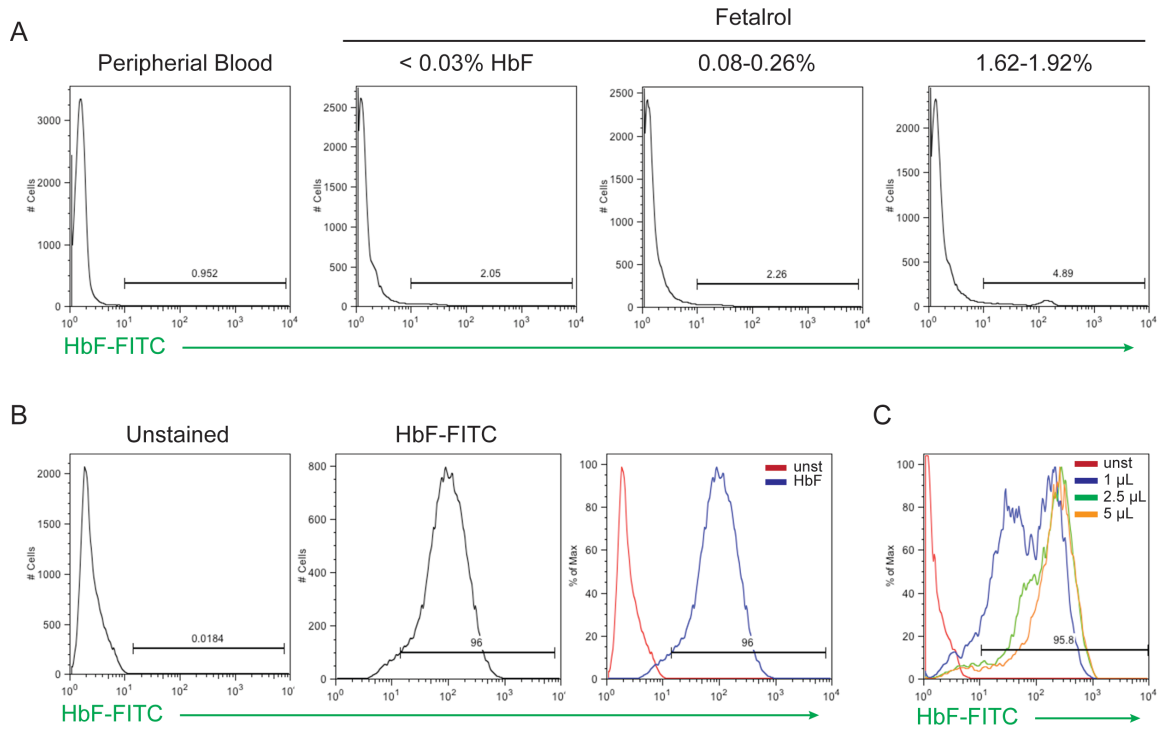

Figure 4.7. Intracellular FACS analysis of HbF protein expression. A) FACS histograms of peripheral blood with increasing amounts of HbF can be detected using an intracellular FACS protocol. B) FACS histograms of iPSC-derived erythroid lineage cells stained for HbF. C) Titering of HbF-FITC antibody in erythroid lineage cells found 2.5 µL to be optimal for detection of low and high HbF expressing cells.

amounts of HbF. I also attempted to simultaneously assess changes in HbF and HBB protein expression using an antibody recognizing HBB. Unfortunately, since RT-PCR quantification of *HBB* gene expression was consistently below the level of detection **(Figure 4.6)**, I was unable to draw any meaningful conclusions.

Both control and SCD cell lines displayed significant variation of HbF levels between cell lines and across time points **(Figure 4.8)**. Wildtype lines BU1, 5, and 6 decrease their HbF levels as the cells mature overtime, mimicking definitive development. Unfortunately, this trend is also seen in SCD-specific lines, suggesting that the cells are undergoing limited maturation and are not switching to HbA expression. Statistical analysis revealed no significant differences in the mean HbF levels amongst the lines or when comparing grouped wildtype and SCD lines. Perhaps a large sample size will give enough power to observe any subtle changes. By not selecting for erythroid specific cells in this assay, the cells that were interrogated for HbF expression were a heterogeneous population. There could be a small subset of cells that are maturing and switching hemoglobin expression, but are masked by the larger population. It was therefore important to interrogate the maturation state simultaneously with HbF expression.

Intracellular FACS assay simultaneously determined maturation and hemoglobin expression

As maturation (progression towards a terminally differentiated erythrocyte) and hemoglobin switching are two separate processes, it is imperative to correlate maturation state with HbF levels. To accomplish this I modified the previously mentioned intracellular HbF FACS assay to include CD235 and CD71. This allows gating for erythroid specific cells with CD235, and subsequent examination CD71 and HbF expression with gates generated with single stains **(Figure 4.9)**. Quantification was done to enable comparisons between the control lines (BU5, BU6) and SCD-specific lines (US2.1, SA018.1) for multiple criteria. There is an increase in most

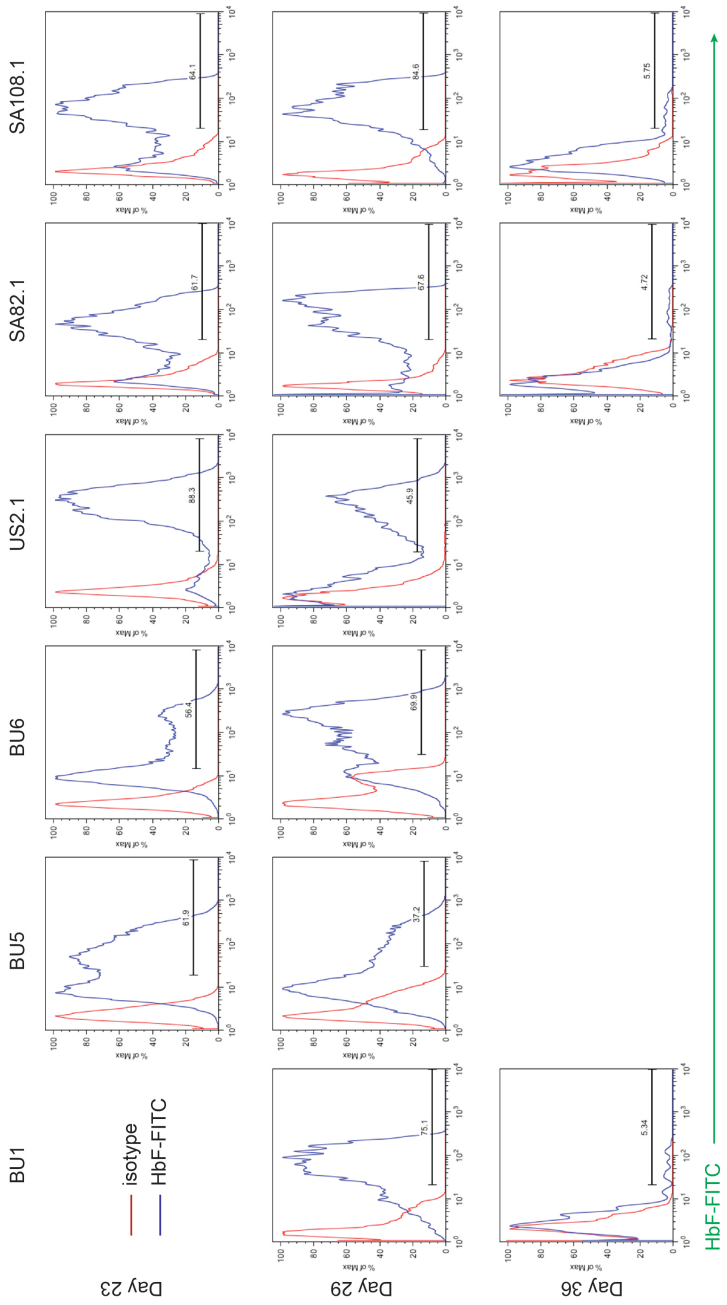

Figure 4.8. HbF levels vary amongst cell lines and over time. HbF levels plotted as histograms in comparison to isotype for three control lines (BU1, BU5, BU6) and three sickle cell lines (US2.1, SA82.1, SA108.1) for days 23, 29, and 36 of the differentiation protocol.

criteria: CD235+ gating (58.7% vs. 92.5%) CD235+ only (34.9% vs. 88.8%), CD235+ CD71+ (20.8% vs. 27.1%), and CD235+ HbF (15.8% vs. 29.8%), between BU5 and SA108.1 **(Figure 4.10 & 4.11)**. It is expected that a SCD line that has higher HbF compared to control *in vivo*, will have more HbF *in vitro*. However, quantitatively the other control line BU6 looks more similar to the disease lines, demonstrating that there is heterogeneity even in the in the control lines **(Figure 4.11)**. This heterogeneity makes seeing a disease specific change difficult. Two populations that are HbF+, a low ($<10^2$) and a high ($>10^2$) are found by dot-plot and histogram analysis. BU6 and SA108.1 have a population of cells that are HbF^{low} and $CD71^{low}$, the description of cells that are maturing (migrating to solely CD235+) and undergoing hemoglobin switching (losing HbF expression) **(Figure 4.11B & C)**.

Discussion

While the use of hES and iPSCs provides an unlimited supply of erythroid progenitors for study, iPSCs allow for the creation of SCD-specific iPSC cells. Generation of iPSCs from mononuclear cells collected during a routine peripheral blood draws, has enabled us to create SCD-specific iPSCs from patients around the world. A diverse library of iPSCs produces patient specific and genetically defined erythroid cells and facilitates our ability to repeatedly examine differences among patients.

A patient's ability to respond to HU cannot be anticipated, nor is fully understood. Initially, the SCD-specific iPSC library was to be utilized to recapitulate a patient's responsiveness to HU, and ultimately for drug screening of potential therapeutics. *HBG* expression increased following *in vitro* treatment of erythroid lineage cells with HU. This effect was seen in one control and two sickle cell lines **(Figure 4.4)**. It was observed that the SCD lines

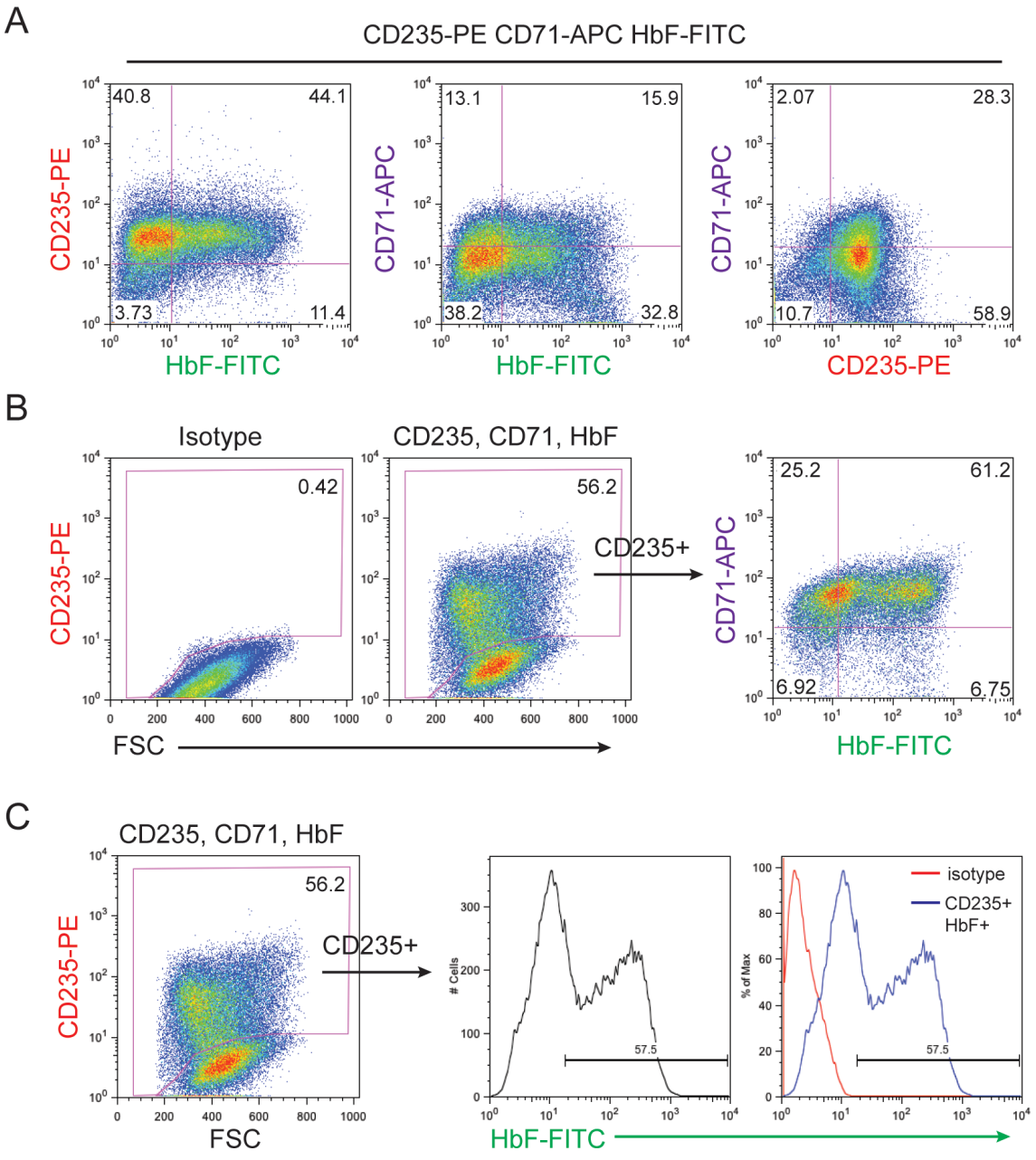

Figure 4.9. 3-color intracellular FACS for HbF, CD235 and CD71 in day 30 erythroid lineage cells. A) Representative FACS dot-plots of triple stained cells B) Representative FACS dot-plots of cells gated for CD235 and then interrogated for CD71 and HbF. C) Representative FACS dot plots for CD235+ cells interrogated solely for HbF expression as displayed in histograms.

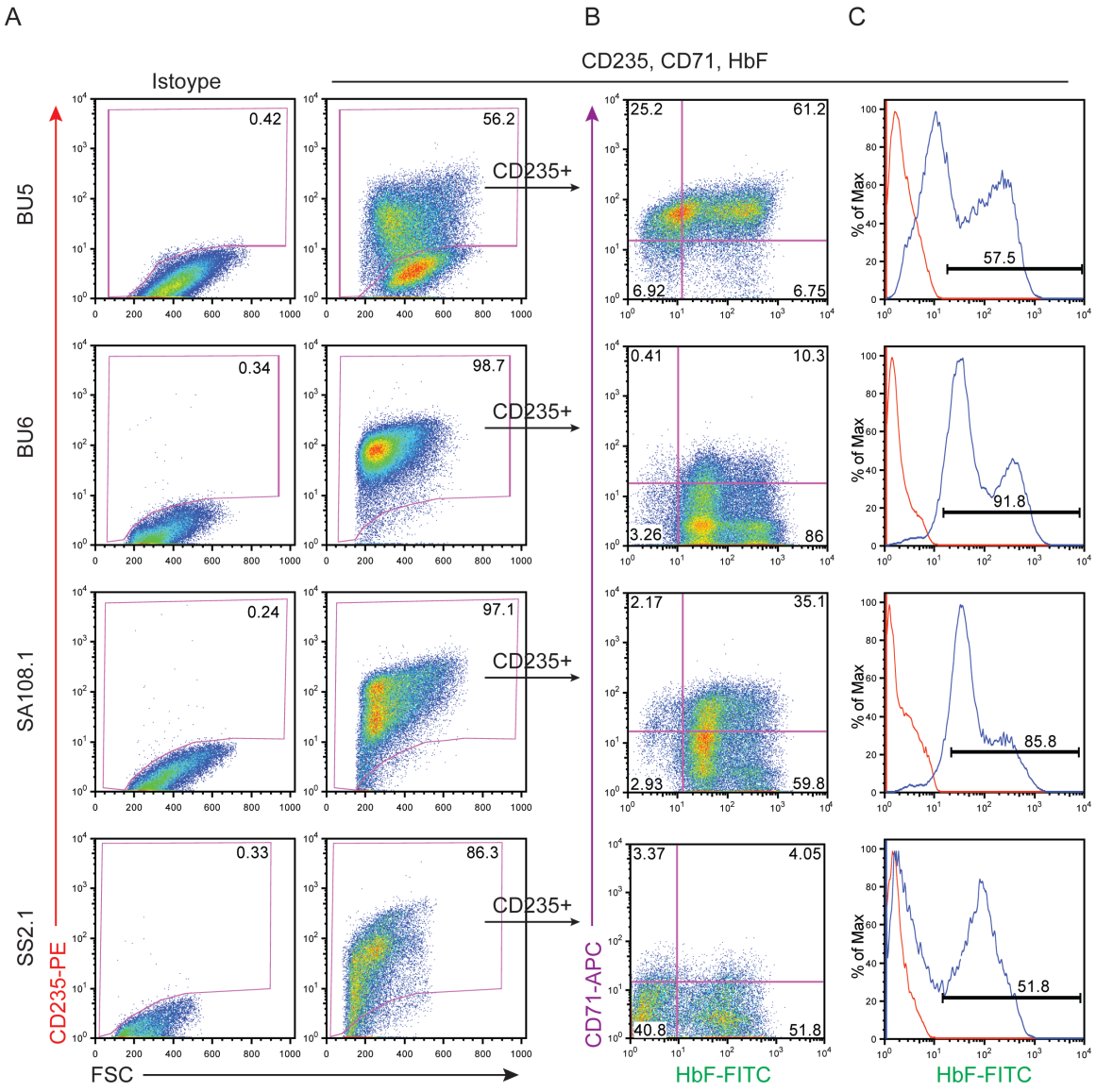

Figure 4.10. Comparison of day 30 control and SCD-specific erythroid lineage cells for HbF, CD235 and CD71 expression. A) Representative FACS dot-plots of triple stained cells subsequent gating for CD235+ cells of two control lines (BU5, BU6) and two SCD-specific lines (US2.1, SA108.1) B) Representative FACS dot-plots of CD235+ cells interrogated for CD71 and HbF expression. C) Representative FACS histograms of CD235+ cells interrogated solely for HbF expression.

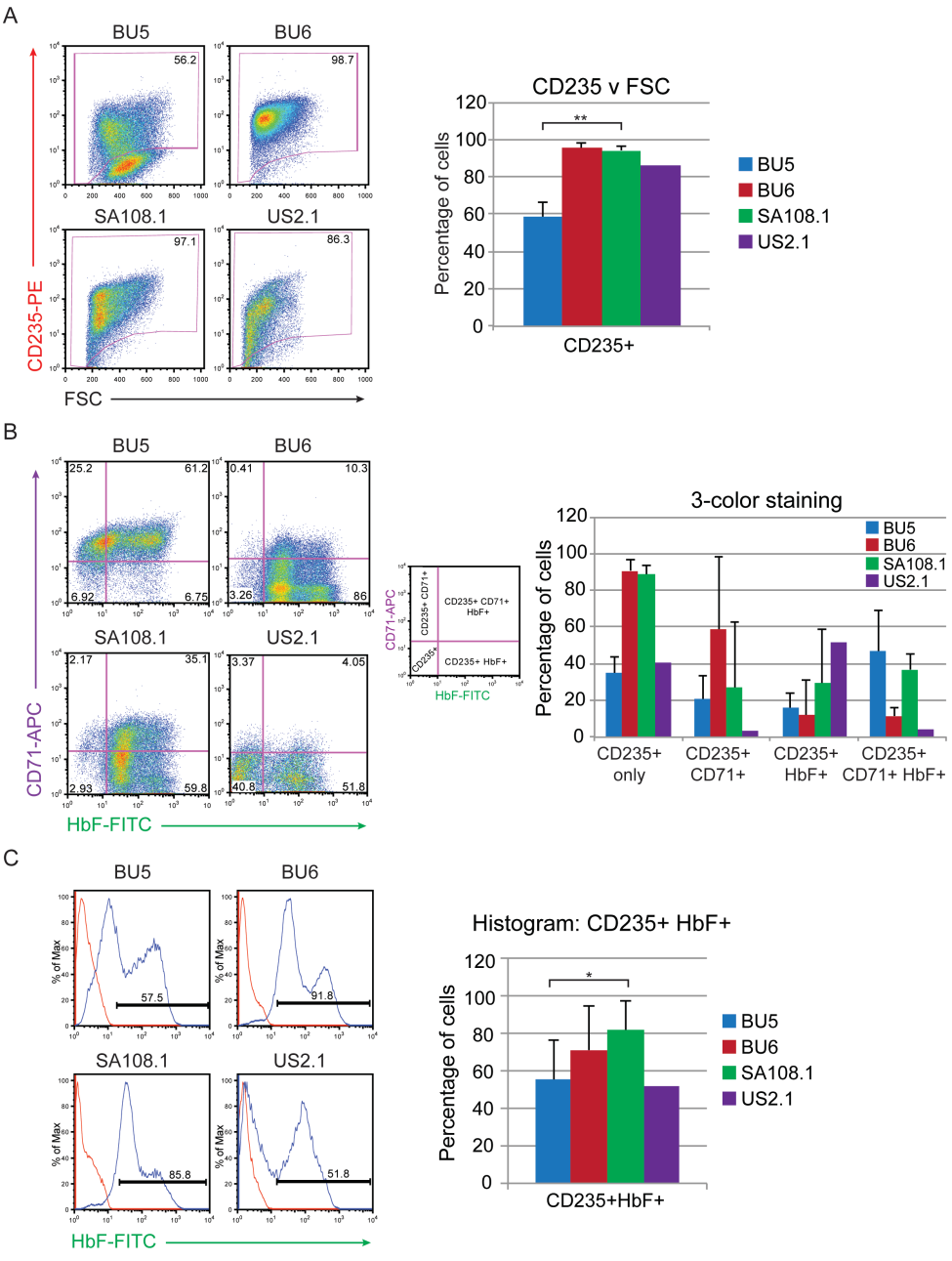

Figure 4.11. Quantification of control and SCD-specific erythroid lineage cells for CD235, HbF and CD71 expression in 3-color intracellular FACS assay. A) Representative FACS dot-plots of triple stained cells gated for CD235+ cells, bar graph of the percentage of CD235+ cells. B) Representative FACS dot-plots of CD235+ interrogated for CD71 and HbF expression, bar graph of the percentage of cells that are CD235+ only, CD235+ CD71+, CD235+ HbF+, or CD235+ CD71+ HbF+. C) Representative FACS histograms of CD235+ cells interrogated solely for HbF expression, bar graph of the percentage of cells CD235+ HbF+ by histogram. All data represents n=3, except US2.1 n=2. *P<.05, **P<.005.

had differential responses to HU *in vitro*, suggesting that I could recapitulate differences seen in the patient.

As elusive as the reasons behind a patient's response to HU are the methods to characterize strong or weak responders. In an ideal situation, HbF levels of individuals taking similar doses of HU could be compared over time, and a percentage increase in HbF levels could be used to differentiate strong from weak responders. As we were not selective in enrolling patients whom were taking a particular dose of HU, we have very few individuals whom could be compared using the above method. This led me to attempt to remove the variability in our clinical data by plotting HbF (percentage) and HU prescription (mg) as a product of time with transfusion history and MCV values noted. I was able to identify responders, greater than a 5% increase in HbF levels with an increase in MCV, weak responders, variable increases in HbF levels with increased MCV, and non-responders, no increase in HbF. Unfortunately, the identified weak and non-responders were either non-compliant or had been taken off HU **(Figure 4.5)**. While other researchers have attempted to classify HU response with other indicators such as *in vitro* RNA expression[303,304] or particular haplotypes[305,306], no one has derived a predictive model for an individual's ability to respond to HU.

Based on the patient information available, I used three SCD iPSC lines to compare to three control lines for the remainder of my studies. The SCD lines represent different haplotypes, Arab-Indian, and Benin, as well as a range of average HbF levels from 6.5-29.6% **(Table 4.5)**. With multiple haplotypes and HbF expression I hoped to visualize differences in HbF expression in my *in vitro* analysis of the lines.

Previous results from in Chapters 2 (Figure 8) & 3 (Figure 5A) demonstrated that the HPs produced through our differentiation methods are capable of limited maturation in the final progenitor media, day 7. I also observed variable HbF expression across iPSC lines by RT-PCR. I

therefore analyzed *HBG* expression in control and SCD-specific lines as a time course in day 7 media. Both *HBG* and *HBA* expression increased over time suggesting the cells ability to alter hemoglobin expression as a result of maturation **(Figure 4.5)**.

Since mRNA expression is not always correlated with protein levels, I sought to corroborate our RT-PCR findings with FACS-based protein quantification[307]. We know from mass spectroscopy results (Chapter 2, figure 9) that these cells had high levels of globins typically expressed during embryonic development, HBE and HBZ, and during fetal development, HBG and HBA. Mass spectrometry is extremely useful for identifying simultaneous expression of hemoglobin, but as performed was not quantitative. I adapted an assay for fetal-maternal hemorrhage using FACS to quickly and quantitatively assess HbF expression in various cell lines over time. This assay allows to me accurately quantify HbF levels in differentiated erythroblast cells and observe the reduction in HbF as cells mature into fully differentiated erythrocyte. Since the reduction in HbF was so dramatic between day 29 and day 36 **(Figure 4.7)** I further analyzed the maturation state and HbF levels of cells at day 30.

Intracellular staining for HbF, while simultaneously staining for maturation markers CD235 and CD71, quantitatively describes the maturation state of the cells in respect to HbF expression. Interestingly, BU6, a control line and SA108.1 have similar levels of CD235 expression and HbF expression when analyzed individually. When compared together, the SCD-specific lines have a higher proportion of CD235+HbF+ cells than the control lines (40.7% vs. 14.0%). Two populations of HbF expression: high and low, were observed both by scatter-plot and histogram analysis of CD235+ cells **(Figure 4.8)**. This suggests that the cells are able to mature and may be capable of hemoglobin switching. It is important to note that without FACS data for other hemoglobins, switching cannot be confirmed and these results may represent

variation in embryonic hemoglobin as well. While these differences are subtle, they do suggest that this system is capable of recapitulating *in vivo* differences seen between individuals.

Each iPSC line, control or SCD-disease specific is capable of creating erythroid lineage cells that can be used to characterize both maturation state and HbF levels. When comparisons were made amongst lines, subtle differences in HbF levels and maturation states were seen. These cells, while expressing primarily HbF, can modulate their HbF levels in response to maturation or HU treatment. These results further demonstrate that iPSC-derived erythroid lineage cells are capable of reflecting the differences seen between individuals. It is interesting to note that most clinical differences are observed in cells that express primarily HbA globin, and little has been done to study HbF modulation in primitive erythroid cells expressing HbF. My results suggest that HbF levels can be modulated in primitive cells, however, I hypothesize that a profound difference, similar to that seen in the patients, in HbF levels will be observed between lines in cells expressing HbA.

CHAPTER 5:

GENERAL DISCUSSION

Erythropoiesis has been studied extensively in xenopus, zebrafish, rats, chickens, mice, and humans. Yet with all we understand about the process of making RBCs, efficiently recapitulating this process *in vitro* continues to elude researchers. The limitation in the production of RBCs has hurt the SCD field's ability to conduct a global study without returning to the patient for fresh samples. The use of hES and iPSCs give researchers an unlimited supply of patient material, but only iPSCs allow for the creation of SCD-specific iPSC cells. By generating iPSCs from mononuclear cells collected during a routine peripheral blood draws; we have been able to create SCD-specific iPSCs from around the world. This diverse library of iPSCs allows for the production of erythroid cells that mimics the genetic context of the patient and facilitates our ability to repeatedly examine differences between patients. Unfortunately, an even more difficult process than making patient specific RBCs, is making RBCs that have matured to produce enucleated RBCs with expression of HbA^{233}. HbA expressing RBCs are an ideal tool for studying novel SCD therapeutics and recapitulating clinical differences observed in the patient. Using erythroid progenitors derived from iPSCs generates large numbers of cells can be obtained for studies into the steps of maturation and hemoglobin switching as well as exploring new HbF inducing drugs.

The goals of this project have evolved as we have learned more about the patients and the cells we have generated. The first goal was the efficient generation of erythroid lineage cells from an iPSC source without the support of co-culturing with feeder cells. Our methodology to produce HPs utilizes a two dimensional system in which the oscillation of cytokine signaling allows the cells to create their own microenvironment. The oscillation mimics the cytokine

gradient seen in early germ layer, tissue, and cell lineage specification. The cells produced are very similar to the short-lived MEP in surface marker expression, mRNA expression, and lineage specification. While the length of time to produce progenitor cells is shorter than previously published results, the limited number cells produced was similar. We then explored a new area of hematopoietic research based on recently published literature suggesting that the AhR is involved in stem cell and progenitor expansion[160].

We discovered that the AhR agonist FICZ has a physiological and functional role in normal hematopoietic development, and that modulation of the AhR in bipotential hematopoietic progenitors can direct cell fate to either the erythroid or megakaryocyte lineage. Incorporation of FICZ in our directed differentiation protocol dramatically increases the number of HPs produced. This is very important for multiple reasons, one the revelation that AhR plays a role in the growth and differentiation of two blood cell types; and two, that the expansion of HPs resulted in tremendous numbers of cells for the further study of both the megakaryocyte and erythroid lineages. We believe that the observed logarithmic expansion of cells is due to decreased cell death and is consistent with previous studies which suggest that the AhR can control apoptosis[211–213]. Our data suggests that FICZ, which is produced naturally as a tryptophan metabolite, could be playing a role in the regulation of hematopoiesis *in vivo*, possibly in concert with additional endogenous AhR ligands.

In addition to allowing for the exponential expansion of HPs, our results indicate that AhR modulation is involved in the further specification of both the erythroid and Mk lineages. We found that increased AhR signaling supports the differentiation of erythroblasts and conversely, antagonism leads to Mk specification. Although EPO and thrombopoietin are the major drivers in RBC and platelet development, our results suggest that AhR may play a cytokine-independent role in the development and specification of these lineages.

With the efficient generation of HPs that could be directed to the erythroid lineage, my subsequent goal became the generation of an *in vitro* system in which to produce enucleated RBCs. Erythroid cell maturation and hemoglobin switching are two separate processes that do not rely on each other. Mature cells can produce HbA or persist in HbF expression, however primitive cells rarely produce HbA. I set out to characterize the ability of iPSCs-derived erythroid lineage cells to mature and express HbA. Erythroid maturation occurs most reliably on stromal cell layers such as murine fetal liver or human bone marrow stroma (OP9). Since co-culturing creates opportunities for contamination of the produced cells, I set out to demonstrate that our cells are capable of maturation, and then to do so in a chemically defined manner. Limited maturation was observed in our HP production media, Day 7, as seen by surface expression of CD235 and CD71. This media, while good for production and expansion of HPs, contains cytokines that block further differentiation and maturation. Ultimately the removal of progenitor producing cytokines with addition of plasmanate, EPO, and transferrin creates a uniform population of CD235+CD71+ cells. Alternatively cells solely CD235+ can be produced in erythroid maturation media 2. This same media was responsible for an increased production of hemoglobin, which is required for maturation. This demonstrates that the cells are capable of maturation.

Very limited, if any enucleation was seen in cells that were capable of maturation. This may result from the lack of supporting macrophages or ideal culturing conditions. Many believe that signaling from the macrophage is responsible for the final stage of maturation, the expulsion of the nucleus[65]. It would be interesting to see if there is an increase in enucleation when cells that have been in EMM2 are co-cultured with macrophages. Similar to the erythrocyte maturation field, only recently has a efficient chemically-based protocol for the production of macrophages from iPSC been developed, as all previous methods required co-culture and purifications steps[308].

These results suggest that soon researchers will be able to produce RBCs and macrophages from the same individual that can be co-cultured for the efficient production of mature, enucleated RBCs.

Cells capable of maturation may not undergo hemoglobin switching and express HbA. This is seen in RBCs produced by the AGM that are capable of maturation, but still express embryonic globin. iPSC-derived erythroid lineage cells are embryonic and fetal in nature, as seen by RNA and protein expression studies. These cells express *HBE, HBZ, HBA*, and *HBG*, but not *HBB*. It is not yet possible to reliably generate large quantities of *HBB* expressing cells from an embryonic source such as hES or iPSC[233]. As the bone marrow niche in which cells mature and undergo hemoglobin switching is extremely complex, consisting of many cell types from multiple cell lineages, it suggest that many factors are involved in the production of HbA expressing RBCs. Replication of that environment *in vitro,* without co-culturing is very difficult. To validate that iPSC can be used for RBC disease modeling, I utilized an *in vivo* environment that can support them through switching and maturation, the humanized mouse model.

The humanized mouse model allowed me to inject human erythroid lineage cells into sub-lethally irradiated mice and compare them before and after they spend time in a natural hematopoietic environment. Early experiments indicated that the cells were capable of homing to the bone marrow and maturation, which resulted in increased splenic clearance of the extra RBCs. This result prompted the creation of a lentiviral vector to transduce a constitutive luciferase expression construct. Cells properly incorporating this sequence into their genome allowed in vivo imaging throughout a multi-day time course. While I was able to visualize the cells for the first week, subsequent imaging revealed decreasing numbers of cells. At 3 weeks post injection, the signal from human cells had decreased below the level of detection using either FACS or

organ-level luciferase imaging. I hypothesized that this diminution of human cells was due to the mouse immune system clearance.

The macrophage is one of the remaining immune cells in NSG mice, and therefore the suspect in the destruction of the human cells. Although others have shown that macrophage cells are responsible for destruction of human erythroid cells in NSG mice and the use of clodronate to deplete macrophage populations can increase human chimerism in this model, this result could not be replicated[287]. Future experiments under this aim should investigate further titration of clodrosome vesicle dosage to increase animal viability. Alternatively, increasing the number of mice in the study would allow for significance despite some premature mortality. I chose to continue this line of investigation by directly blocking macrophage identification of human cells.

CD47 is an integrin-associating protein (IAP) expressed on the surface of both human and mouse cells. Upon CD47 binding to signal-regulatory protein-α (SIRPα) on macrophages, macrophages identify the presenting cell as "self" or "foreign", with foreign cells being phagocytized. Expression of murine CD47 on human cells can prevent phagocytosis by changing the "eat me signal" to a "self" signal[288]. Others have adapted mice to express human CD47 as another method for preventing destruction of human cells in mice[288,289]. As our cells are easily transduced with lentivirus, my future goal is to create a pHAGE expression plasmid that contains murine CD47, which can be infected into the human erythroid lineage cells and hinder their phagocytosis when injected into mice.

By optimizing mouse *in vivo* imaging, cellular assays, and erythroid maturation procedures I have laid a solid groundwork for establishing an *in vivo* and *in vitro* model for RBC maturation. Methods to assess cell morphology and surface markers to determine the maturation state can be used to compare iPSC-derived erythroid lineage cells. Furthermore, once the cause of human cell loss is counteracted, NSG mice should serve as the ideal vessel for studying the

process of hemoglobin switching, which ultimately can be determined by subsequent mass spectrometry. Conditions for the isolation of human cells from murine peripheral blood and spleen homogenates by cell sorting have been established. This allows for a pure population of human cells to be analyzed after maturing and switching *in vivo*. Regardless of an iPSC-derived human cell's ability to undergo hemoglobin switching, this model is crucial for testing human cells ability to mature, navigate the spleen and survive an *in vivo* environment, prior to being used in a clinical setting.

With the ability to create erythroid lineage cells I was able to pursue the last goal of this project, the comparison of wildtype and SCD-specific iPSC-derived erythroid cells. Since iPSCs mimic the genetic context of the patient I hypothesized that not only would I see differences between wildtype and SCD-specific cells, but also within SCD lines in regards to HbF expression and response to HU.

The ability of a patient to respond to HU is unpredictable. With a library of SCD-specific iPSC I proposed to study HU responders versus poor responders in the hope of identifying differences that would allow for a targeted search for novel therapeutics. My experiments demonstrated that *HBG* expression increased following *in vitro* treatment of erythroid lineage cells with HU. This effect was observed in both control and sickle cell lines. SCD lines showed a range of differential responses to HU *in vitro*, suggesting that the ability to recapitulate differences seen in the patient was feasible. Unfortunately, due to irregular clinical treatment and HbF readings, patient responses to HU could not be reliably determined.

In an ideal situation, HbF levels of individuals taking similar doses of HU could be compared over time, and a percentage increase in HbF levels could be used to differentiate strong from weak responders. In the creation of our library we were not critical in enrolling patients prescribed a common dose of HU, nor were we able to define the frequency with which their HbF

levels were measured, two facets which led to confounding results. In an attempt to extract cryptic trends in our clinical data we charted HbF (percentage) and HU prescription (mg) as a product of time with transfusion history and MCV values noted. This method identifies HU responders as those with greater than a 5% increase in HbF levels upon HU prescription with a corresponding increase in MCV. Weak responders had variable increases and decreases in HbF levels less than 5% with increased MCV, and non-responders showed no significant change in HbF. Regrettably, all patients identified as weak or non-responsive were flagged as either non-compliant or had been taken off HU, leaving nothing to compare with the HU responders. While other researchers have attempted to classify HU response with other indicators such as *in vitro* RNA expression[303] or particular haplotypes[305,306], no one has derived a predictive model for an individual's ability to respond to HU. I believe that utilization of a SCD-specific iPSC library is a valuable tool to study HU response, however, establishment of such a model system first requires validation with individuals that have a thorough history of HbF levels, minimal transfusions and consistent HU prescription.

Using the patient information available, I decided to use three SCD iPSC lines to compare to three control lines for the remainder of my studies. The SCD lines represent distinct haplotypes Arab-Indian, and Benin. These SCD lines all show an increase in HbF expression (6.5-29.6%) compared with the <0.5% HbF seen in control lines. With multiple haplotypes and HbF expression I hoped to visualize differences in HbF expression in my *in vitro* analysis of the lines.

Previous results demonstrated that HPs are capable of limited maturation in the final progenitor media, day 7. I conducted a time course to observe mRNA expression changes in day 7 media that revealed both *HBG* and *HBA* expression increased over time. This suggested that the cells are capable of altering hemoglobin expression as a result of maturation. I sought to

corroborate my RT-PCR findings with FACS-based protein quantification[307]. Mass spectrometric results revealed that the erythroid lineage cells had high levels HBE, HBZ, HBG and HBA. While mass spectrometry is extremely useful for identifying simultaneous expression of hemoglobin, it is typically not quantitative. I adapted a clinical fetal-maternal hemorrhage FACS assay to quickly and quantitatively assess HbF levels in various iPSC derived erythroid cells. With this assay I was able to quantify HbF levels in differentiated erythroblast cells and observe the changes in HbF levels as cells mature. I observed a dramatic reduction in HbF between day 29 and day 36, prompting me to analyze the maturation state and HbF levels of cells at day 30. To analyze maturation and HbF levels simultaneously required further adaptation of the intracellular HbF FACS assay. Analysis of multiple control and SCD-specific lines revealed interesting trends. BU6, a control line and SA108.1 had similar expression levels of CD235 and HbF. The SCD-specific lines had a higher proportion of CD235+HbF+ cells than the control lines (40.7% vs. 14.0%), which may reflect the higher levels of HbF seen in the patients compared to control. Two populations of HbF expression: high and low, were observed both by scatter-plot and histogram analysis of CD235+ cells. This suggested that day 30 cells were currently in the process of maturation and hemoglobin switching. Despite the small number of lines used for these experiments, we were able to identify trends in our *in vitro* iPSC based system that recapitulated *in vivo* observations.

Collectively, these results demonstrate that each iPSC line, control or SCD-disease specific, is capable of creating erythroid lineage cells that can be used to characterize *in vitro* and *in vivo* maturation states as well as hemoglobin expression. Evaluation of HbF in each line revealed subtle differences in HbF levels and maturation states while still demonstrating the ability of the cells to modulate their HbF levels in response to maturation or HU treatment. These results validate my original hypothesis that iPSC-derived erythroid lineage cells are capable of

reflecting a similar range of differences observed in individuals. However, it is important to acknowledge that the observed clinical differences are seen in mature erythroid cells that express HbA globin, and little has been done to study HbF modulation in primitive erythroid cells expressing HbF. While my results suggest that HbF levels can be modulated in primitive cells, I hypothesize the profound differences in HbF levels will be seen once cells expressing HbA are produced.

Since our *in vitro* differentiation procedure appeared to be producing mature erythroblasts without the accompanying hemoglobin switching, we became convinced that we were modeling primitive erythropoiesis. Primitive erythropoiesis, which takes place during embryonic and fetal development results in RBCs, which are capable of maturation, but will express primarily embryonic and HbF. Historically, multiple cells types derived from iPSCs have been observed to be fetal in nature, unable to express proteins typical of adult cells. This is highlighted by the difficulty of altering erythroid lineage cells to produce HbA, despite repeated advances in the production of the cells. Mass spectrometry data showing embryonic and fetal hemoglobin expression supports the model of primitive erythropoiesis and is reinforced by FACS analysis of the adherent and non-adherent layers. We found that the non-adherent population we were collecting had fewer hematopoietic stem cell-like cells than the small population found in the adherent layer. This suggested to us that altering an early step to allow for definitive erythropoiesis is key **(Figure 5.1)**. An early cell type of interest is the hemogenic endothelium from which definitive HSC arise. If we are capable of producing the environment that HSC are derived from, we should be able to capture HSC-like cells for expansion and differentiation. Very preliminary results from our lab suggest that this is possible with the addition of SB431542, an activin and nodal inhibitor, at day 4 of our differentiation protocol. Addition of SB43152 on day 4 increased the CD34+, and HSC surface marker, cell population from 3 to 21%. These HSC-like

cells can be purified from the rest of the adherent layer, re-plated, and allowed to continue producing HPs. The HPs that are produced are capable of expressing *HBB* under maturation conditions, as seen by RT-PCR. The ability to harness these HSC-like cells for the support of a definitive erythropoietic environment will allow for optimal comparisons of wildtype and SCD-specific erythroid cells.

In addition to answering basic biological questions concerning hematopoietic and erythroid development, our *in vitro* platform could also be used for the production of

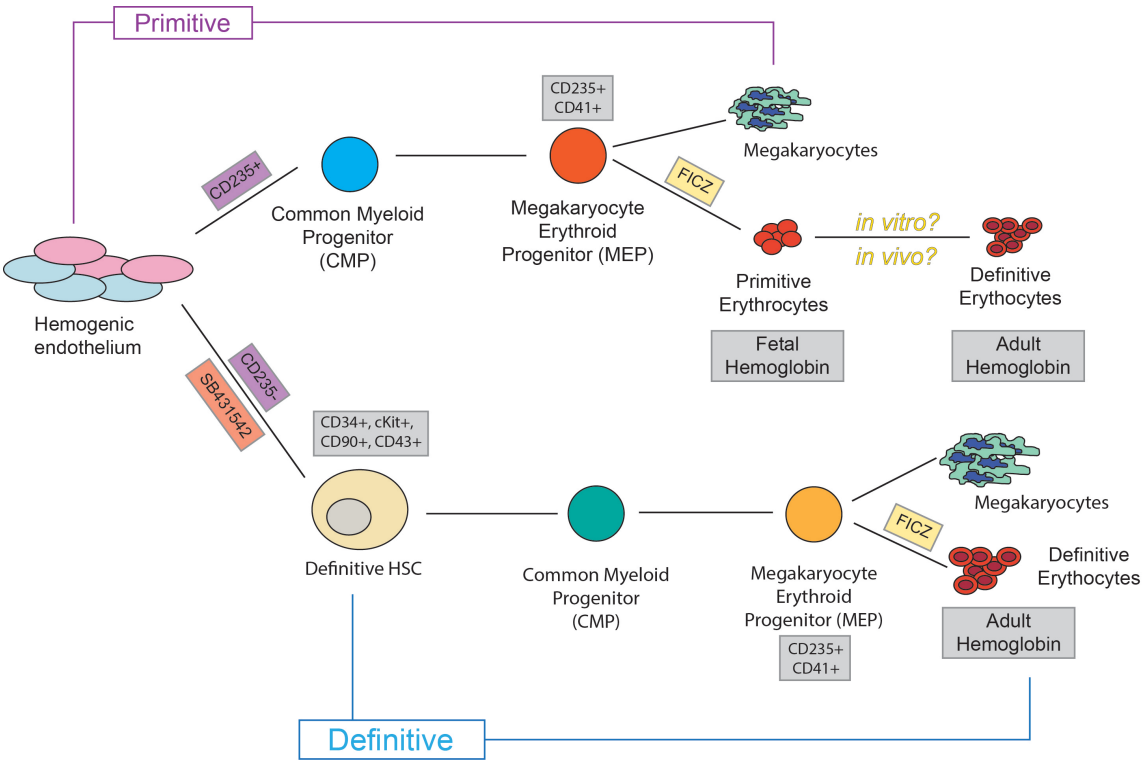

Figure 5.1. Diagram illustrating differences in cells generated from primitive or definitive hematopoiesis.

blood products in a chemically defined and xenobiotic agent-free differentiation scheme. As blood transfusions are an indispensable cell therapy, and the safety and adequacy of the blood supply are of national and international concern, an iPSC-based system could allow for red blood cell and platelet transfusion, without problems related to immunogenicity, contamination, or supply. It has been posited that only a few individuals will be needed for iPSC generation to be able to create blood products for all HLA matched groups[309]. Furthermore, the ability to produce multiple populations of cells from a single source, coupled with the fact that both platelets and mature RBCs contain no nuclear genetic material, decreases safety concerns with the use of iPSC-derived cells and paves the way for clinical utility.

REFERENCES

1. Pietras EM, Warr MR, Passegué E. Cell cycle regulation in hematopoietic stem cells. *The Journal of cell biology*. 2011;195(5):709–20. doi:10.1083/jcb.201102131.

2. Akashi K, Traver D, Miyamoto T, Weissman IL. A clonogenic common myeloid progenitor that gives rise to all myeloid lineages. *Nature*. 2000;404(6774):193–7. doi:10.1038/35004599.

3. Kondo M, Weissman IL, Akashi K. Identification of clonogenic common lymphoid progenitors in mouse bone marrow. *Cell*. 1997;91(5):661–72.

4. Alberts B, Johnson A, Lewis J, Raff M, Keith R, Walter P. Adaptive Immune System. In: *Molecular Biology of the Cell*. 4th ed. Garland Science; 2002.

5. Alberts B, Johnson A, Lewis J, Raff M, Keith R, Walter P. Renewal by Multipotent Stem Cells: Blood Cell Formation. In: *Molecular Biology of the Cell*. 4th ed. Garland Science; 2002.

6. Orkin SH, Zon LI. Hematopoiesis: an evolving paradigm for stem cell biology. *Cell*. 2008;132(4):631–44. doi:10.1016/j.cell.2008.01.025.

7. Palis J, Yoder MC. Yolk-sac hematopoiesis: the first blood cells of mouse and man. *Experimental hematology*. 2001;29(8):927–36.

8. Tavian M, Biasch K, Sinka L, Vallet J, Péault B. Embryonic origin of human hematopoiesis. *The International journal of developmental biology*. 2010;54(6-7):1061–5. doi:10.1387/ijdb.103097mt.

9. Kennedy M, Firpo M, Choi K, et al. A common precursor for primitive erythropoiesis and definitive haematopoiesis. *Nature*. 1997;386(6624):488–93. doi:10.1038/386488a0.

10. Zambidis ET, Park TS, Yu W, et al. Expression of angiotensin-converting enzyme (CD143) identifies and regulates primitive hemangioblasts derived from human pluripotent stem cells. *Blood*. 2008;112(9):3601–14. doi:10.1182/blood-2008-03-144766.

11. Ivanovs A, Rybtsov S, Welch L, Anderson RA, Turner ML, Medvinsky A. Highly potent human hematopoietic stem cells first emerge in the intraembryonic aorta-gonad-mesonephros region. *The Journal of experimental medicine*. 2011;208(12):2417–27. doi:10.1084/jem.20111688.

12. Laird DJ, von Andrian UH, Wagers AJ. Stem cell trafficking in tissue development, growth, and disease. *Cell*. 2008;132(4):612–30. doi:10.1016/j.cell.2008.01.041.

13. Cumano A, Godin I. Ontogeny of the hematopoietic system. *Annual review of immunology*. 2007;25:745–85. doi:10.1146/annurev.immunol.25.022106.141538.

14. Jagannathan-Bogdan M, Zon LI. Hematopoiesis. *Development (Cambridge, England)*. 2013;140(12):2463–7. doi:10.1242/dev.083147.

15. Mahmud DL, G-Amlak M, Deb DK, Platanias LC, Uddin S, Wickrema A. Phosphorylation of forkhead transcription factors by erythropoietin and stem cell factor prevents acetylation and their interaction with coactivator p300 in erythroid progenitor cells. *Oncogene*. 2002;21(10):1556–62. doi:10.1038/sj.onc.1205230.

16. Goodman JW, Hall EA, Miller KL, Shinpock SG. Interleukin 3 promotes erythroid burst formation in "serum-free" cultures without detectable erythropoietin. *Proceedings of the National Academy of Sciences of the United States of America*. 1985;82(10):3291–5.

17. Böhmer RM. IL-3-dependent early erythropoiesis is stimulated by autocrine transforming growth factor beta. *Stem cells (Dayton, Ohio)*. 2004;22(2):216–24. doi:10.1634/stemcells.22-2-216.

18. Umemura T, al-Khatti A, Donahue RE, Papayannopoulou T, Stamatoyannopoulos G. Effects of interleukin-3 and erythropoietin on in vivo erythropoiesis and F-cell formation in primates. *Blood*. 1989;74(5):1571–6.

19. Wojchowski DM, Menon MP, Sathyanarayana P, et al. Erythropoietin-dependent erythropoiesis: New insights and questions. *Blood cells, molecules & diseases*. 2006;36(2):232–8. doi:10.1016/j.bcmd.2006.01.007.

20. Lin CS, Lim SK, D'Agati V, Costantini F. Differential effects of an erythropoietin receptor gene disruption on primitive and definitive erythropoiesis. *Genes & development*. 1996;10(2):154–64. doi:10.1101/gad.10.2.154.

21. Tsang AP, Visvader JE, Turner CA, et al. FOG, a multitype zinc finger protein, acts as a cofactor for transcription factor GATA-1 in erythroid and megakaryocytic differentiation. *Cell*. 1997;90(1):109–19.

22. Coghill E, Eccleston S, Fox V, et al. Erythroid Kruppel-like factor (EKLF) coordinates erythroid cell proliferation and hemoglobinization in cell lines derived from EKLF null mice. *Blood*. 2001;97(6):1861–8. doi:10.1182/blood.V97.6.1861.

23. Tallack MR, Perkins AC. KLF1 directly coordinates almost all aspects of terminal erythroid differentiation. *IUBMB life*. 2010;62(12):886–90. doi:10.1002/iub.404.

24. Testa U, Fossati C, Samoggia P, et al. Expression of growth factor receptors in unilineage differentiation culture of purified hematopoietic progenitors. *Blood*. 1996;88(9):3391–406.

25. Munugalavadla V, Dore LC, Tan BL, et al. Repression of c-kit and its downstream substrates by GATA-1 inhibits cell proliferation during erythroid maturation. *Molecular and cellular biology*. 2005;25(15):6747–59. doi:10.1128/MCB.25.15.6747-6759.2005.

26. Huddleston H, Tan B, Yang F-C, et al. Functional p85alpha gene is required for normal murine fetal erythropoiesis. *Blood*. 2003;102(1):142–5. doi:10.1182/blood-2002-10-3245.

27. Bakker WJ, van Dijk TB, Parren-van Amelsvoort M, et al. Differential regulation of Foxo3a target genes in erythropoiesis. *Molecular and cellular biology*. 2007;27(10):3839–3854. doi:10.1128/MCB.01662-06.

28. Jayapal SR, Lee KL, Ji P, Kaldis P, Lim B, Lodish HF. Down-regulation of Myc is essential for terminal erythroid maturation. *The Journal of biological chemistry*. 2010;285(51):40252–65. doi:10.1074/jbc.M110.181073.

29. Broudy VC, Lin NL, Priestley G V, Nocka K, Wolf NS. Interaction of stem cell factor and its receptor c-kit mediates lodgment and acute expansion of hematopoietic cells in the murine spleen. *Blood*. 1996;88(1):75–81.

30. Goldberg MA, Dunning SP, Bunn HF. Regulation of the erythropoietin gene: evidence that the oxygen sensor is a heme protein. *Science (New York, NY)*. 1988;242(4884):1412–5.

31. Eschbach JW, Egrie JC, Downing MR, Browne JK, Adamson JW. Correction of the anemia of end-stage renal disease with recombinant human erythropoietin. Results of a combined phase I and II clinical trial. *The New England journal of medicine*. 1987;316(2):73–8. doi:10.1056/NEJM198701083160203.

32. Von Lindern M, Deiner EM, Dolznig H, et al. Leukemic transformation of normal murine erythroid progenitors: v- and c-ErbB act through signaling pathways activated by the EpoR and c-Kit in stress erythropoiesis. *Oncogene*. 2001;20(28):3651–64. doi:10.1038/sj.onc.1204494.

33. Socolovsky M, Nam H, Fleming MD, Haase VH, Brugnara C, Lodish HF. Ineffective erythropoiesis in Stat5a(-/-)5b(-/-) mice due to decreased survival of early erythroblasts. *Blood*. 2001;98(12):3261–73.

34. Dolznig H, Habermann B, Stangl K, et al. Apoptosis protection by the Epo target Bcl-X(L) allows factor-independent differentiation of primary erythroblasts. *Current biology : CB*. 2002;12(13):1076–85.

35. Busfield SJ, Klinken SP. Erythropoietin-induced stimulation of differentiation and proliferation in J2E cells is not mimicked by chemical induction. *Blood*. 1992;80(2):412–9.

36. Minegishi N, Minegishi M, Tsuchiya S, et al. Erythropoietin-dependent induction of hemoglobin synthesis in a cytokine-dependent cell line M-TAT. *The Journal of biological chemistry*. 1994;269(44):27700–4.

37. Ronzoni L, Bonara P, Rusconi D, Frugoni C, Libani I, Cappellini MD. Erythroid differentiation and maturation from peripheral CD34+ cells in liquid culture: cellular and molecular characterization. *Blood cells, molecules & diseases*. 2007;40(2):148–55. doi:10.1016/j.bcmd.2007.07.006.

38. Fujiwara Y, Browne CP, Cunniff K, Goff SC, Orkin SH. Arrested development of embryonic red cell precursors in mouse embryos lacking transcription factor GATA-1. *Proceedings of the National Academy of Sciences of the United States of America*. 1996;93(22):12355–8.

39. Fujiwara T, O'Geen H, Keles S, et al. Discovering hematopoietic mechanisms through genome-wide analysis of GATA factor chromatin occupancy. *Molecular cell*. 2009;36(4):667–81. doi:10.1016/j.molcel.2009.11.001.

40. Yu M, Riva L, Xie H, et al. Insights into GATA-1-mediated gene activation versus repression via genome-wide chromatin occupancy analysis. *Molecular cell*. 2009;36(4):682–95. doi:10.1016/j.molcel.2009.11.002.

41. Cheng Y, Wu W, Kumar SA, et al. Erythroid GATA1 function revealed by genome-wide analysis of transcription factor occupancy, histone modifications, and mRNA expression. *Genome research*. 2009;19(12):2172–84. doi:10.1101/gr.098921.109.

42. Tripic T, Deng W, Cheng Y, et al. SCL and associated proteins distinguish active from repressive GATA transcription factor complexes. *Blood*. 2009;113(10):2191–201. doi:10.1182/blood-2008-07-169417.

43. Cantor AB, Orkin SH. Transcriptional regulation of erythropoiesis: an affair involving multiple partners. *Oncogene*. 2002;21(21):3368–76. doi:10.1038/sj.onc.1205326.

44. Kassouf MT, Hughes JR, Taylor S, et al. Genome-wide identification of TAL1's functional targets: insights into its mechanisms of action in primary erythroid cells. *Genome research*. 2010;20(8):1064–83. doi:10.1101/gr.104935.110.

45. Shivdasani RA, Mayer EL, Orkin SH. Absence of blood formation in mice lacking the T-cell leukaemia oncoprotein tal-1/SCL. *Nature*. 1995;373(6513):432–4. doi:10.1038/373432a0.

46. Miller IJ, Bieker JJ. A novel, erythroid cell-specific murine transcription factor that binds to the CACCC element and is related to the Krüppel family of nuclear proteins. *Molecular and cellular biology*. 1993;13(5):2776–86.

47. Tallack MR, Whitington T, Yuen WS, et al. A global role for KLF1 in erythropoiesis revealed by ChIP-seq in primary erythroid cells. *Genome research*. 2010;20(8):1052–63. doi:10.1101/gr.106575.110.

48. Kerenyi MA, Orkin SH. Networking erythropoiesis. *The Journal of experimental medicine*. 2010;207(12):2537–41. doi:10.1084/jem.20102260.

49. Schoenfelder S, Sexton T, Chakalova L, et al. Preferential associations between co-regulated genes reveal a transcriptional interactome in erythroid cells. *Nature genetics*. 2010;42(1):53–61. doi:10.1038/ng.496.

50. Zhou D, Liu K, Sun C-W, Pawlik KM, Townes TM. KLF1 regulates BCL11A expression and gamma- to beta-globin gene switching. *Nature genetics*. 2010;42(9):742–4. doi:10.1038/ng.637.

51. Borg J, Papadopoulos P, Georgitsi M, et al. Haploinsufficiency for the erythroid transcription factor KLF1 causes hereditary persistence of fetal hemoglobin. *Nat Genet*. 2010;42(9):801–805. doi:10.1038/ng.630.

52. Mancini E, Sanjuan-Pla A, Luciani L, et al. FOG-1 and GATA-1 act sequentially to specify definitive megakaryocytic and erythroid progenitors. *The EMBO journal*. 2012;31(2):351–65. doi:10.1038/emboj.2011.390.

53. Chang AN, Cantor AB, Fujiwara Y, et al. GATA-factor dependence of the multitype zinc-finger protein FOG-1 for its essential role in megakaryopoiesis. *Proceedings of the National Academy of Sciences of the United States of America*. 2002;99(14):9237–42. doi:10.1073/pnas.142302099.

54. Crispino JD, Lodish MB, MacKay JP, Orkin SH. Use of altered specificity mutants to probe a specific protein-protein interaction in differentiation: the GATA-1:FOG complex. *Molecular cell*. 1999;3(2):219–28.

55. Muntean AG, Crispino JD. Differential requirements for the activation domain and FOG-interaction surface of GATA-1 in megakaryocyte gene expression and development. *Blood*. 2005;106(4):1223–31. doi:10.1182/blood-2005-02-0551.

56. Pal S, Cantor AB, Johnson KD, et al. Coregulator-dependent facilitation of chromatin occupancy by GATA-1. *Proceedings of the National Academy of Sciences of the United States of America*. 2004;101(4):980–5. doi:10.1073/pnas.0307612100.

57. Hong W, Nakazawa M, Chen Y-Y, et al. FOG-1 recruits the NuRD repressor complex to mediate transcriptional repression by GATA-1. *The EMBO journal*. 2005;24(13):2367–78. doi:10.1038/sj.emboj.7600703.

58. Sankaran VG, Nathan DG. Reversing the hemoglobin switch. *The New England journal of medicine*. 2010;363(23):2258–60. doi:10.1056/NEJMcibr1010767.

59. Hunefeld FL. *Die Chemismus in der thierischen Organization*. Leipzig, Brockhaus; 1840.

60. Hoppe-Seyer F. Uber di Chemischn und OptischenEigenschaftern des Blutsfarbstoffs. *Arch F Path Anat U Physiol (Virchow's Arcihv)*. 1864;29:233–235.

61. Tavian M, Péault B. Embryonic development of the human hematopoietic system. *The International journal of developmental biology*. 2005;49(2-3):243–50. doi:10.1387/ijdb.041957mt.

62. Philipsen S, Wood WG. Erythropoiesis. In: *Disorders of Hemoglobin*. Second. Cambridge University Press; 2009:22–45. doi:http://dx.doi.org/10.1017/CBO9780511596582.

63. Hanspal M, Hanspal JS. The association of erythroblasts with macrophages promotes erythroid proliferation and maturation: a 30-kD heparin-binding protein is involved in this contact. *Blood*. 1994;84(10):3494–504.

64. Chasis JA, Mohandas N. Erythroblastic islands: niches for erythropoiesis. *Blood*. 2008;112(3):470–8. doi:10.1182/blood-2008-03-077883.

65. Mao X, Shi X, Liu F, Li G, Hu L. Evaluation of erythroblast macrophage protein related to erythroblastic islands in patients with hematopoietic stem cell transplantation. *European journal of medical research*. 2013;18:9. doi:10.1186/2047-783X-18-9.

66. Yamaguchi K, Jürgens KD, Bartels H, Scheid P, Piiper J. Dependence of O2 transfer conductance of red blood cells on cellular dimensions. *Advances in experimental medicine and biology*. 1988;222:571–8.

67. Herrick JB. Peculiar elongated and sickle-shaped red blood corpuscles in a case of severe anemia. *Archives of Internal Medicine*. 1910;VI(5):517. doi:10.1001/archinte.1910.00050330050003.

68. Hanh E, Gillespie E. Sickle cell anemia. *Arch Int Med*. 1927;39:233.

69. Pauling L. Molecular disease and evolution. *Bulletin of the New York Academy of Medicine*. 1964;40:334–42.

70. Pauling L, Itano HA. Sickle cell anemia, a molecular disease. *Science (New York, NY)*. 1949;109(2865):443.

71. Neel J V. The Inheritance of Sickle Cell Anemia. *Science (New York, NY)*. 1949;110(2846):64–6. doi:10.1126/science.110.2846.64.

72. Watson J. The significance of the paucity of sickle cells in newborn Negro infants. *The American journal of the medical sciences*. 1948;215(4):419–23.

73. Ingram VM. Abnormal human haemoglobins. III. The chemical difference between normal and sickle cell haemoglobins. *Biochimica et biophysica acta*. 1959;36:402–11.

74. Steinberg MH. Predicting clinical severity in sickle cell anaemia. *Br J Haematol*. 2005;129(4):465–481. doi:10.1111/j.1365-2141.2005.05411.x.

75. Letvin NL, Linch DC, Beardsley GP, McIntyre KW, Nathan DG. Augmentation of fetal-hemoglobin production in anemic monkeys by hydroxyurea. *The New England journal of medicine*. 1984;310(14):869–73. doi:10.1056/NEJM198404053101401.

76. Rodgers GP, Dover GJ, Noguchi CT, Schechter AN, Nienhuis AW. Hematologic responses of patients with sickle cell disease to treatment with hydroxyurea. *The New England journal of medicine*. 1990;322(15):1037–45. doi:10.1056/NEJM199004123221504.

77. Charache S, Terrin ML, Moore RD, et al. Effect of hydroxyurea on the frequency of painful crises in sickle cell anemia. Investigators of the Multicenter Study of Hydroxyurea in Sickle Cell Anemia. *The New England journal of medicine*. 1995;332(20):1317–22. doi:10.1056/NEJM199505183322001.

78. Steinberg MH, Barton F, Castro O, et al. Effect of hydroxyurea on mortality and morbidity in adult sickle cell anemia: risks and benefits up to 9 years of treatment. *JAMA*. 2003;289(13):1645–1651. doi:10.1001/jama.289.13.1645.

79. Steinberg MH, Forget BG, Higgs DR, Wetheral DJ. *Disorders Hemoglobin Genetics Pathophysiology And Clinical Management 2nd Edition :: Hematology :: Cambridge University Press*.; 2009.

80. Hoover R, Rubin R, Wise G, Warren R. Adhesion of normal and sickle erythrocytes to endothelial monolayer cultures. *Blood*. 1979;54(4):872–6.

81. Hebbel RP, Yamada O, Moldow CF, Jacob HS, White JG, Eaton JW. Abnormal adherence of sickle erythrocytes to cultured vascular endothelium: possible mechanism for microvascular occlusion in sickle cell disease. *The Journal of clinical investigation*. 1980;65(1):154–60. doi:10.1172/JCI109646.

82. Reiter CD, Wang X, Tanus-Santos JE, et al. Cell-free hemoglobin limits nitric oxide bioavailability in sickle-cell disease. *Nature medicine*. 2002;8(12):1383–9. doi:10.1038/nm799.

83. Steinberg MH, Rodgers GP. Pharmacologic modulation of fetal hemoglobin. *Medicine (Baltimore)*. 2001;80(5):328–344.

84. Nagel RL, Fleming AF. Genetic epidemiology of the beta s gene. *Baillière's clinical haematology*. 1992;5(2):331–65.

85. Pagnier J, Mears JG, Dunda-Belkhodja O, et al. Evidence for the multicentric origin of the sickle cell hemoglobin gene in Africa. *Proceedings of the National Academy of Sciences of the United States of America*. 1984;81(6):1771–3.

86. Powars DR, Chan L, Schroeder WA. Beta S-gene-cluster haplotypes in sickle cell anemia: clinical implications. *The American journal of pediatric hematology/oncology*. 1990;12(3):367–74.

87. Padmos MA, Roberts GT, Sackey K, et al. Two different forms of homozygous sickle cell disease occur in Saudi Arabia. *British journal of haematology*. 1991;79(1):93–8.

88. Menzel S, Thein SL. Genetic architecture of hemoglobin F control. *Curr Opin Hematol*. 2009;16(3):179–186.

89. Garner C, Tatu T, Reittie JE, et al. Genetic influences on F cells and other hematologic variables: a twin heritability study. *Blood*. 2000;95(1):342–346.

90. Yin W, Barkess G, Fang X, et al. Histone acetylation at the human beta-globin locus changes with developmental age. *Blood*. 2007;110(12):4101–4107. doi:10.1182/blood-2007-05-091256.

91. Mabaera R, Richardson CA, Johnson K, Hsu M, Fiering S, Lowrey CH. Developmental- and differentiation-specific patterns of human gamma- and beta-globin promoter DNA methylation. *Blood*. 2007;110(4):1343–1352. doi:10.1182/blood-2007-01-068635.

92. Arbane M, Morle L, Dessi E, et al. Genetic control of the proportion of gamma chains of human fetal haemoglobin. *Nouv Rev Fr Hematol*. 1986;28(4):235–242.

93. Thein SL, Menzel S, Peng X, et al. Intergenic variants of HBS1L-MYB are responsible for a major quantitative trait locus on chromosome 6q23 influencing fetal hemoglobin levels in adults. *Proc Natl Acad Sci U S A*. 2007;104(27):11346–11351. doi:10.1073/pnas.0611393104.

94. Menzel S, Garner C, Gut I, et al. A QTL influencing F cell production maps to a gene encoding a zinc-finger protein on chromosome 2p15. *Nat Genet*. 2007;39(10):1197–1199. doi:10.1038/ng2108.

95. Thein SL, Menzel S. Discovering the genetics underlying foetal haemoglobin production in adults. *British journal of haematology*. 2009;145(4):455–67. doi:10.1111/j.1365-2141.2009.07650.x.

96. Stamatoyannopoulos G. Control of globin gene expression during development and erythroid differentiation. *Exp Hematol*. 2005;33(3):259–271. doi:10.1016/j.exphem.2004.11.007.

97. Sunshine HR, Hofrichter J, Eaton WA. Requirement for therapeutic inhibition of sickle haemoglobin gelation. *Nature*. 1978;275(5677):238–240.

98. Platt OS. Hydroxyurea for the treatment of sickle cell anemia. *N Engl J Med*. 2008;358(13):1362–1369. doi:10.1056/NEJMct0708272.

99. Arlt MF, Ozdemir AC, Birkeland SR, Wilson TE, Glover TW. Hydroxyurea induces de novo copy number variants in human cells. *Proc Natl Acad Sci U S A*. 2011;108(42):17360–17365. doi:10.1073/pnas.1109272108.

100. Lozzio CB, Lozzio BB. Human chronic myelogenous leukemia cell-line with positive Philadelphia chromosome. *Blood*. 1975;45(3):321–334.

101. Liang DC, Shih LY, Kuo MC, et al. The synergistic effect of thrombopoietin in erythropoiesis with erythropoietin and/or IL-3 and myelopoiesis with G-CSF or IL-3 from umbilical cord blood cells of full-term neonates. *Pediatric hematology and oncology*. 2001;18(6):383–91. doi:10.1080/088800101316922001.

102. Villeval JL, Pelicci PG, Tabilio A, et al. Erythroid properties of K562 cells. Effect of hemin, butyrate and TPA induction. *Exp Cell Res*. 1983;146(2):428–435.

103. Fusaki N, Ban H, Nishiyama A, Saeki K, Hasegawa M. Efficient induction of transgene-free human pluripotent stem cells using a vector based on Sendai virus, an RNA virus that does not integrate into the host genome. *Proc Jpn Acad Ser B Phys Biol Sci*. 2009;85(8):348–362.

104. Cioe L, McNab A, Hubbell HR, Meo P, Curtis P, Rovera G. Differential expression of the globin genes in human leukemia K562(S) cells induced to differentiate by hemin or butyric acid. *Cancer Research*. 1981;41(1):237–243.

105. Plonczynski M, Hardy CL, Safaya S, et al. Induction of Globin Synthesis in K562 Cells Is Associated with Differential Expression of Transcription Factor Genes. *Blood Cells, Molecules, and Diseases*. 1999;25(3):156–165. doi:http://dx.doi.org/10.1006/bcmd.1999.0241.

106. Moon AM, Ley TJ. Functional properties of the beta-globin locus control region in K562 erythroleukemia cells. *Blood*. 1991;77(10):2272–2284.

107. Dean A, Ley TJ, Humphries RK, Fordis M, Schechter AN. Inducible transcription of five globin genes in K562 human leukemia cells. *Proc Natl Acad Sci U S A*. 1983;80(18):5515–5519.

108. Zein S, Li W, Ramakrishnan V, et al. Identification of fetal hemoglobin-inducing agents using the human leukemia KU812 cell line. *Experimental biology and medicine (Maywood, NJ)*. 2010;235(11):1385–1394. doi:10.1258/ebm.2010.010129.

109. Flomenberg N, Devine SM, Dipersio JF, et al. The use of AMD3100 plus G-CSF for autologous hematopoietic progenitor cell mobilization is superior to G-CSF alone. *Blood*. 2005;106(5):1867–74. doi:10.1182/blood-2005-02-0468.

110. Liles WC, Broxmeyer HE, Rodger E, et al. Mobilization of hematopoietic progenitor cells in healthy volunteers by AMD3100, a CXCR4 antagonist. *Blood*. 2003;102(8):2728–30. doi:10.1182/blood-2003-02-0663.

111. Ings SJ, Balsa C, Leverett D, Mackinnon S, Linch DC, Watts MJ. Peripheral blood stem cell yield in 400 normal donors mobilised with granulocyte colony-stimulating factor (G-CSF): impact of age, sex, donor weight and type of G-CSF used. *British Journal of Haematology*. 2006;134(5):517–525.

112. Mueller MM, Bialleck H, Bomke B, et al. Safety and efficacy of healthy volunteer stem cell mobilization with filgrastim G-CSF and mobilized stem cell apheresis: results of a prospective longitudinal 5-year follow-up study. *Vox sanguinis*. 2013;104(1):46–54.

113. Perrine SP, Miller BA, Faller D V, et al. Sodium butyrate enhances fetal globin gene expression in erythroid progenitors of patients with Hb SS and beta thalassemia. *Blood*. 1989;74(1):454–459.

114. Hsiao CH, Li W, Lou TF, Baliga BS, Pace BS. Fetal hemoglobin induction by histone deacetylase inhibitors involves generation of reactive oxygen species. *Exp Hematol*. 2006;34(3):264–273. doi:10.1016/j.exphem.2005.12.009.

115. Lavelle D, Saunthararajah Y, Vaitkus K, et al. S110, a novel decitabine dinucleotide, increases fetal hemoglobin levels in baboons (P. anubis). *J Transl Med*. 2010;8:92. doi:10.1186/1479-5876-8-92.

116. Makala L, Di Maro S, Lou TF, Sivanand S, Ahn JM, Pace BS. FK228 Analogues Induce Fetal Hemoglobin in Human Erythroid Progenitors. *Anemia*. 2012;2012:428137. doi:10.1155/2012/428137.

117. Bianchi N, Chiarabelli C, Borgatti M, Mischiati C, Fibach E, Gambari R. Accumulation of gamma-globin mRNA and induction of erythroid differentiation after treatment of human leukaemic K562 cells with tallimustine. *Br J Haematol*. 2001;113(4):951–961.

118. Fibach E, Bianchi N, Borgatti M, Prus E, Gambari R. Mithramycin induces fetal hemoglobin production in normal and thalassemic human erythroid precursor cells. *Blood*. 2003;102(4):1276–1281. doi:10.1182/blood-2002-10-3096.

119. Van den Akker E, Satchwell TJ, Pellegrin S, Daniels G, Toye AM. The majority of the in vitro erythroid expansion potential resides in CD34(-) cells, outweighing the contribution of CD34(+) cells and significantly increasing the erythroblast yield from peripheral blood samples. *Haematologica*. 2010;95(9):1594–1598.

120. Pászty C, Brion CM, Manci E, et al. Transgenic knockout mice with exclusively human sickle hemoglobin and sickle cell disease. *Science (New York, NY)*. 1997;278(5339):876–8.

121. Ryan TM, Townes TM, Reilly MP, et al. Human sickle hemoglobin in transgenic mice. *Science (New York, NY)*. 1990;247(4942):566–8.

122. Takahashi K, Yamanaka S. Induction of pluripotent stem cells from mouse embryonic and adult fibroblast cultures by defined factors. *Cell*. 2006;126(4):663–676. doi:10.1016/j.cell.2006.07.024.

123. Takahashi K, Tanabe K, Ohnuki M, et al. Induction of pluripotent stem cells from adult human fibroblasts by defined factors. *Cell*. 2007;131(5):861–872. doi:10.1016/j.cell.2007.11.019.

124. Yu J, Vodyanik MA, Smuga-Otto K, et al. Induced pluripotent stem cell lines derived from human somatic cells. *Science*. 2007;318(5858):1917–1920. doi:10.1126/science.1151526.

125. Brambrink T, Foreman R, Welstead GG, et al. Sequential expression of pluripotency markers during direct reprogramming of mouse somatic cells. *Cell Stem Cell*. 2008;2(2):151–159. doi:10.1016/j.stem.2008.01.004.

126. Maherali N, Sridharan R, Xie W, et al. Directly reprogrammed fibroblasts show global epigenetic remodeling and widespread tissue contribution. *Cell Stem Cell*. 2007;1(1):55–70. doi:10.1016/j.stem.2007.05.014.

127. Mikkelsen TS, Ku M, Jaffe DB, et al. Genome-wide maps of chromatin state in pluripotent and lineage-committed cells. *Nature*. 2007;448(7153):553–560. doi:10.1038/nature06008.

128. Stadtfeld M, Maherali N, Breault DT, Hochedlinger K. Defining molecular cornerstones during fibroblast to iPS cell reprogramming in mouse. *Cell Stem Cell*. 2008;2(3):230–240. doi:10.1016/j.stem.2008.02.001.

129. Sommer CA, Stadtfeld M, Murphy GJ, Hochedlinger K, Kotton DN, Mostoslavsky G. Induced pluripotent stem cell generation using a single lentiviral stem cell cassette. *Stem cells (Dayton, Ohio)*. 2009;27(3):543–549. doi:10.1634/stemcells.2008-1075.

130. Somers A, Jean J-CJM, Sommer CA, et al. Generation of transgene-free lung disease-specific human induced pluripotent stem cells using a single excisable lentiviral stem cell cassette. *Stem cells (Dayton, Ohio)*. 2010;28(10):1728–40. doi:10.1002/stem.495.

131. Sommer CA, Sommer AG, Longmire T a, et al. Excision of reprogramming transgenes improves the differentiation potential of iPS cells generated with a single excisable vector. *Stem Cells*. 2010;28(1):64–74. doi:10.1002/stem.255.

132. Okita K, Matsumura Y, Sato Y, et al. A more efficient method to generate integration-free human iPS cells. *Nat Methods*. 2011;8(5):409–412.

133. Niwa A, Umeda K, Chang H, et al. Orderly hematopoietic development of induced pluripotent stem cells via Flk-1(+) hemoangiogenic progenitors. *Journal of cellular physiology*. 2009;221(2):367–377. doi:10.1002/jcp.21864.

134. Stadtfeld M, Nagaya M, Utikal J, Weir G, Hochedlinger K. Induced pluripotent stem cells generated without viral integration. *Science (New York, NY)*. 2008;322(5903):945–949.

135. Warren L, Manos PD, Ahfeldt T, et al. Highly efficient reprogramming to pluripotency and directed differentiation of human cells with synthetic modified mRNA. *Cell Stem Cell*. 2010;7(5):618–630.

136. Kim D, Kim C-H, Moon J-I, et al. Generation of human induced pluripotent stem cells by direct delivery of reprogramming proteins. *Cell Stem Cell*. 2009;4(6):472–476.

137. Seki T, Yuasa S, Oda M, et al. Generation of induced pluripotent stem cells from human terminally differentiated circulating T cells. *Cell Stem Cell*. 2010;7(1):11–14.

138. Anokye-Danso F, Trivedi CM, Juhr D, et al. Highly efficient miRNA-mediated reprogramming of mouse and human somatic cells to pluripotency. *Cell stem cell*. 2011;8(4):376–88. doi:10.1016/j.stem.2011.03.001.

139. Miyoshi N, Ishii H, Nagano H, et al. Reprogramming of mouse and human cells to pluripotency using mature microRNAs. *Cell stem cell*. 2011;8(6):633–8. doi:10.1016/j.stem.2011.05.001.

140. Ye Z, Zhan H, Mali P, et al. Human-induced pluripotent stem cells from blood cells of healthy donors and patients with acquired blood disorders. *Blood*. 2009;114(27):5473–5480.

141. Staerk J, Dawlaty MM, Gao Q, et al. Reprogramming of human peripheral blood cells to induced pluripotent stem cells. *Cell Stem Cell*. 2010;7(1):20–24.

142. Loh Y-H, Agarwal S, Park I-H, et al. Generation of induced pluripotent stem cells from human blood. *Blood*. 2009;113(22):5476–5479.

143. Sommer AG, Rozelle SS, Sullivan S, et al. Generation of human induced pluripotent stem cells from peripheral blood using the STEMCCA lentiviral vector. *Journal of visualized experiments : JoVE*. 2012;(68).

144. Lian Q, Chow Y, Esteban MA, Pei D, Tse HF. Future perspective of induced pluripotent stem cells for diagnosis, drug screening and treatment of human diseases. *Thromb Haemost*. 2010;104(1):39–44. doi:10.1160/th10-05-0269.

145. Deshmukh RS, Kovacs KA, Dinnyes A. Drug discovery models and toxicity testing using embryonic and induced pluripotent stem-cell-derived cardiac and neuronal cells. *Stem Cells Int*. 2012;2012:379569. doi:10.1155/2012/379569.

146. Chun YS, Byun K, Lee B. Induced pluripotent stem cells and personalized medicine: current progress and future perspectives. *Anat Cell Biol*. 2011;44(4):245–255. doi:10.5115/acb.2011.44.4.245.

147. Grskovic M, Javaherian A, Strulovici B, Daley GQ. Induced pluripotent stem cells--opportunities for disease modelling and drug discovery. *Nat Rev Drug Discov*. 2011;10(12):915–929. doi:10.1038/nrd3577.

148. Egawa N, Kitaoka S, Tsukita K, et al. Drug screening for ALS using patient-specific induced pluripotent stem cells. *Sci Transl Med*. 2012;4(145):145ra104. doi:10.1126/scitranslmed.3004052.

149. Ebert AD, Yu J, Rose Jr. FF, et al. Induced pluripotent stem cells from a spinal muscular atrophy patient. *Nature*. 2009;457(7227):277–280. doi:10.1038/nature07677.

150. Itzhaki I, Maizels L, Huber I, et al. Modelling the long QT syndrome with induced pluripotent stem cells. *Nature*. 2011;471(7337):225–229. doi:10.1038/nature09747.

151. Lee G, Papapetrou EP, Kim H, et al. Modelling pathogenesis and treatment of familial dysautonomia using patient-specific iPSCs. *Nature*. 2009;461(7262):402–406. doi:10.1038/nature08320.

152. Leung A, Nah SK, Reid W, et al. Induced pluripotent stem cell modeling of multisystemic, hereditary transthyretin amyloidosis. *Stem cell reports*. 2013;1(5):451–63. doi:10.1016/j.stemcr.2013.10.003.

153. McNeish J, Roach M, Hambor J, et al. High-throughput screening in embryonic stem cell-derived neurons identifies potentiators of alpha-amino-3-hydroxyl-5-methyl-4-isoxazolepropionate-type glutamate receptors. *J Biol Chem*. 2010;285(22):17209–17217. doi:10.1074/jbc.M109.098814.

154. Buzanska L, Sypecka J, Nerini-Molteni S, et al. A human stem cell-based model for identifying adverse effects of organic and inorganic chemicals on the developing nervous system. *Stem cells (Dayton, Ohio)*. 2009;27(10):2591–601. doi:10.1002/stem.179.

155. Takayama K, Kawabata K, Nagamoto Y, et al. 3D spheroid culture of hESC/hiPSC-derived hepatocyte-like cells for drug toxicity testing. *Biomaterials*. 2013;34(7):1781–9. doi:10.1016/j.biomaterials.2012.11.029.

156. Moretti A, Bellin M, Welling A, et al. Patient-specific induced pluripotent stem-cell models for long-QT syndrome. *N Engl J Med*. 2010;363(15):1397–1409. doi:10.1056/NEJMoa0908679.

157. Liang P, Lan F, Lee AS, et al. Drug screening using a library of human induced pluripotent stem cell-derived cardiomyocytes reveals disease-specific patterns of cardiotoxicity. *Circulation*. 2013;127(16):1677–91. doi:10.1161/CIRCULATIONAHA.113.001883.

158. Giarratana M-C, Rouard H, Dumont A, et al. Proof of principle for transfusion of in vitro-generated red blood cells. *Blood*. 2011;118(19):5071–9. doi:10.1182/blood-2011-06-362038.

159. Giarratana M-C, Kobari L, Lapillonne H, et al. Ex vivo generation of fully mature human red blood cells from hematopoietic stem cells. *Nature biotechnology*. 2005;23(1):69–74.

160. Boitano AE, Wang J, Romeo R, et al. Aryl hydrocarbon receptor antagonists promote the expansion of human hematopoietic stem cells. *Science (New York, NY)*. 2010;329(5997):1345–1348.

161. Robinson SN, Ng J, Niu T, et al. Superior ex vivo cord blood expansion following co-culture with bone marrow-derived mesenchymal stem cells. *Bone marrow transplantation*. 2006;37(4):359–366.

162. Robinson SN, Simmons PJ, Yang H, Alousi AM, Marcos de Lima J, Shpall EJ. Mesenchymal stem cells in ex vivo cord blood expansion. *Best practice & research Clinical haematology*. 2011;24(1):83–92.

163. Zhang CC, Lodish HF. Murine hematopoietic stem cells change their surface phenotype during ex vivo expansion. *Blood*. 2005;105(11):4314–4320.

164. Drake AC, Khoury M, Leskov I, et al. Human CD34+ CD133+ hematopoietic stem cells cultured with growth factors including Angptl5 efficiently engraft adult NOD-SCID Il2rγ-/- (NSG) mice. *PLoS One*. 2011;6(4):e18382.

165. Cerdan C, Rouleau A, Bhatia M. VEGF-A165 augments erythropoietic development from human embryonic stem cells. *Blood*. 2004;103(7):2504–2512. doi:10.1182/blood-2003-07-2563.

166. Zambidis ET, Peault B, Park TS, Bunz F, Civin CI. Hematopoietic differentiation of human embryonic stem cells progresses through sequential hematoendothelial, primitive, and definitive stages resembling human yolk sac development. *Blood*. 2005;106(3):860–870.

167. Chang K, Nelson AM, Cao H, et al. Definitive-like erythroid cells derived from human embryonic stem cells coexpress high levels of embryonic and fetal globins with little or no adult globin. *Blood*. 2006;108(5):1515–23. doi:10.1182/blood-2005-11-011874.

168. Chang K-H, Huang A, Hirata RK, Wang P-R, Russell DW, Papayannopoulou T. Globin phenotype of erythroid cells derived from human induced pluripotent stem cells. *Blood*. 2010;115(12):2553–4. doi:10.1182/blood-2009-11-252650.

169. Kaufman DS, Hanson ET, Lewis RL, Auerbach R, Thomson JA. Hematopoietic colony-forming cells derived from human embryonic stem cells. *Proceedings of the National Academy of Sciences of the United States of America*. 2001;98(19):10716–10721. doi:10.1073/pnas.191362598.

170. Dias J, Gumenyuk M, Kang H, et al. Generation of red blood cells from human induced pluripotent stem cells. *Stem cells and development*. 2011;20(9):1639–1647.

171. Ma F, Ebihara Y, Umeda K, et al. Generation of functional erythrocytes from human embryonic stem cell-derived definitive hematopoiesis. *Proceedings of the National Academy of Sciences of the United States of America*. 2008;105(35):13087–13092. doi:10.1073/pnas.0802220105.

172. Salvagiotto G, Burton S, Daigh CA, Rajesh D, Slukvin II, Seay NJ. A defined, feeder-free, serum-free system to generate in vitro hematopoietic progenitors and differentiated blood cells from hESCs and hiPSCs. *PLoS One*. 2011;6(3):e17829.

173. Niwa A, Heike T, Umeda K, et al. A novel serum-free monolayer culture for orderly hematopoietic differentiation of human pluripotent cells via mesodermal progenitors. *PLoS One*. 2011;6(7):e22261.

174. Lin J, Fernandez I, Roy K. Development of feeder-free culture systems for generation of ckit+sca1+ progenitors from mouse iPS cells. *Stem cell reviews*. 2011;7(3):736–747.

175. Olivier EN, Qiu C, Velho M, Hirsch RE, Bouhassira EE. Large-scale production of embryonic red blood cells from human embryonic stem cells. *Experimental hematology*. 2006;34(12):1635–1642.

176. Si-Tayeb K, Noto FK, Nagaoka M, et al. Highly efficient generation of human hepatocyte-like cells from induced pluripotent stem cells. *Hepatology*. 2010;51(1):297–305. doi:10.1002/hep.23354.

177. Qiu C, Olivier EN, Velho M, Bouhassira EE. Globin switches in yolk sac-like primitive and fetal-like definitive red blood cells produced from human embryonic stem cells. *Blood*. 2008;111(4):2400–2408.

178. Chang K-H, Nelson AM, Fields PA, et al. Diverse hematopoietic potentials of five human embryonic stem cell lines. *Experimental cell research*. 2008;314(16):2930–2940.

179. Lu S-JJ, Feng Q, Park JS, et al. Biologic properties and enucleation of red blood cells from human embryonic stem cells. *Blood*. 2008;112(12):4475–4484. doi:10.1182/blood-2008-05-157198.

180. Lapillonne H, Kobari L, Mazurier C, et al. Red blood cell generation from human induced pluripotent stem cells: perspectives for transfusion medicine. *Haematologica*. 2010;95(10):1651–1659.

181. Liu Y, Yue W, Ji L, Nan X, Pei X. Production of erythriod cells from human embryonic stem cells by fetal liver cell extract treatment. *BMC developmental biology*. 2010;10:85.

182. Kobari L, Yates F, Oudrhiri N, et al. Human induced pluripotent stem cells can reach complete terminal maturation: in vivo and in vitro evidence in the erythropoietic

differentiation model. *Haematologica*. 2012;97(12):1795–803. doi:10.3324/haematol.2011.055566.

183. Hahn ME. Aryl hydrocarbon receptors: diversity and evolution. *Chemico-biological interactions*. 2002;141(1-2):131–160.

184. Gu YZ, Hogenesch JB, Bradfield CA. The PAS superfamily: sensors of environmental and developmental signals. *Annual review of pharmacology and toxicology*. 2000;40:519–561. doi:10.1146/annurev.pharmtox.40.1.519.

185. Maltepe E, Schmidt J V, Baunoch D, Bradfield CA, Simon MC. Abnormal angiogenesis and responses to glucose and oxygen deprivation in mice lacking the protein ARNT. *Nature*. 1997;386(6623):403–407. doi:10.1038/386403a0.

186. Chan WK, Yao G, Gu YZ, Bradfield CA. Cross-talk between the aryl hydrocarbon receptor and hypoxia inducible factor signaling pathways. Demonstration of competition and compensation. *The Journal of biological chemistry*. 1999;274(17):12115–12123.

187. Taylor BL, Zhulin IB. PAS domains: internal sensors of oxygen, redox potential, and light. *Microbiology and molecular biology reviews : MMBR*. 1999;63(2):479–506.

188. Hankinson O, Brooks BA, Weir-Brown KI, et al. Genetic and molecular analysis of the Ah receptor and of Cyp1a1 gene expression. *Biochimie*. 1991;73(1):61–66.

189. Beischlag T V, Luis Morales J, Hollingshead BD, Perdew GH. The aryl hydrocarbon receptor complex and the control of gene expression. *Critical reviews in eukaryotic gene expression*. 2008;18(3):207–250.

190. Nebert DW, Petersen DD, Puga A. Human AH locus polymorphism and cancer: inducibility of CYP1A1 and other genes by combustion products and dioxin. *Pharmacogenetics*. 1991;1(2):68–78.

191. Liu RM, Vasiliou V, Zhu H, et al. Regulation of [Ah] gene battery enzymes and glutathione levels by 5,10-dihydroindeno[1,2-b]indole in mouse hepatoma cell lines. *Carcinogenesis*. 1994;15(10):2347–52.

192. Liu H, Santostefano M, Safe S. 2-Phenylphenanthridinone and related compounds: aryl hydrocarbon receptor agonists and suicide inactivators of P4501A1. *Archives of biochemistry and biophysics*. 1994;313(2):206–214. doi:10.1006/abbi.1994.1378.

193. Spink BC, Hussain MM, Katz BH, Eisele L, Spink DC. Transient induction of cytochromes P450 1A1 and 1B1 in MCF-7 human breast cancer cells by indirubin. *Biochemical pharmacology*. 2003;66(12):2313–2321.

194. Spink BC, Pang S, Pentecost BT, Spink DC. Induction of cytochrome P450 1B1 in MDA-MB-231 human breast cancer cells by non-ortho-substituted polychlorinated biphenyls.

Toxicology in vitro : an international journal published in association with BIBRA. 2002;16(6):695–704.

195. Reiners JJ, Jones CL, Hong N, Clift RE, Elferink C. Downregulation of aryl hydrocarbon receptor function and cytochrome P450 1A1 induction by expression of Ha-ras oncogenes. *Molecular carcinogenesis*. 1997;19(2):91–100.

196. Santini RP, Myrand S, Elferink C, Reiners JJ. Regulation of Cyp1a1 induction by dioxin as a function of cell cycle phase. *The Journal of pharmacology and experimental therapeutics*. 2001;299(2):718–728.

197. Funatake CJ, Marshall NB, Steppan LB, Mourich D V, Kerkvliet NI. Cutting edge: activation of the aryl hydrocarbon receptor by 2,3,7,8-tetrachlorodibenzo-p-dioxin generates a population of CD4+ CD25+ cells with characteristics of regulatory T cells. *Journal of immunology (Baltimore, Md : 1950)*. 2005;175(7):4184–4188.

198. Apetoh L, Quintana FJ, Pot C, et al. The aryl hydrocarbon receptor interacts with c-Maf to promote the differentiation of type 1 regulatory T cells induced by IL-27. *Nature immunology*. 2010;11(9):854–861. doi:10.1038/ni.1912.

199. Li Y, Innocentin S, Withers DR, et al. Exogenous stimuli maintain intraepithelial lymphocytes via aryl hydrocarbon receptor activation. *Cell*. 2011;147(3):629–640. doi:10.1016/j.cell.2011.09.025.

200. Martin B, Hirota K, Cua DJ, Stockinger B, Veldhoen M. Interleukin-17-producing gammadelta T cells selectively expand in response to pathogen products and environmental signals. *Immunity*. 2009;31(2):321–330. doi:10.1016/j.immuni.2009.06.020.

201. Veldhoen M, Hirota K, Christensen J, O'Garra A, Stockinger B. Natural agonists for aryl hydrocarbon receptor in culture medium are essential for optimal differentiation of Th17 T cells. *The Journal of experimental medicine*. 2009;206(1):43–49. doi:10.1084/jem.20081438.

202. Veldhoen M, Hirota K, Westendorf AM, et al. The aryl hydrocarbon receptor links TH17-cell-mediated autoimmunity to environmental toxins. *Nature*. 2008;453(7191):106–109. doi:10.1038/nature06881.

203. Quintana FJ, Basso AS, Iglesias AH, et al. Control of T(reg) and T(H)17 cell differentiation by the aryl hydrocarbon receptor. *Nature*. 2008;453(7191):65–71. doi:10.1038/nature06880.

204. Quintana FJ, Murugaiyan G, Farez MF, et al. An endogenous aryl hydrocarbon receptor ligand acts on dendritic cells and T cells to suppress experimental autoimmune encephalomyelitis. *Proceedings of the National Academy of Sciences of the United States of America*. 2010;107(48):20768–20773. doi:10.1073/pnas.1009201107.

205. Mezrich JD, Fechner JH, Zhang X, Johnson BP, Burlingham WJ, Bradfield CA. An interaction between kynurenine and the aryl hydrocarbon receptor can generate regulatory T cells. *Journal of immunology (Baltimore, Md : 1950)*. 2010;185(6):3190–3198. doi:10.4049/jimmunol.0903670.

206. Kimura A, Naka T, Nohara K, Fujii-Kuriyama Y, Kishimoto T. Aryl hydrocarbon receptor regulates Stat1 activation and participates in the development of Th17 cells. *Proceedings of the National Academy of Sciences of the United States of America*. 2008;105(28):9721–9726. doi:10.1073/pnas.0804231105.

207. Abdelrahim M, Smith R, Safe S. Aryl hydrocarbon receptor gene silencing with small inhibitory RNA differentially modulates Ah-responsiveness in MCF-7 and HepG2 cancer cells. *Molecular pharmacology*. 2003;63(6):1373–1381. doi:10.1124/mol.63.6.1373.

208. Barouki R, Aggerbeck M, Aggerbeck L, Coumoul X. The aryl hydrocarbon receptor system. *Drug metabolism and drug interactions*. 2012;27(1):3–8. doi:10.1515/dmdi-2011-0035.

209. Miller ME, Holloway AC, Foster WG. Benzo-[a]-pyrene increases invasion in MDA-MB-231 breast cancer cells via increased COX-II expression and prostaglandin E2 (PGE2) output. *Clinical & experimental metastasis*. 2005;22(2):149–156. doi:10.1007/s10585-005-6536-x.

210. Mulero-Navarro S, Pozo-Guisado E, Pérez-Mancera PA, et al. Immortalized mouse mammary fibroblasts lacking dioxin receptor have impaired tumorigenicity in a subcutaneous mouse xenograft model. *The Journal of biological chemistry*. 2005;280(31):28731–28741. doi:10.1074/jbc.M504538200.

211. Marlowe JL, Fan Y, Chang X, et al. The aryl hydrocarbon receptor binds to E2F1 and inhibits E2F1-induced apoptosis. *Molecular biology of the cell*. 2008;19(8):3263–3271. doi:10.1091/mbc.E08-04-0359.

212. Matikainen T, Perez GI, Jurisicova A, et al. Aromatic hydrocarbon receptor-driven Bax gene expression is required for premature ovarian failure caused by biohazardous environmental chemicals. *Nature genetics*. 2001;28(4):355–360. doi:10.1038/ng575.

213. Robles R, Morita Y, Mann KK, et al. The aryl hydrocarbon receptor, a basic helix-loop-helix transcription factor of the PAS gene family, is required for normal ovarian germ cell dynamics in the mouse. *Endocrinology*. 2000;141(1):450–453. doi:10.1210/endo.141.1.7374.

214. Caruso JA, Mathieu PA, Joiakim A, Zhang H, Reiners JJ. Aryl hydrocarbon receptor modulation of tumor necrosis factor-alpha-induced apoptosis and lysosomal disruption in a hepatoma model that is caspase-8-independent. *The Journal of biological chemistry*. 2006;281(16):10954–10967. doi:10.1074/jbc.M508383200.

215. Schlezinger JJ, Liu D, Farago M, et al. A role for the aryl hydrocarbon receptor in mammary gland tumorigenesis. *Biological chemistry*. 2006;387(9):1175–1187. doi:10.1515/BC.2006.145.

216. Hayashibara T, Yamada Y, Mori N, et al. Possible involvement of aryl hydrocarbon receptor (AhR) in adult T-cell leukemia (ATL) leukemogenesis: constitutive activation of AhR in ATL. *Biochemical and biophysical research communications*. 2003;300(1):128–134.

217. Zudaire E, Cuesta N, Murty V, et al. The aryl hydrocarbon receptor repressor is a putative tumor suppressor gene in multiple human cancers. *The Journal of clinical investigation*. 2008;118(2):640–650. doi:10.1172/JCI30024.

218. Kawajiri K, Kobayashi Y, Ohtake F, et al. Aryl hydrocarbon receptor suppresses intestinal carcinogenesis in ApcMin/+ mice with natural ligands. *Proceedings of the National Academy of Sciences of the United States of America*. 2009;106(32):13481–13486. doi:10.1073/pnas.0902132106.

219. Opitz CA, Litzenburger UM, Sahm F, et al. An endogenous tumour-promoting ligand of the human aryl hydrocarbon receptor. *Nature*. 2011;478(7368):197–203. doi:10.1038/nature10491.

220. Lawrence BP, Sherr DH. You AhR what you eat? *Nature immunology*. 2012;13(2):117–119. doi:10.1038/ni.2213.

221. Singh KP, Garrett RW, Casado FL, Gasiewicz T a. Aryl hydrocarbon receptor-null allele mice have hematopoietic stem/progenitor cells with abnormal characteristics and functions. *Stem cells and development*. 2011;20(5):769–84. doi:10.1089/scd.2010.0333.

222. Hirabayashi Y, Inoue T. Aryl hydrocarbon receptor biology and xenobiotic responses in hematopoietic progenitor cells. *Biochemical pharmacology*. 2009;77(4):521–35. doi:10.1016/j.bcp.2008.09.030.

223. Singh KP, Casado FL, Opanashuk LA, Gasiewicz TA. The aryl hydrocarbon receptor has a normal function in the regulation of hematopoietic and other stem/progenitor cell populations. *Biochemical pharmacology*. 2009;77(4):577–87. doi:10.1016/j.bcp.2008.10.001.

224. Lindsey S, Papoutsakis ET. The aryl hydrocarbon receptor (AHR) transcription factor regulates megakaryocytic polyploidization. *British journal of haematology*. 2011;152(4):469–484. doi:10.1111/j.1365-2141.2010.08548.x.

225. Thurmond TS, Staples JE, Silverstone AE, Gasiewicz TA. The aryl hydrocarbon receptor has a role in the in vivo maturation of murine bone marrow B lymphocytes and their response to 3,7,8-tetrachlorodibenzo-p-dioxin. Toxicol Appl Pharmacol 165, . . 2000;2:227–236.

226. Jude CD, Climer L, Xu D, Artinger E, Fisher JK, Ernst P. Unique and independent roles for MLL in adult hematopoietic stem cells and progenitors. *Cell stem cell*. 2007;1(3):324–337. doi:10.1016/j.stem.2007.05.019.

227. Minami Y, Kajiguchi T, Abe A, Ohno T, Kiyoi H, Naoe T. Expanded distribution of the T315I mutation among hematopoietic stem cells and progenitors in a chronic myeloid leukemia patient during imatinib treatment. *International journal of hematology*. 2010;92(4):664–666. doi:10.1007/s12185-010-0706-6.

228. Choi K-D, Yu J, Smuga-Otto K, et al. Hematopoietic and endothelial differentiation of human induced pluripotent stem cells. *Stem cells (Dayton, Ohio)*. 2009;27(3):559–567. doi:10.1634/stemcells.2008-0922.

229. Takayama N, Nishikii H, Usui J, et al. Generation of functional platelets from human embryonic stem cells in vitro via ES-sacs, VEGF-promoted structures that concentrate hematopoietic progenitors. *Blood*. 2008;111(11):5298–5306. doi:10.1182/blood-2007-10-117622.

230. Eisen MB, Spellman PT, Brown PO, Botstein D. Cluster analysis and display of genome-wide expression patterns. *Proceedings of the National Academy of Sciences of the United States of America*. 1998;95(25):14863–14868.

231. Chambers J, TJ H. *Statistical Models in S*.; 1991.

232. Novershtern N, Subramanian A, Lawton LN, et al. Densely interconnected transcriptional circuits control cell states in human hematopoiesis. *Cell*. 2011;144(2):296–309. doi:10.1016/j.cell.2011.01.004.

233. Chang K-H, Bonig H, Papayannopoulou T. Generation and characterization of erythroid cells from human embryonic stem cells and induced pluripotent stem cells: an overview. *Stem cells international*. 2011;2011:791604. doi:10.4061/2011/791604.

234. Schlezinger JJ, Bernard PL, Haas A, Grandjean P, Weihe P, Sherr DH. Direct assessment of cumulative aryl hydrocarbon receptor agonist activity in sera from experimentally exposed mice and environmentally exposed humans. *Environmental health perspectives*. 2010;118(5):693–698. doi:10.1289/ehp.0901113.

235. Han D, Nagy SR, Denison MS. Comparison of recombinant cell bioassays for the detection of Ah receptor agonists. *BioFactors (Oxford, England)*. 2004;20(1):11–22.

236. Kim SH. Novel compound 2-methyl-2H-pyrazole-3-carboxylic acid (2-methyl-4-o-tolylazo-phenyl)-amide (CH-223191) prevents 2,3,7,8-TCDD-induced toxicity by antagonizing the aryl hydrocarbon receptor. *Mol Pharmacol 69 Epub Mar 60 Transversal study of breast cancer treatment in Spain Farm Hosp 32 139*. 2006;147(2008):1871–1878.

237. Hahn ME, Allan LL, Sherr DH. Regulation of constitutive and inducible AHR signaling: complex interactions involving the AHR repressor. *Biochemical pharmacology*. 2009;77(4):485–497. doi:10.1016/j.bcp.2008.09.016.

238. Evans BR, Karchner SI, Allan LL, et al. Repression of aryl hydrocarbon receptor (AHR) signaling by AHR repressor: role of DNA binding and competition for AHR nuclear translocator. *Molecular pharmacology*. 2008;73(2):387–398. doi:10.1124/mol.107.040204.

239. Lindsey S, Papoutsakis ET. The evolving role of the aryl hydrocarbon receptor (AHR) in the normophysiology of hematopoiesis. *Stem cell reviews*. 2012;8(4):1223–35. doi:10.1007/s12015-012-9384-5.

240. Rannug U, Rannug A, Sjöberg U, Li H, Westerholm R, Bergman J. Structure elucidation of two tryptophan-derived, high affinity Ah receptor ligands. *Chemistry & biology*. 1995;2(12):841–845.

241. Wincent E, Amini N, Luecke S, et al. The suggested physiologic aryl hydrocarbon receptor activator and cytochrome P4501 substrate 6-formylindolo[3,2-b]carbazole is present in humans. *The Journal of biological chemistry*. 2009;284(5):2690–2696. doi:10.1074/jbc.M808321200.

242. Gasiewicz TA, Singh KP, Casado FL. The aryl hydrocarbon receptor has an important role in the regulation of hematopoiesis: implications for benzene-induced hematopoietic toxicity. *Chemico-biological interactions*. 2010;184(1-2):246–251. doi:10.1016/j.cbi.2009.10.019.

243. Scott EW, Simon MC, Anastasi J, Singh H. Requirement of transcription factor PU.1 in the development of multiple hematopoietic lineages. *Science (New York, NY)*. 1994;265(5178):1573–7.

244. Rekhtman N, Radparvar F, Evans T, Skoultchi AI. Direct interaction of hematopoietic transcription factors PU.1 and GATA-1: functional antagonism in erythroid cells. *Genes & development*. 1999;13(11):1398–411.

245. Zhang P, Zhang X, Iwama A, et al. PU.1 inhibits GATA-1 function and erythroid differentiation by blocking GATA-1 DNA binding. *Blood*. 2000;96(8):2641–8.

246. Doré LC, Crispino JD. Transcription factor networks in erythroid cell and megakaryocyte development. *Blood*. 2011;118(2):231–9. doi:10.1182/blood-2011-04-285981.

247. Kelley LL, Koury MJ, Bondurant MC, Koury ST, Sawyer ST, Wickrema A. Survival or death of individual proerythroblasts results from differing erythropoietin sensitivities: a mechanism for controlled rates of erythrocyte production. *Blood*. 1993;82(8):2340–52.

248. Marieb EN, Hoehn K. *Human Anatomy & Physiology, 7/E*. 7E ed. Pearson; :page 652 and figure 17.5.

249. Gahmberg CG, Jokinen M, Andersson LC. Expression of the major sialoglycoprotein (glycophorin) on erythroid cells in human bone marrow. *Blood*. 1978;52(2):379–87.

250. Kudo S, Onda M, Fukuda M. Characterization of glycophorin A transcripts: control by the common erythroid-specific promoter and alternative usage of different polyadenylation signals. *Journal of biochemistry*. 1994;116(1):183–92.

251. Loken MR, Civin CI, Bigbee WL, Langlois RG, Jensen RH. Coordinate glycosylation and cell surface expression of glycophorin A during normal human erythropoiesis. *Blood*. 1987;70(6):1959–61.

252. Dong HY, Wilkes S, Yang H. CD71 is selectively and ubiquitously expressed at high levels in erythroid precursors of all maturation stages: a comparative immunochemical study with glycophorin A and hemoglobin A. *The American journal of surgical pathology*. 2011;35(5):723–32. doi:10.1097/PAS.0b013e31821247a8.

253. Lesley J, Hyman R, Schulte R, Trotter J. Expression of transferrin receptor on murine hematopoietic progenitors. *Cellular immunology*. 1984;83(1):14–25.

254. Nakahata T, Okumura N. Cell surface antigen expression in human erythroid progenitors: erythroid and megakaryocytic markers. *Leukemia & lymphoma*. 1994;13(5-6):401–9. doi:10.3109/10428199409049629.

255. Sieff C, Bicknell D, Caine G, Robinson J, Lam G, Greaves MF. Changes in cell surface antigen expression during hemopoietic differentiation. *Blood*. 1982;60(3):703–13.

256. Sargent PJ, Farnaud S, Evans RW. Structure/function overview of proteins involved in iron storage and transport. *Current medicinal chemistry*. 2005;12(23):2683–93.

257. Aisen P. Transferrin receptor 1. *The international journal of biochemistry & cell biology*. 2004;36(11):2137–43. doi:10.1016/j.biocel.2004.02.007.

258. Kansas GS, Muirhead MJ, Dailey MO. Expression of the CD11/CD18, leukocyte adhesion molecule 1, and CD44 adhesion molecules during normal myeloid and erythroid differentiation in humans. *Blood*. 1990;76(12):2483–92.

259. McCarthy EF. The oxygen affinity of human maternal and foetal haemoglobin. *The Journal of physiology*. 1943;102(1):55–61.

260. André MC, Erbacher A, Gille C, et al. Long-term human CD34+ stem cell-engrafted nonobese diabetic/SCID/IL-2R gamma(null) mice show impaired CD8+ T cell maintenance and a functional arrest of immature NK cells. *Journal of immunology (Baltimore, Md : 1950)*. 2010;185(5):2710–20. doi:10.4049/jimmunol.1000583.

261. Broxmeyer HE, Lee M-R, Hangoc G, et al. Hematopoietic stem/progenitor cells, generation of induced pluripotent stem cells, and isolation of endothelial progenitors from

21- to 23.5-year cryopreserved cord blood. *Blood*. 2011;117(18):4773–7. doi:10.1182/blood-2011-01-330514.

262. Rörby E, Hägerström MN, Blank U, Karlsson G, Karlsson S. Human hematopoietic stem/progenitor cells overexpressing Smad4 exhibit impaired reconstitution potential in vivo. *Blood*. 2012;120(22):4343–51. doi:10.1182/blood-2012-02-408658.

263. Risueño RM, Sachlos E, Lee J-HJB, Hong S-H, Szabo E, Bhatia M. Inability of human induced pluripotent stem cell-hematopoietic derivatives to downregulate microRNAs in vivo reveals a block in xenograft hematopoietic regeneration. *Stem cells (Dayton, Ohio)*. 2012;30(2):131–9. doi:10.1002/stem.1684.

264. Majeti R, Park CY, Weissman IL. Identification of a hierarchy of multipotent hematopoietic progenitors in human cord blood. *Cell stem cell*. 2007;1(6):635–45. doi:10.1016/j.stem.2007.10.001.

265. Chen Q, Khoury M, Limmon G, Choolani M, Chan JKY, Chen J. Human fetal hepatic progenitor cells are distinct from, but closely related to, hematopoietic stem/progenitor cells. *Stem cells (Dayton, Ohio)*. 2013;31(6):1160–9. doi:10.1002/stem.1359.

266. Amabile G, Welner RS, Nombela-Arrieta C, et al. In vivo generation of transplantable human hematopoietic cells from induced pluripotent stem cells. *Blood*. 2013;121(8):1255–64. doi:10.1182/blood-2012-06-434407.

267. Hayakawa J, Hsieh MM, Anderson DE, et al. The assessment of human erythroid output in NOD/SCID mice reconstituted with human hematopoietic stem cells. *Cell transplantation*. 2010;19(11):1465–73. doi:10.3727/096368910X314161.

268. Brehm M a, Shultz LD, Luban J, Greiner DL. Overcoming current limitations in humanized mouse research. *The Journal of infectious diseases*. 2013;208 Suppl(Suppl 2):S125–30. doi:10.1093/infdis/jit319.

269. Mosier DE, Gulizia RJ, Baird SM, Wilson DB. Transfer of a functional human immune system to mice with severe combined immunodeficiency. *Nature*. 1988;335(6187):256–9. doi:10.1038/335256a0.

270. Bosma GC, Custer RP, Bosma MJ. A severe combined immunodeficiency mutation in the mouse. *Nature*. 1983;301(5900):527–30.

271. McCune JM, Namikawa R, Kaneshima H, Shultz LD, Lieberman M, Weissman IL. The SCID-hu mouse: murine model for the analysis of human hematolymphoid differentiation and function. *Science (New York, NY)*. 1988;241(4873):1632–9.

272. Ito M, Hiramatsu H, Kobayashi K, et al. NOD/SCID/gamma(c)(null) mouse: an excellent recipient mouse model for engraftment of human cells. *Blood*. 2002;100(9):3175–82. doi:10.1182/blood-2001-12-0207.

273. Tanaka S, Saito Y, Kunisawa J, et al. Development of mature and functional human myeloid subsets in hematopoietic stem cell-engrafted NOD/SCID/IL2rγKO mice. *Journal of immunology (Baltimore, Md : 1950)*. 2012;188(12):6145–55. doi:10.4049/jimmunol.1103660.

274. Shultz LD, Lyons BL, Burzenski LM, et al. Human lymphoid and myeloid cell development in NOD/LtSz-scid IL2R gamma null mice engrafted with mobilized human hemopoietic stem cells. *Journal of immunology (Baltimore, Md : 1950)*. 2005;174(10):6477–89.

275. Shultz LD, Ishikawa F, Greiner DL. Humanized mice in translational biomedical research. *Nature reviews Immunology*. 2007;7(2):118–30. doi:10.1038/nri2017.

276. McDermott SP, Eppert K, Lechman ER, Doedens M, Dick JE. Comparison of human cord blood engraftment between immunocompromised mouse strains. *Blood*. 2010;116(2):193–200. doi:10.1182/blood-2010-02-271841.

277. Ishikawa F, Yasukawa M, Lyons B, et al. Development of functional human blood and immune systems in NOD/SCID/IL2 receptor {gamma} chain(null) mice. *Blood*. 2005;106(5):1565–73. doi:10.1182/blood-2005-02-0516.

278. Smith BW, Rozelle SS, Leung A, et al. The aryl hydrocarbon receptor directs hematopoietic progenitor cell expansion and differentiation. *Blood*. 2013. doi:10.1182/blood-2012-11-466722.

279. England SJ, McGrath KE, Frame JM, Palis J. Immature erythroblasts with extensive ex vivo self-renewal capacity emerge from the early mammalian fetus. *Blood*. 2011;117(9):2708–17. doi:10.1182/blood-2010-07-299743.

280. Miharada K, Hiroyama T, Sudo K, Nagasawa T, Nakamura Y. Efficient enucleation of erythroblasts differentiated in vitro from hematopoietic stem and progenitor cells. *Nature biotechnology*. 2006;24(10):1255–6. doi:10.1038/nbt1245.

281. Van Rooijen N. The liposome-mediated macrophage "suicide" technique. *Journal of immunological methods*. 1989;124(1):1–6.

282. Lehenkari PP, Kellinsalmi M, Näpänkangas JP, et al. Further insight into mechanism of action of clodronate: inhibition of mitochondrial ADP/ATP translocase by a nonhydrolyzable, adenine-containing metabolite. *Molecular pharmacology*. 2002;61(5):1255–62.

283. Bergh A, Damber JE, van Rooijen N. Liposome-mediated macrophage depletion: an experimental approach to study the role of testicular macrophages in the rat. *The Journal of endocrinology*. 1993;136(3):407–13.

284. Van Lent PL, van den Bersselaar L, van den Hoek AE, et al. Reversible depletion of synovial lining cells after intra-articular treatment with liposome-encapsulated dichloromethylene diphosphonate. *Rheumatology international*. 1993;13(1):21–30.

285. Van Rooijen N, van Nieuwmegen R. Elimination of phagocytic cells in the spleen after intravenous injection of liposome-encapsulated dichloromethylene diphosphonate. An enzyme-histochemical study. *Cell and tissue research*. 1984;238(2):355–8.

286. Biewenga J, van der Ende MB, Krist LF, Borst A, Ghufron M, van Rooijen N. Macrophage depletion in the rat after intraperitoneal administration of liposome-encapsulated clodronate: depletion kinetics and accelerated repopulation of peritoneal and omental macrophages by administration of Freund's adjuvant. *Cell and tissue research*. 1995;280(1):189–96.

287. Hu Z, Van Rooijen N, Yang Y-G. Macrophages prevent human red blood cell reconstitution in immunodeficient mice. *Blood*. 2011;118(22):5938–5946. doi:10.1182/blood-2010-11-321414.

288. Takenaka K, Prasolava TK, Wang JCY, et al. Polymorphism in Sirpa modulates engraftment of human hematopoietic stem cells. *Nature immunology*. 2007;8(12):1313–23. doi:10.1038/ni1527.

289. Strowig T, Rongvaux A, Rathinam C, et al. Transgenic expression of human signal regulatory protein alpha in Rag2-/-gamma(c)-/- mice improves engraftment of human hematopoietic cells in humanized mice. *Proceedings of the National Academy of Sciences of the United States of America*. 2011;108(32):13218–23. doi:10.1073/pnas.1109769108.

290. Weatherall DJ. The inherited diseases of hemoglobin are an emerging global health burden. *Blood*. 2010;115(22):4331–4336. doi:10.1182/blood-2010-01-251348.

291. Gilman JG, Huisman TH. DNA sequence variation associated with elevated fetal G gamma globin production. *Blood*. 1985;66(4):783–7.

292. Craig JE, Rochette J, Fisher CA, et al. Dissecting the loci controlling fetal haemoglobin production on chromosomes 11p and 6q by the regressive approach. *Nature genetics*. 1996;12(1):58–64. doi:10.1038/ng0196-58.

293. Akinsheye I, Solovieff N, Ngo D, et al. Fetal hemoglobin in sickle cell anemia: molecular characterization of the unusually high fetal hemoglobin phenotype in African Americans. *American journal of hematology*. 2012;87(2):217–9. doi:10.1002/ajh.22221.

294. Uda M, Galanello R, Sanna S, et al. Genome-wide association study shows BCL11A associated with persistent fetal hemoglobin and amelioration of the phenotype of beta-thalassemia. *Proc Natl Acad Sci U S A*. 2008;105(5):1620–1625. doi:10.1073/pnas.0711566105.

295. Alsultan A, Solovieff N, Aleem A, et al. Fetal hemoglobin in sickle cell anemia: Saudi patients from the Southwestern province have similar HBB haplotypes but higher HbF levels than African Americans. *American journal of hematology*. 2011;86(7):612–4. doi:10.1002/ajh.22032.

296. Ballas SK, Barton FB, Waclawiw M a, et al. Hydroxyurea and sickle cell anemia: effect on quality of life. *Health and quality of life outcomes*. 2006;4:59. doi:10.1186/1477-7525-4-59.

297. Steinberg MH, McCarthy WF, Castro O, et al. The risks and benefits of long-term use of hydroxyurea in sickle cell anemia: A 17.5 year follow-up. *Am J Hematol*. 2010;85(6):403–408. doi:10.1002/ajh.21699.

298. Ma Q, Wyszynski DF, Farrell JJ, et al. Fetal hemoglobin in sickle cell anemia: genetic determinants of response to hydroxyurea. *The pharmacogenomics journal*. 2007;7(6):386–394. doi:10.1038/sj.tpj.6500433.

299. Dover GJ, Charache S. Hydroxyurea induction of fetal hemoglobin synthesis in sickle-cell disease. *Seminars in oncology*. 1992;19(3 Suppl 9):61–66.

300. Steinberg MH, Lu ZH, Barton FB, Terrin ML, Charache S, Dover GJ. Fetal hemoglobin in sickle cell anemia: determinants of response to hydroxyurea. Multicenter Study of Hydroxyurea. *Blood*. 1997;89(3):1078–1088.

301. Orringer EP, Blythe DS, Johnson AE, Phillips G, Dover GJ, Parker JC. Effects of hydroxyurea on hemoglobin F and water content in the red blood cells of dogs and of patients with sickle cell anemia. *Blood*. 1991;78(1):212–6.

302. Smith BW, Rozelle SS, Leung A, et al. The aryl hydrocarbon receptor directs hematopoietic progenitor cell expansion and differentiation. *Blood*. 2013;122(3):376–85. doi:10.1182/blood-2012-11-466722.

303. Italia K, Jijina F, Merchant R, et al. Comparison of in-vitro and in-vivo response to fetal hemoglobin production and γ-mRNA expression by hydroxyurea in Hemoglobinopathies. *Indian journal of human genetics*. 2013;19(2):251–8.

304. Pecoraro A, Rigano P, Troia A, et al. Quantification of HBG mRNA in primary erythroid cultures: prediction of the response to hydroxyurea in sickle cell and beta-thalassemia. *European journal of haematology*. 2014;92(1):66–72. doi:10.1111/ejh.12204.

305. Silva DGH, Belini Junior E, Carrocini GC de S, et al. Genetic and biochemical markers of hydroxyurea therapeutic response in sickle cell anemia. *BMC medical genetics*. 2013;14:108. doi:10.1186/1471-2350-14-108.

306. Al-Nood HA, Al-Khawlani MM, Al-Akwa A. Fetal hemoglobin response to hydroxyurea in Yemeni sickle cell disease patients. *Hemoglobin*. 2011;35(1):13–21. doi:10.3109/03630269.2011.551748.

307. Vogel C, Marcotte EM. Insights into the regulation of protein abundance from proteomic and transcriptomic analyses. *Nature reviews Genetics*. 2012;13(4):227–32. doi:10.1038/nrg3185.

308. Van Wilgenburg B, Browne C, Vowles J, Cowley SA. Efficient, long term production of monocyte-derived macrophages from human pluripotent stem cells under partly-defined and fully-defined conditions. *PloS one*. 2013;8(8):e71098. doi:10.1371/journal.pone.0071098.

309. Taylor CJ, Peacock S, Chaudhry AN, Bradley JA, Bolton EM. Generating an iPSC bank for HLA-matched tissue transplantation based on known donor and recipient HLA types. *Cell stem cell*. 2012;11(2):147–52. doi:10.1016/j.stem.2012.07.014.

CURRICULUM VITAE